ABSTRACT

TITLE OF THESIS: Multiphase Solid-Liquid-Liquid Mixing in Stirred Tanks

INVESTIGATOR: George R. DeRitter
Master of Science in Chemical Engineering

ADVISOR: Dr. Piero M. Armenante
Assistant Professor Of Chemical Engineering

A large number of investigations can be found in the literature which examine the effect of mixing parameters in both solid-liquid and liquid-liquid systems. However, very little is currently available for solid-liquid-liquid systems. It is the intent of this study to look at the various parameters affecting the point of complete dispersion for a liquid and the point of complete suspension for a solid phase, in a three phase liquid-liquid-solid system.

A model has been developed for the dispersion of each phase based on a momentum balance of forces on an individual particle of solid or an individual droplet of liquid. Kolmogoroff's theory of isotropic turbulence has been utilized to predict the behavior of the system. Similar equations have been previously applied successfully to two phase systems. A wide variety of agitation systems with both radial and axial discharge was employed in this investigation to experimentally validate the model prediction. In particular, the disk turbine (representative of radial flow impellers) and the pitched blade turbine (representative of axial flow impellers) were studied in greater detail. All of the experiments conducted in this work involved three phase systems.

A comparison between the experimental results obtained in this work and those predicted by the model equations is provided. The agreement was found to be very good. In addition, comparisons between the current work and previously reported data on two phase systems is given. Again, good agreement was obtained. These results indicate that for systems involving only moderate concentrations of solid and dispersed liquid, the role of the key variables can be successfully predicted by considering each phase independently.

MULTIPHASE SOLID-LIQUID-LIQUID MIXING IN STIRRED TANKS

by George R. DeRitter

Thesis submitted to the Faculty of the Graduate School of
New Jersey Institute of Technology
in partial fulfillment of the requirements for the degree of
Master of Science in Chemical Engineering
1990

Blank Page

APPROVAL SHEET

Title of Thesis: Multiphase Solid-Liquid-Liquid Mixing in Stirred Tanks

Name of Candidate: George R. DeRitter
Master of Science in Chemical Engineering 1990

Thesis and Abstract

Approved:

5/10/90
Date

Dr. Piero M. Armenante
Assistant Professor
Department of Chemical Engineering, Chemistry, and Environmental Science

5-10-90
Date

Dr. Dana Knox
Associate Professor
Department of Chemical Engineering, Chemistry, and Environmental Science

5-10-90
Date

Dr. Basil Baltzis
Associate Professor
Department of Chemical Engineering, Chemistry, and Environmental Science

V I T A

Name: George R. DeRitter

Permanent Address:

Degree and date to be conferred: Master of Science in Chemical Engineering, 1990

Date of birth:

Place of birth:

Secondary Education: Hawthorne High School
Hawthorne, NJ 1983

Collegiate Institutions Attended:

	Dates	Degree	Date of Degree
N.J. Institute of Technology	1983-1988	BS	1988
N.J. Institute of Technology	1988-1990	MS	1990

Major: Chemical Engineering

ACKNOWLEDGEMENT

I would like to sincerely acknowledge the guidance and support of my thesis advisor, Dr. Piero M. Armenante. He served as a continuous source of direction and advise. His efforts were truly appreciated.

I would also like to acknowledge the members of my thesis committee, Dr. Dana Knox and Dr. Basil Baltzis, for their support and constructive criticism.

TABLE OF CONTENTS

LIST OF TABLES

LIST OF FIGURES

Chapter 1
INTRODUCTION

Multiphase fluid mixing is one of the most common and most important operations in the chemical process industry. It finds extensive application in the manufacture of chemicals, pharmaceuticals, and food products as well as many separation operations such as potable water and wastewater treatment.

Significant efforts have been devoted to mixing in recent years. By looking at the effects of the various mixing parameters such as system geometry, impeller type and size, and impeller clearance, it is possible to optimize the operation and effectively develop scale-up rules.

Of particular significance in multiphase systems is the achievement of complete suspension or dispersion. In a liquid-liquid system this point represents an important balance in the maximization of contact between the two phases and the minimization of power input. Below this point, each increase in agitation brings about a sizable increase in the amount of phase contact. Beyond this point, however, the return on investment is not nearly so significant. In a solid-liquid system the point of minimum suspension speed represents the point at which the entire solid surface is in contact with the continuous fluid.

A number of mixing parameters have been investigated as part of this study, with special focus placed on the effect of the impeller clearance on the attainment of complete dispersion. In systems involving the dispersion/suspension of

phases from both the top and the bottom of the vessel, consideration of the impeller clearance can improve the effectiveness of agitation in both tank regions.

Chapter 2
LITERATURE SURVEY

Mixing refers to the random distribution, into and through one another, of two or more initially separate phases. This is in contrast to agitation, where motion is induced in a material in a specified way. A single homogeneous material can be agitated, but it cannot be mixed until another material is added to the system. Mixing operations are employed widely in industry for the contacting of multiple phases for chemical reaction as well as the contacting of phases for the transfer of mass or heat (10).

In the systems of interest in this study, external forces are provided by a rotating agitator. These forces overcome resisting forces exerted by the dispersed particles or liquids. The two primary forces to be overcome are related to inertial and viscous resistances.

A number of factors play a role in determining the rate at which energy is supplied to the system (i.e. the power) to provide a desired degree of agitation. The power is dependent not only on the impeller type and agitation speed, but also the physical characteristics of the fluid, the shape of the vessel, and the relative location of the components of the system.

Before it is possible to expand the current body of knowledge on mixing to three phase systems, it is necessary to more fully understand the interactions between each of the two phase combinations of interest here.

2.1 KOLMOGOROFF'S THEORY OF ISOTROPIC TURBULENCE

Since Kolmogoroff's theory will be employed in most of the theoretical discussions presented in this work, a brief description of the main principles is presented here.

Contained within the turbulent flow of a stirred tank are large primary eddies which have relatively large velocity fluctuations of low frequency and are of a size comparable to the physical dimensions of the system. These eddies contain most of the kinetic energy which is transferred to them by the rotation of the impeller. These eddies represent the first stage in a downward cascade of energy which continually produces smaller eddies with higher frequencies. The smaller eddies are produced as a result of the motion of the larger eddies through slower moving streams of fluid. The disintegration of the eddies with associated decrease of their size continues to the point where the remaining kinetic energy is dissipated into heat by viscous forces. As the kinetic energy is transferred down the smaller eddies, the directional element associated with the bulk flow in the vessel is gradually lost.

Kolmogoroff then argued that in a turbulent system, the smaller eddies are independent of the bulk flow in the vessel and are isotropic. The properties of these eddies are primarily a function of the energy dissipation rate per unit mass and the size of the eddies. The size range where the eddies are isotropic but energy is transferred without viscous dissi-

pation is referred to as the inertial subrange.

Eventually a state of equilibrium is reached where the rate of energy supply from the impeller is equal to the rate of dissipation by fluid kinematic viscosity. The size of eddies where the inertial and viscous forces are in balance has been defined as the Kolmogoroff length scale. The scale is defined as $(\nu^3/\epsilon)^{1/4}$. Eddies that are smaller than this scale are considered part of the viscous subrange, in which viscosity plays a major role.

2.2 THE SUSPENSION OF SOLIDS IN LIQUIDS

A large number of industrial operations rely on the suspension of a solid in a liquid. Included here are crystallization, precipitation, dissolution, leaching, ion-exchange, adsorption, and catalyzed chemical reactions. In these processes it is generally safe to assume that the impeller Reynold's number, ND^2/ν, is greater than 2×10^4 so that the system can be considered to be fully turbulent.

There are several steps involved in the suspension of particles in an agitated vessel. First the particles have to be lifted from the base of the vessel and then dispersed throughout. The lifting of a particle involves the movement of the particle across the base to the point where suspension takes place and then the actual lifting of the particle into the moving fluid. Both drag forces, involved with the move-

ment of the particle, and gravitational forces, involved with the actual lifting, need to be overcome in order to achieve suspension. The point of suspension is a function of both the impeller type and the distance between the impeller and the vessel base.

2.2.1 Levels of Suspension in Solid-Liquid Systems

There are two main levels of suspension in solid-liquid systems. The first is the "just completely suspended" state. This represents the lowest agitator speed, Njs, at which all of the surface area of the particles is available for processing. This is the most important speed since in systems involving mass transfer many workers have shown that the rate increases relatively rapidly with increase in agitation speed up to this point but only slowly above it.

The second level of suspension which received a fair amount of attention in solid-liquid systems is the state of "homogeneous suspension". This represents the minimum agitation speed required to achieve a roughly constant concentration of particles throughout the vessel. This is an important criterion for systems designed for continuous discharge or for those which are to be modeled as a continuous stirred tank reactor (CSTR).

A visual method is typically used to determine Njs. Zwietering (18) outlined a procedure which states that the agitation speed at which no particle is observed to be at rest for more than 1 or 2 seconds is recorded as Njs. Several investigators have employed methods which are less subjective

and are based on sampling techniques. This type of method is based on the measurement of the particle concentration just above the base of the vessel and determination of the point at which a maximum or a discontinuity exists in the plot of concentration vs. agitation speed. This behavior can be explained by considering the fact that at low agitator speeds, most of the particles are at rest on the bottom so that the concentration measurements are very low. As the agitation speed is increased, the solids begin to become suspended, so the concentration increases. This continues until the particle supply on the vessel base is exhausted. At this point further increases in agitation speed are used to distribute the particles more uniformly throughout the vessel, thus lowering the local concentration near the bottom.

Work performed by Bourne and Sharma (2) has shown that the minimum agitation speed determined by the sampling method correlated well with the visually determined value. This result was confirmed in work performed by Susanto (15).

2.2.2 Available Models for Solid Suspension

Due to the complexity of the fluid dynamics in the stirred tank, most of the models developed up to this point have had a largely empirical basis. The most famous of these is that of Zwietering. In 1958, Zwietering published an empirical correlation for the minimum agitation speed required to suspend solids. The extensive experimental program covered a wide range of variables including: vessel diameter, impeller type,

impeller diameter, solid particle size, solid density, solid concentration, liquid density, liquid viscosity, and impeller clearance. The resulting empirical expression is:

$$Njs = S\ \nu^{0.1}\ Dp^{0.2}\ (g\Delta\rho/\rho c)^{0.45}\ Xs^{0.13}\ D^{-0.85}$$

More theoretical approaches were taken by both Narayanan (12) and Musil (11). Narayanan based his expression on a balance of the gravity force of a particle with the upward drag force due to the vertical component of the fluid velocity. The weakness of this expression is due to the failure to consider the effect of the drag coefficient and the solid concentration.

Musil's suspension theory is based on the assumption that all energy supplied in the vessel is available to suspend the solid and there is a loss due to viscous dissipation within the descending stream of slurry.

The semitheoretical expression developed by Baldi et. al. (1) will be evaluated in this work. In this expression it is assumed that suspension is caused by turbulent eddies of the same length scale as the particles themselves. Because of its significance, this expression will be examined in greater detail in Chapter 3.

2.3 The Dispersion of Liquids in Liquids

There are a number of industrial processes which rely on the contacting of immiscible liquids in stirred tanks. There are four principal purposes of operations involving the direct

contact of immiscible liquids: separation of components in solution, chemical reaction, cooling or heating by direct contact, and the creation of permanent emulsions (13).

Although several investigators have looked at liquid-liquid systems, most of the resulting correlations are exclusively based on the statistical regression of the experimental data and dimensional analysis.

2.3.1 Degrees of Dispersion

As in the solid-liquid case, there are two main degrees of dispersion of interest. The first, "just completely dispersed" state, represents the point at which there are no large drops or agglomerates of droplets found on the bottom of the vessel or at the liquid surface (depending on whether the dispersed phase is heavier or lighter than the continuous phase, respectively). The second state is that of the homogeneous dispersion, in which the concentration of the dispersed liquid is approximately constant throughout the vessel.

2.3.2 Available Models for Liquid Dispersion

A number of investigators have considered liquid-liquid systems (8, 17, 14, 7, 5), but there is little agreement between them in terms of the resulting correlations. The correlations are based on a purely experimental approach relying heavily on dimensional analysis. The agreement among the various authors is very poor. For example, if the correlation is expressed in the form:

$$Rem = k\ Su^{x}\ Ar^{y},$$

where:

k = proportionality constant

$Rem = \rho c\ Njd\ D^2/\mu c$

$Su = g\ \rho c\ \Delta\rho\ D^3/\mu c^2$

$Ar = \rho c\ \sigma\ D/\mu c^2,$

then, depending on the author, x varies between 0.08 and 0.25 while y varies between 0.32 and 0.39.

This method of forcing experimental data to fit a dimensionless equation has produced potentially unreal interrelations between variables. For example, according to Carpenter (3), the recent results of Godfrey et. al. (8) can be equally well represented by:

$$Njd \propto \sigma^{0.47}\ \rho c^{-0.53}\ \mu c^{0.06}$$

or

$$Njd \propto \sigma^{0.14}\ \Delta\rho^{0.33}\ \rho c^{-0.33}\ \mu c^{0.06}.$$

From Carpenter, "Clearly using these equations to assess the effect on a working extraction vessel of changing the dispersed phase would give very different results". As an additional example, van Heuven and Beek (17) state that:

$$Njd \propto (\rho c + X1\ \Delta\rho)^{-0.47}$$

and

$$Njd \propto \mu c^{0.076},$$

even though they never actually varied μc and ρc in their experiments.

The theoretical approach to be evaluated in this work for three phase systems has been developed and successfully applied in two phase systems by Tsai (16).

Chapter 3

Development of Theoretical Models

3.1 Theoretical Model for Njs

The model used in this work to predict the minimum agitation speed for complete solid suspension, Njs, is the semitheoretical model developed by Baldi et. al. (1).

Baldi began by observing that particles have a tendency to be suspended and then settle for a very short time before becoming resuspended. He then assumed that the suspension of solid particles is caused by turbulent bursts rather than the average velocity field near the vessel base. He then went on to assume that there was a critical size for the eddies responsible for suspension. Eddies smaller than the critical size would not have enough energy to suspend the particles. Eddies which were too large would be less likely to hit the particles because of their lower frequency.

Kuboi (9) observed that the velocity fluctuations of suspended particles are the same as those of eddies in that size range. From this observation, Kuboi assumed that the critical size eddies have a scale of the same order as the particles themselves. So, from an energy balance:

$$\rho c\ (v')^2 \propto \Delta\rho\ Dp\ g$$

v' is the fluctuating velocity of the critical eddies. If we then assume that the critical eddies are within the inertial subrange, the following expression for the velocity can be

used:

$$v' \propto (Dp\epsilon\ b/\rho c)^{1/3}$$

Here, b is the local dissipated power per unit volume near the vessel base.

Next, Baldi assumed that the power dissipated near the base is proportional to the average power dissipated:

$$\epsilon_b \propto \epsilon$$

Then, for a cylindrical vessel with height equal to diameter, the average power dissipated is given by:

$$\epsilon = 4\ Np\ \rho c\ Njs^3\ D^5/(\pi T^3)$$

This expression can then be combined with the energy balance expression and arranged to arrive at an expression for Z, where Z is a dimensionless group consisting of the ratio of the energy dissipated near the vessel base to the average energy dissipated in the vessel:

$$Z = \frac{(g\Delta\rho/\rho c)^{1/2}\ T\ Dp^{1/6}}{Np^{1/3}\ D^{5/3}\ Njs}$$

Since Z is assumed to be constant, this expression can be rearranged to arrive at the final expression for the minimum agitation speed required for suspension.

$$Njs = \frac{(g\Delta\rho/\rho c)^{1/2} T\ Dp^{1/6}}{Np^{1/3}\ D^{5/3}\ Z}$$

3.2 Theoretical Model for Njd

The model for Njd has been previously developed and applied to two phase systems by Tsai (16).

In order to generate a dispersion, the disrupting inertial forces associated with the turbulent microeddies must be of the same order of magnitude as the resisting buoyancy forces acting to reform the droplets. Therefore the inertial forces are proportional to the buoyancy forces at the minimum agitation speed required for dispersion, Njd:

$$\gamma D^2 \propto g \Delta\rho' D^3$$

Next, we assume that once a droplet has been pulled into the dispersion, the forces acting to continue breaking up the droplet are balanced by the interfacial tension forces which are working to keep the droplet together.

$$\gamma D^2 \propto \sigma D$$

These three forces are then proportional to each other:

$$\gamma D^2 \propto g \Delta\rho' D^3 \propto \sigma D$$

Next, we assume that the droplet size is much larger than the Kolmogoroff length scale and much smaller than the primary eddies. This then puts the size of the eddies within the inertial subrange where Kolmogoroff's expression for the inertial force can be applied:

$$\gamma D^2 \propto \rho c \, (\epsilon D)^{2/3} D^2$$

The average power dissipated in the vessel is then given by this expression:

$$\epsilon = (4/\pi) \; Np \; Njd^3 \; D^2 \; (D/T)^3$$

These expressions can then be substituted back into the force balance and rearranged to provide a final expression for Njd:

$$Njd = A(g\,\Delta\rho')^{5/12}\sigma^{1/12}\rho_c^{-0.5}\,D^{-2/3}\,(T/D)^{0.67}\,(H/D)^{0.33} * Np^{-1/3}$$

This expression can also be arranged in the following dimensionless form:

$$Rem = A\,Su^{1/12}\,Ar^{5/12}\,(T/D)^{0.67}\,(H/D)^{0.33}\,Np^{-1/3}$$

We will now incorporate the semitheoretical expression for the concentration effect developed by Delichatsios and Probstein (6). This expression is based on a balance of the frequency of coalescence with the frequency of droplet break-up.

$$f(Xl) = ((-\ln(0.011 + 0.68\,Xl))/4.5)^{-0.5}$$

This then results in the following expression for Njd and Rem:

$$Njd = A((-\ln(0.011 + 0.68\,Xl))/4.5)^{-0.5}\,(g\,\Delta\rho')^{5/12}\,\sigma^{1/12}\,\rho c^{-0.5}\,D^{-2.3}\,(T/D)^{0.67}\,(H/D)^{0.33}\,Np^{-1/3}$$

and

$$Rem = A((-\ln(0.011 + 0.68\,Xl))/4.5)^{-0.5}\,Su^{1/12}\,Ar^{5/12}\,(T/D)^{0.67}\,(H/D)^{0.33}\,Np^{-1/3}$$

Chapter 4
Description of Apparatus and Materials

The vessels employed in this work were cylindrical with flat bottoms. Four baffles were mounted along the vessel periphery, each spaced by 90 degrees. The baffle width was equal to one tenth of the vessel diameter. The baffles extended from the top to the bottom of the vessel. Vessel diameters ranged from 7.625" to 23.5". Table 13 contains the vessel dimensions as well as the materials of construction.

The majority of the experiments were conducted using a 0.25 horsepower variable speed motor (G.K. Heller, Corp.) which had a maximum speed of 1500 Rpm. The speed and power measurements were taken with a digital multimeter apparatus which gave the speed of rotation in Rpm and the power reading in watts. The experiments in the 23.5" vessel were conducted using a 2 horsepower variable speed motor (G.K. Heller, Corp.) which also featured a digital multimeter apparatus.

A variety of impellers were used in this work. The disk turbine and the flat blade turbine, with diameters ranging from 2.5" to 8", were investigated as examples of radial flow. Axial flow was examined using the Lightnin A310 (Mixing Equipment Co.) fluid foil impeller with a diameter range from 3.8" to 4.5". The pitched blade turbine, which exhibits mixed flow, was examined in the range from D = 2.5" to D = 8". Table 14 contains impeller dimensional information.

Distilled water was used as the continuous phase in all experiments except those with T = 23.5". Normal tap water was used in this case. White mineral oil (Ruger Chemical

Company), methylisobutyl ketone, and hexane were used as dispersed phases in this work. The density range was from 673 to 828 kg/m^3. The interfacial tension ranged from 9.2 to 46.6 dynes/cm. The physical properties of the fluids are listed in table 11.

The solid phase used in these experiments was glass beads. The beads were spherically shaped and had diameters ranging from 60 to 200 microns. The density of the beads was 2500 kg/m^3. Table 12 contains physical property information for the glass beads. The beads were sieved before use to obtain a tight size distribution.

The interfacial tension for the dispersed liquids was measured using a Cenco-DuNuoy Interfacial Tensiometer. The densities were measured using a pycnometer and an electronic balance. Distilled water was used to calibrate the pycnometer.

Chapter 5
Experimental Procedure

The vessel was charged with the liquids (an organic phase and an aqueous phase) and solid particles and the agitator of choice was placed at the preselected clearance off the tank bottom. The vessel was leveled before the beginning of each run. The agitation level was then slowly increased, by approximately 10% of the previous value, until the point of complete suspension/dispersion for each phase was achieved. Approximately 15 to 20 minutes were required for stabilization at each mixing speed. Visual observation was used to identify the point of complete suspension. For the solid phase, the procedure described by Zweitering was employed (18). This method is based on the observation that, at the point just below complete suspension, particles settle temporarily at the bottom and for a short time (1-2 seconds) are in a fixed position relative to each other. Careful attention was also paid to the point within the vessel where the particles became suspended. This often provided information about the flow pattern near the vessel bottom. A conceptually similar procedure was employed for the liquid phase. Here, the focus was on the disappearance of the liquid-liquid interface. As the dispersion point was approached, it became necessary to closely observe the liquid surface since the dispersed phase layer became extremely thin. Small patches of undispersed liquid could still be detected. It is the disappearance of these patches which constitutes the point of complete suspension.

For each run, the minimum agitation speed required for suspension of the solid, Njs, and for dispersion of the liquid phase, Njd, was recorded. A power measurement was also taken at each of the points where either the solids or the organic liquid phase was completely dispersed. In some cases, it was not possible to achieve complete suspension. In these cases, the experiment was stopped at the point of excessive aeration for failure to suspend the solid phase or at the maximum motor speed achievable for failure to disperse the liquid phase.

Chapter 6
Results and Discussion

6.1 IMPELLER CLEARANCE EFFECTS

6.1.1 Effect of Impeller Clearance off the Tank Bottom on Njs

The effect of impeller clearance off the tank bottom on Njs was examined in the 11.5" vessel using both the disk turbine and the A310 impeller. This clearance, C, was varied from 1" to 4.5" for the disk turbine and from 1" to 8.5" for the A310 impeller. At C = 4.5" (C/T = 0.391), the point of air entrainment was reached before suspension of the solid phase, using the disk turbine. This occurred at C = 8.5" (C/T = 0.739) for the A310 impeller.

The data for the disk turbine are plotted in Figure 1. As the value of C/T is increased, a change in the flow pattern below the impeller occurred. At low clearances (C/T < 0.174), suspension occurred from the periphery of the vessel. At C/T = 0.174 suspension was occurring from both the center and the periphery of the vessel. Beyond this point (C/T > 0.217), suspension occurred exclusively from the center of the vessel. This behavior was previously reported by Susanto (15). A similar pattern was detected for the case of the power number, Np, although not nearly as pronounced as the effect on Njs. Figure 2 shows a plot of the power number, Np, versus the C/T ratio.

This behavior is related to the establishment of a vortex in the region below the impeller. At low clearances, the

impeller is primarily fed from above and the radial discharge causes the solid suspension to occur at the vessel periphery. At higher clearances (C/T > 0.2), the characteristic "figure eight" flow pattern is fully developed and suspension occurs at the center of the vessel. Between these two regions, there is a region of instability in which the suspension occurs at both the vessel center and the periphery.

Figure 3 shows the results achieved with the A310 impeller. The value of Njs increases only gradually as the clearance is increased, up to C/T = 0.6. For values of C/T higher than this, Njs increases rapidly with C/T. The A310 impeller is designed to both draw and discharge flow uniformly in a cylindrical pattern. In a stirred tank, the point is eventually reached where the impeller discharge reverses direction and forms an upwardly moving hollow cylinder, outside but concentric to the discharge cylinder. This upwardly moving hollow cylinder then moves to the top of the vessel where it again reverses direction and becomes the input cylinder which will then be drawn into the impeller. This is likely to have contributed to the sharp increase in Njs exhibited beyond C/T = 0.6. The power number is plotted against C/T in Figure 4. Here, Np increases gradually throughout the investigated range. The relatively large scatter in this data is due to the measurement of the power in the low range (< 1 watt).

6.1.2 Effect of Impeller Clearance off the Liquid Surface on Njd

The effect of impeller clearance off the liquid surface, C', on Njd was also investigated with both the disk turbine and the A310 impeller (Note that C' + C = H = T). The range of C' was 2" to 10.5" for the disk turbine and 3" to 10.5" for the A310 impeller. At C' < 7" (C'/T < 0.609), using the disk turbine, air became entrained before solid suspension could occur. With the A310 impeller, entrainment occurred before dispersion of the liquid phase at C' < 3" (C'/T < 0.261).

In Figure 5, the results obtained with the disk turbine are plotted. The value of Njd was observed to increase rapidly with C'/T up to approximately C'/T = 0.7, and only gradually beyond this point. In the plot of power number, Np, versus C'/T (Figure 6), a sharp increase is noted in the curve between C'/T of 0.09 and 0.35. It is suspected that this behavior is related to the behavior observed near the bottom of the vessel in the case of the effect of clearance on Njs. At C' values less than 2" (C'/T < 0.174), it is impossible to achieve dispersion without significant aeration. This corresponds to the region of periphery suspension in the solid case.

At higher values of C', dispersion is achieved, but often with significant distortion of the liquid surface. This distorted condition of the liquid surface leads to areas which are highly dynamic in flow to those which are more static. The net result is a higher speed required for dispersion. At C'/T > 0.7 the upper vortex can be formed without deforming the liquid surface. This then results in a more gradual increase

in Njd since the upper vortex can be formed without lifting the fluid significantly.

The effect of impeller clearance, C', on Np is shown in Figure 7. The behavior observed in this figure can be partially attributed to the fact that the resistance to formation of an upper vortex is less than the resistance to formation of a lower vortex. The lower vortex has the vessel base as a stationary boundary. The upper vortex is bounded by the liquid-air interface. Since this boundary is able to become distorted, the upper vortex is more easily formed.

The results obtained with the A310 impeller are plotted in Figure 8. Here, there is very little change in the value of Njd for C'/T < 0.7. Past this point the value of Njd increases slightly with the C'/T ratio. This is similar to the behavior noted in the Njs case. Once the impeller is at a sufficient distance from the interface of interest, the flow intensity lessens significantly due to the reversal of the hollow cylinder as discussed in section 6.1.1. The result is a higher value of Njd in this case. Figure X17 shows the power number plotted against C'/T for the A310 impeller. The power number remains essentially constant throughout the range investigated with the scatter in the data again being caused by the low power measurements.

6.2 IMPELLER DIAMETER EFFECTS

6.2.1 Effect of Impeller Diameter on Njs

In this work, the effect of impeller diameter was examined by keeping the value of C/D constant as the impeller size was varied. This procedure was previously employed by both Baldi et. al. (1) and Susanto (15). This procedure is in contrast to that employed by both Zwietering and Chapman (4) where the impeller clearance was held constant as the impeller diameter was varied.

Baldi found that for an eight bladed disk turbine,

$$Njs \propto D^{-1.67} \quad \text{at } C/D = 0.5$$

and

$$Njs \propto D^{-1.89} \quad \text{at } C/D = 1.0.$$

Baldi proposed that the exponent on D was a function of the C/D ratio. In Susanto's work, it was found that:

$$Njs \quad D^{-1.68} \quad \text{for all impeller types } (C/D = 0.25).$$

Susanto also found the exponent on D to be dependent on the value of C/D.

Figure 9 shows the results obtained in this work for a six bladed disk turbine. Here it was found that:

$$Njs \propto D^{-1.695} \quad \text{at } C/D = 0.5$$

and

$$Njs \propto D^{-1.918} \quad \text{at } C/D = 1.0$$

The correlation coefficients for these relationships were -0.9994 and 0.9998 for C/D values of 0.5 and 1.0 respectively. This result is in close agreement with that of Baldi. A

similar dependence of the exponent on the C/D ratio was noted. The results for the pitched blade turbine (pumping down), shown in Figure 10, indicate that:

$$Njs \propto D^{-1.744} \quad \text{at } C/D = 0.5$$

and

$$Njs \propto D^{-1.608} \quad \text{at } C/D = 1.0$$

Here, the correlation coefficients were 0.9946 and 0.9984 for C/D values of 0.5 and 1.0 respectively. These results are in reasonable agreement with the theoretical value of -1.67. The dependence of the exponent on the value of C/D, observed with the disk turbine, was not observed in the experiments with the pitched blade turbine. This can be partially attributed to the change in the flow pattern observed near the vessel base when using a disk turbine. At a C/D value of 0.5, all suspension occurred from the periphery of the vessel with the exception of the 4" impeller which seemed to be entering the range of instability discussed in Section 6.1. This impeller exhibited suspension at both the vessel center and the periphery. The C/T ratio for this case was 0.174. At C/D equal to 1.0, a full vortex was formed in the region below the impeller and the suspension occurred exclusively from the vessel center. For the pitched blade turbine, suspension occurred from the vessel periphery at both values of C/D.

6.2.2 Effect of Impeller Diameter on Njd

As in the case of solid suspension, the effect of impeller diameter on Njd was examined at a constant value of C'/D.

Figure 11 shows the results for the disk turbine at a C'/D value of 1.0. The following relationship was found:

$$Njd \propto D^{-1.724}$$

This value shows reasonable agreement with the theoretical value of -1.67 and the value of -1.63 previously reported by Tsai (16) for two phase systems. The correlation coefficient was -0.9902.

Figure 12 shows the data for the pitched blade turbine at C'/D = 1.0. The relationship, which exhibited a correlation coefficient of 0.9974, was found to be:

$$Njd \propto D^{-1.812}.$$

This again shows reasonable agreement with the value of -1.75 reported by Tsai and the theoretical value of -1.67. In each of the experiments at a C'/D value = 1.0, it was not possible to suspend the solid phase before the point of air entrainment. This was true for both the disk turbine and the pitched blade turbine (pumping down).

6.3 EFFECT OF PARTICLE SIZE ON Njs

The effect of particle size was examined in the 11" tank by varying Dp over a range from 60 to 200 microns. The concentration of the solid, Xs, was held constant at 0.5% (by weight). Readings were taken at C/D values of 0.5 and 1.0 for both the disk turbine and the A310 impeller.

Figures 13 and 14 show the results for the disk turbine.

Figure 13 contains the results at C/D = 0.5 and Figure 14 contains results for C/D = 1.0. The values of Njd are also found in these plots. The following relationships were found:

$$Njs \propto Dp^{0.1322} \quad \text{at } C/D = 0.5$$

and

$$Njs \propto Dp^{0.1716} \quad \text{at } C/D = 1.0.$$

The correlation coefficient for the linear regression at C/D = 0.5 was 0.9624 while at C/D = 1.0, the value was 0.9977. The value of the exponent at C/D = 1.0 is in very good agreement with the theoretically predicted value of 0.167. The poorer agreement with theory found at C/D = 0.5 can be partially attributed to the fact that this value of impeller clearance is in the range of instability for a disk turbine. In each case, the suspension occurred at both the vessel center and the periphery while at C/D = 1.0, the suspension was exclusively from the vessel center. The slightly poorer fit at C/D = 0.5 may also be caused by the unstable flow pattern observed.

At C/D = 0.5, the average value for Njd was 452 Rpm and the standard deviation was 7.7. The corresponding values at C/D = 1.0 were 379.5 for the mean and 1.9 for the standard deviation. These results indicate that dispersion of the liquid was not influenced by the change in particle size.

The results achieved with the A310 impeller are plotted in Figures 15 (C/D = 0.5) and 16 (C/D = 1.0). In these experiments it was found that:

$$Njs \propto Dp^{0.1653} \quad \text{at } C/D = 0.5$$

and

$$Njs \propto Dp^{0.1875} \quad \text{at } C/D = 1.0.$$

Correlation coefficients of 0.9486 and 1.0 were found for C/D values of 0.5 and 1.0 respectively. For the case of C/D = 0.5, the exponent of 0.1653 agrees very well with the theoretical value of 0.167. Reasonable agreement was also observed at C/D = 1.0. The average value of Njd was 854 with a standard deviation of 25.5 at C/D = 0.5, while at C/D = 1.0 an average of 818 with standard deviation = 11.0 was observed. These results confirm the observations noted with the disk turbine. The dispersion of the liquid phase is not affected by variation of the particle size of the solid.

6.4 EFFECT OF DISPERSED PHASE PROPERTIES ON Njd

The effect of dispersed phase properties was investigated by changing the organic fluid used for this phase. The value of C'/D was 1.0 and both the disk turbine and the pitched blade turbine (pumping down) were investigated. The following fluids were used: mineral oil, methylisobutyl ketone, and hexane. Since it is difficult to change the interfacial tension or the density difference without changing the other, the following quantity is plotted directly: $\sigma^{1/12} \Delta\rho^{5/12}$. This represents the theoretically predicted dependencies from Tsai(16). Figure 17 shows the results obtained. The theoretical value for the exponent was 1.0, since the anticipated dependence was plotted directly. A value of 1.0367 was obtained for the disk turbine and a value of 1.0392 was obtained

for the pitched blade turbine. These results are in very good agreement with the theoretically predicted value of 1.0. Tsai (16) also investigated this dependence and found an exponent of 0.92.

Figures 18 and 19 show the values of Njd and Nje plotted for the disk turbine and the pitched blade turbine respectively. Nje represents the minimum speed required for aeration (See Section 6.7). The average values of Nje in these runs were 469 for the disk turbine and 594 for the pitched turbine. The standard deviations were 14.7 and 12.5 for the disk turbine and the pitched blade turbine respectively. This demonstrates that changing the dispersed liquid, in the region of densities and viscosities used here, did not have a significant effect on the dispersion of an additional phase (air).

6.5 DISPERSED PHASE CONCENTRATION EFFECTS

6.5.1 Effect of Solid Concentration on Njs

The effect of solid concentration was examined in the range from 0.5% to 4.0% using both the disk turbine and the A310 impeller. The results for the disk turbine are plotted in Figure 20 and the results for the A310 impeller are found in Figure 21. The value of C/D was constant at 0.744 in these experiments. The following relationships were observed:

$$Njs \propto Xs^{0.1236} \quad \text{for the disk turbine}$$

and

$$Njs \propto Xs^{0.2219} \quad \text{for the A310 impeller.}$$

The correlation coefficient for the disk turbine was 0.9992 and for the A310 impeller the value was 0.9766. The value of the exponent for the disk turbine is in very good agreement with the value of 0.125 observed by Baldi (1) and the value of 0.124 observed by Susanto (15). Close agreement was also found with the results obtained by Zwietering (18) and Chapman et. al. (4), who observed values of 0.13 and 0.12 respectively. The value of the exponent observed with the A310 impeller is significantly higher than previously obtained results. It is, however, in reasonable agreement with the result obtained by Chapman et. al. for a downward pumping pitched blade turbine. A result of 0.21 was obtained. The value of C/D was 1.0 in this case, however. This result indicates that a higher value of the exponent is appropriate for mixed or axial flow impellers.

As in previous experiments, the dispersion of the liquid was unaffected by the varying solid concentration. The average value of Njd for the disk turbine was 400 Rpm with a standard deviation of 2.5. The corresponding values for the A310 impeller were 840 for the mean and 6.5 for the standard deviation.

6.5.2 Effect of Liquid Concentration on Njd

The liquid concentration was varied from 5% to 20% in the 11 inch vessel. The C'/D ratio was held constant at 1.0 and

both the disk turbine and the A310 impeller was examined. The values of both Njd and Nje are plotted in Figure 22 for the disk turbine. Figure 23 contains values of Njd and Njs obtained with the A310 impeller. The following relationships were found:

$$Njd \propto Xl^{0.1460} \quad \text{for the disk turbine}$$

and

$$Njd \propto Xl^{0.1600} \quad \text{for the A310 impeller.}$$

The correlation coefficients were 0.9808 for the disk turbine and 0.9853 for the A310 impeller. These results lie roughly between the values found in the case of solid concentration.

These results were also analyzed by using the expression developed by Delichatsios and Probstein (6). This expression is based on a balance of the frequency of coalescence and the frequency droplet breakup. The semitheoretical expression takes the following form:

$$f(Xl) = \{-1/4.5*\ln(0.011 + 0.68*Xl)\}^{-3.5}.$$

In Figure 24, the values of Njd are plotted versus f(Xl). The following results were obtained:

$$Njd \propto (f(Xl))^{0.716} \quad \text{for the disk turbine}$$

and

$$Njd \propto (f(Xl))^{0.758} \quad \text{for the A310 impeller.}$$

These values are significantly lower than the theoretical value of 1.0. Correlation coefficients of 0.9935 and 0.9639 were obtained for the disk turbine and the A310 impeller respectively.

In each run involving the disk turbine, the point of aeration, Nje, was reached before Njs. The average value for Nje was 364 Rpm with a standard deviation of 4.3. This shows that the entrainment of air occurred reproducibly in these runs and that this point is not a function of Xl. This point offers additional support to the possibility of theoretically predicting Nje, taken up in section 6.7. The A310 impeller was able to achieve solid suspension from C'/D = 1.0. The average value of Njs was 862 with standard deviation = 16.9. This again confirms previous results by showing no dependence of Njs on the value of Xl in this range (5% - 20%).

6.6 SCALE-UP EFFECTS

The effect of scale-up was investigated using four vessels. The T values were 7.625", 9.5", 11.5", and 23.5". Measurements of both Njs and Njd were taken at C/D = 0.5 and 1.0 and at C'/T = 1.0. Results for the disk turbine, flat blade turbine, and pitched blade turbine (pumping down) are reported. The ratio of T/D was approximately 3.0 in each case.

6.6.1 Effect of Scale-up on Njs

The results obtained at C/D = 0.5 are plotted in Figure 25. The following relationships were obtained:

Njs T^-0.8255 for the disk turbine,

$$Njs \propto T^{-0.9133} \quad \text{for the pitched blade turbine,}$$

and

$$Njs \propto T^{-0.7996} \quad \text{for the flat blade turbine.}$$

The correlation coefficients were -0.9968, -0.9968, and -0.9969 for the disk turbine, pitched turbine, and flat turbine respectively. These values are all in reasonable agreement with the theoretically predicted value of -0.67. The results for C/D = 1.0 are plotted in Figure 26. The following expressions resulted:

$$Njs \propto T^{-0.8224} \quad \text{for the disk turbine,}$$

$$Njs \propto T^{-0.6810} \quad \text{for the pitched turbine,}$$

and

$$Njs \propto T^{-0.7283} \quad \text{for the flat turbine.}$$

Here, the linear correlation coefficients were -0.9937, -0.9850, and -1.0000 for the disk turbine, pitched turbine, and flat turbine respectively. Again, reasonable agreement with theory was observed.

The experimentally obtained values for the exponents are consistently slightly higher than the value predicted by theory. This can be partially attributed to the fact that although the ratio of T/D was assumed to be constant at 3.0. The actual values for this ratio were 3.05, 3.167, 2.875, and 2.938 for vessel diameters of 7.625", 9.5", 11.5", and 23.5" respectively. In the two smaller vessels, the impellers were slightly small, while in the two larger vessels, the impellers were slightly large. This would result in lower values of Njs in the larger vessels and higher values in the smaller ves-

sels. The net result would be a higher slope. In an effort to correct for this variation in T/D, the values of Njs were multiplied by the actual T/D ratio and divided by 3.0.

After applying this correction, the dependencies were recalculated. Figure 27 contains a plot of the corrected values. The following results were obtained at C/D = 0.5.:

$Njs \propto T^{-0.7303}$ for the disk turbine,

$Njs \propto T^{-0.8189}$ for the pitched blade turbine,

and

$Njs \propto T^{-0.7028}$ for the flat blade turbine.

The resulting correlation coefficients for these corrected relationships were -0.9958, -0.9861, and -0.9961 for the disk turbine, the pitched blade turbine, and the flat blade turbine respectively. The correction has improved the agreement with the theoretical value of -0.67. Similarly, the correction was applied at C/D = 1.0 and the data was replotted in Figure 28. The following relationships were obtained:

$Njs \propto T^{-0.7290}$ for the disk turbine,

$Njs \propto T^{-0.5872}$ for the pitched blade turbine,

and

$Njs \propto T^{-0.6324}$ for the flat blade turbine.

Correlation coefficients of -0.9931, -0.9310, and -0.9826 were obtained for the disk turbine, the pitched blade turbine, and the flat blade turbine respectively. With the exception of the pitched blade turbine results, the correction improved the agreement with theory.

6.6.2 Effect of Scale-up on Njd

The effect of Scale-up on Njd was investigated at C'/D values of 1.0 and 1.875 (C'/D = 1.875 corresponds to a C/D = 1.0). The results for C'/D = 1.0 are found in Figure 29. The following relationships were found:

$$Njd \propto T^{-0.7307} \quad \text{for the disk turbine,}$$

$$Njd \propto T^{-0.7927} \quad \text{for the pitched blade turbine,}$$

and

$$Njd \propto T^{-0.7998} \quad \text{for the flat blade turbine.}$$

These values are all slightly higher, but in reasonable agreement with the theoretical value of -0.67. The correlation coefficients were -0.9983, -0.9988, and -0.9964 for the disk turbine, pitched blade turbine, and flat blade turbine respectively. In Figure 30, the results obtained at C'/D = 1.875 are plotted. Here, the dependencies were:

$$Njd \propto T^{-0.7980} \quad \text{for the disk turbine,}$$

$$Njd \propto T^{-0.8556} \quad \text{for the pitched blade turbine,}$$

and

$$Njd \propto T^{-0.7686} \quad \text{for the flat blade turbine.}$$

Again, reasonable agreement was obtained. The correlation coefficients were -0.9995, -0.9979, and -0.9999 for the disk turbine, pitched blade turbine, and flat blade turbine respectively.

As discussed in Section 6.6.1, the variation of T/D in these experiments contributed to the consistently higher slopes. The theoretical correction for T/D was again applied. The corrected data for C'/D = 1.0 is plotted in Figure 31.

The dependencies were:

$$Njd \propto T^{-0.6388} \quad \text{for the disk turbine,}$$

$$Njd \propto T^{-0.7003} \quad \text{for the pitched blade turbine,}$$

and

$$Njd \propto T^{-0.7042} \quad \text{for the flat blade turbine.}$$

The correlation coefficients were -0.9879, -0.9749, and -0.9654 for the disk turbine, the pitched blade turbine, and the flat blade turbine respectively. The agreement with theory has again been improved (as in the Njs case).

The corrected values of Njd at C'/D = 1.875 are plotted in Figure 32. The following relationships were found:

$$Njd \propto T^{-0.7028} \quad \text{for the disk turbine,}$$

$$Njd \propto T^{-0.7612} \quad \text{for the pitched blade turbine,}$$

and

$$Njd \propto T^{-0.6753} \quad \text{for the flat blade turbine.}$$

The correlation coefficients for these relationships were -0.9860, -0.9832, and -0.9862 for the disk turbine, the pitched blade turbine, and the flat blade turbine respectively. Again, improved agreement with theory was noted as a result of the correction.

For comparison purposes, the Njd results obtained at C'/D = 1.875 are plotted along with the values of Njs. This corresponds to a C/D value of 1.0. Figures 33, 34, and 35 contain data for the disk turbine, the pitched blade turbine, and the flat blade turbine respectively. All values contained in these three plots have been corrected for variation in T/D.

6.7 MINIMUM SPEED REQUIRED FOR AERATION, Nje

As part of this work, the point of air entrainment was investigated with respect to several parameters. This was primarily investigated since in several case the minimum speed for aeration, Nje, was reached before Njs. It is suspected that the dependence of Nje on the various mixing parameters will be similar to that of Njs and Njd. This is based on the fact that Nje merely represents the dispersion of an additional fluid phase (air).

6.7.1 Effect of Impeller Diameter on Nje

The value of Nje is plotted against the impeller diameter, D, in Figure 36. A correlation coefficient of -0.9999 was obtained for the disk turbine and a value of -0.9857 was obtained for the pitched blade turbine. The following relationships were found:

$$Nje \propto D^{-1.7827} \quad \text{for the disk turbine}$$

and

$$Nje \propto D^{-1.7434} \quad \text{for the pitched blade turbine.}$$

These results are in very good agreement with the theoretically predicted value of -1.67

6.7.2 Effect of Scale-up on Nje

The effect of vessel diameter on Nje was investigated at

C'/D = 1.0. The results are found in Figure 37. The resulting dependencies were as follows:

$$Nje \propto T^{-0.7307} \quad \text{for the disk turbine,}$$

$$Nje \propto T^{-0.7927} \quad \text{for the pitched blade turbine,}$$

and

$$Nje \propto T^{-0.7536} \quad \text{for the flat blade turbine.}$$

Correlation coefficients of -0.9949, -0.9893, and -0.9310 were observed for the disk turbine, pitched blade turbine, and flat blade turbine respectively. Although the data for the flat blade turbine is more scattered than in the other cases, there is clearly good agreement with the theoretically predicted value of -0.67. The previously applied correction (Section 6.6) was again applied in this case in an effort to improve the agreement with theory. The results, plotted in Figure 38, exhibited the following dependencies:

$$Nje \propto T^{-0.6974} \quad \text{for the disk turbine,}$$

$$Nje \propto T^{-0.6909} \quad \text{or the pitched blade turbine,}$$

and

$$Nje \propto T^{-0.6603} \quad \text{for the flat blade turbine.}$$

The correlation coefficients were -0.9929, -0.9640, and -0.8503 for the disk turbine, the pitched blade turbine, and the flat blade turbine respectively. Again, improved agreement with theory resulted from the correction.

The values of Nje obtained at C'/D = 1.0 are plotted with the corresponding values of Njd in Figures 39, 40, and 41. Figure 39 covers the disk turbine, Figure 40 contains data for the pitched blade turbine, and Figure 41 contains flat blade turbine data. Corrected values are plotted in each case.

Chapter 7
Presentation of the Final Equation

7.1 Final Equation for Solid-Liquid Systems

The final expression for Njs is plotted in Figures 42, 43, and 44. Figure 42 contains the data for the disk turbine. The values of Njs at C/D = 0.5 are plotted separately from the values at C/D = 1.0. The differences in the proportionality constant, Z, are due to the change in flow pattern observed between these two values of C/D (See Section 6.1.1). The value of Z at C/D = 0.5 was 0.9734 and the correlation coefficient was 0.9895. At C/D = 1.0, the value of Z was 1.0697 and the correlation coefficient was 0.9876. The fit is very good in both cases.

Figure 43 contains the data for the A310 impeller. The values of Njs are plotted for C/D ranging from 0.5 to 1.6. The value of Z obtained here was 0.6737 and the correlation coefficient was 0.9452. Again, the fit is very good.

The data for the pitched blade turbine are plotted in Figure 44. The value of Z was found to be 0.9704 and the correlation coefficient was 0.9139. The plot represents both data at C/D = 0.5 and C/D = 1.0. The fit for the pitched blade turbine is slightly poorer than the disk turbine and the A310 impeller.

7.2 Final Equation for Liquid-Liquid Systems

The final equation for Njd is plotted in Figures 45, 46,

and 47. Figure 45 contains the data for the disk turbine. As in Section 7.1, the data for the disk turbine is split due to the change in flow pattern. Here, the data at C'/D = 1.0 is plotted separately from the data for C'/D between 1.8 and 2.4. At C'/D = 1.0, the value of the proportionality constant, A, was 0.8425 and the correlation coefficient was 0.9124. For 1.8 < C'/D < 2.4, the value of A was 1.1946 and the correlation coefficient was 0.9750.

The data for the A310 impeller are plotted in Figure 46. The data shown correspond to C'/D between 0.5 and 1.9. The value of A obtained for the A310 impeller was 0.7773 and the correlation coefficient was 0.8513.

Figure 47 contains the pitched blade turbine results for C'/D between 0.5 and 1.9. A value of 1.0380 was obtained for A and a value of 0.8810 was obtained for the correlation coefficient.

Chapter 8
Conclusions

From this study it has been shown that, for systems involving moderate concentrations of solid and dispersed liquid, semitheoretical models can predict agitation parameter dependencies successfully. This was demonstrated by correctly predicting the effect of impeller diameter, particle size, dispersed phase properties, solid and liquid concentration, and vessel diameter. It was shown that, within the ranges investigated here, each phase can be considered independently.

A change in the flow pattern was observed as the impeller clearance was increased with the disk turbine. This behavior was previously observed in two phase systems. A change in flow pattern was also observed with the A310 impeller at high values of impeller clearance.

Theoretical dependence can be applied to overcome geometric inconsistencies for scale-up. This was demonstrated in the case of variation in T/D (Section 6.6).

The dependence of Nje on several mixing variables was shown to be similar to that observed for Njs and Njd.

Chapter 9
Nomenclature

A	constant of proportionality
Ar	Archimedes number = $g \rho c \Delta \rho' D^3/\mu c^2$
C	impeller clearance measured from the base of the vessel
C'	impeller clearance measured from the liquid surface
D	impeller diameter
Dp	solid particle diameter
g	acceleration due to gravity
H	liquid height
N	impeller speed
Njd	minimum speed required to "just disperse" the liquid phase
Nje	minimum speed required to "just entrain" air at the liquid surface
Njs	minimum speed required to "just suspend" the solid phase
Np	power number = $P/(\rho c\ N^3\ D^5)$
P	power input
Rem	impeller Reynold's number = $\rho c\ N\ D^2/\mu c$
S	proportionality constant
Su	Suratman number = $\rho c \Delta \rho' D/\mu c^2$
T	vessel diameter
v'	fluctuating velocity of the critical eddies
Xl	dispersed liquid volume fraction
Xs	solid mass fraction
ϵ	average power dissipation per unit mass
ϵb	power dissipation per unit mass near the vessel base

μ_c	continuous phase viscosity
μ_d	dispersed phase viscosity
η	Kolmogoroff's length scale
ρ_c	continuous phase density
ρ_d	dispersed liquid density
ρ_s	solid phase density
$\Delta\rho$	$(\rho_s - \rho_c)$
$\Delta\rho'$	$(\rho_c - \rho_d)$
σ	interfacial tension
τ	shear stress
ν	kinematic viscosity of the continuous phase

Chapter 10
Appendix

Experimental Data

Table 1

Effect of Impeller Clearance on Njs and Njd

Solid: Glass beads (150 microns); concentration = 0.5% (weight)

Dispersed Liquid: White mineral oil; concentration = 5% (volume)

Continuous Liquid: Distilled Water

T = 11.5"; D(disk turbine) = 4"; D(A310) = 3.8"

impeller type	C/T ratio	Njs	Power	C'/T ratio	Njd	Power
DT	0.087	231	2	0.913	407	16.5
	0.13	246	3	0.87	396	16
	0.174	256	3.5	0.826	402	17
	0.217	318	7.5	0.783	404	16.5
	0.261	337	10	0.739	400	16
	0.304	353	11	0.696	392	15.5
	0.348	368	13	0.652	380	14
	0.391	entrainment @ 393		0.609	363	12
	0.652	entrainment @ 390		0.348	273	5
	0.826	entrainment @ 331		0.174	199	1
A310	0.087	364	0.25	0.913	918	11
	0.13	389	0.5	0.87	863	9
	0.165	401	0.5	0.835	847	8.5
	0.217	420	0.5	0.783	835	8
	0.243	432	0.5	0.757	832	8
	0.296	444	0.75	0.704	829	8
	0.33	454	1	0.67	805	7
	0.391	467	1	0.609	803	7
	0.435	476	1	0.565	802	6
	0.478	489	1	0.522	803	6
	0.522	502	1	0.478	801	6
	0.565	511	1.5	0.435	812	7
	0.609	528	2	0.391	809	7
	0.67	541	2	0.33	809	7
	0.696	571	2	0.304	803	7
	0.739	608	3	0.261	entrainment @ 752	

Table 2

The Effect of Impeller Diameter

Solid: Glass beads (150 microns); concentration = 0.5% (weight)

Dispersed Liquid: White mineral oil; concentration = 5% (volume)

Continuous Liquid: Distilled Water

T = 11.5"; D(disk turbine) = 2.5-4"; D(A310) = 3.8-4.5"

Effect of Impeller Diameter on Njs

impeller type	C/D ratio	Njs	Power	Njd	Power	Impeller Diameter
DT	0.5	552	3	1190	32	2.5
	0.5	395	3	808	27	3
	0.5	248	3	456	20	4
	1.0	887	16	1156	36	2.5
	1.0	637	16	689	21	3
	1.0	368	13	380	14	4
PT	0.5	610	1	1678	30	2.5
	0.5	407	1	850	12	3
	0.5	262	1	511	10	4
	1.0	773	3	1635	25	2.5
	1.0	554	3	916	14	3
	1.0	361	3	584	14	4

Effect of Impeller Diameter on Njd

impeller type	C′/D ratio	Njs	Power	Njd	Power	Impeller Diameter
DT	1.0	entrainment	@ 900	623	5	2.5
	1.0	entrainment	@ 658	409	4	3
	1.0	entrainment	@ 390	273	5	4
PT	1.0	entrainment	@ 1190	1120	7	2.5
	1.0	entrainment	@ 807	760	7	3
	1.0	entrainment	@ 515	474	7	4

Table 3

Effect of Particle Size on Njs

Solid: Glass beads (size in microns); concentration = 0.5% (weight)

Dispersed Liquid: White mineral oil; concentration = 5% (volume)

Continuous Liquid: Distilled Water

T = 11.5"; D(disk turbine) = 4"; D(A310) = 3.8"

impeller type	C/D ratio	Njs	Power	Njd	Power	Particle Size
DT	0.5	227	2.5	460	20	60
	0.5	234	3	448	20	75
	0.5	248	3	456	20	150
	0.5	271	4	443	20	200
	1.0	309	7	378	14	60
	1.0	325	9	382	15	75
	1.0	361	3	380	14	150
	1.0	383	15	378	14	200
A310	0.5	352	0.5	871	9	60
	0.5	382	1	821	7	75
	0.5	401	0.5	847	8.5	150
	0.5	446	1	877	9	200
	1.0	382	1	821	7	60
	1.0	399	1	814	17	75
	1.0	454	1	805	7	150
	1.0	479	1	831	8	200

Table 4

Effect of Liquid Properties on Njd

Solid: Glass beads (150 microns); concentration = 0.5% (weight)

Dispersed Liquid: concentration = 5.0% (volume)

Continuous Liquid: Distilled Water

T = 9.5"; D(disk turbine) = 3"; D(pitched turbine) = 3"

impeller type	C'/D ratio	Njs	Power	Njd	Power	Dispersed Liquid
DT	1.0	entrainment @	456	306	1.5	MIBK
	1.0	entrainment @	485	325	2	Oil
	1.0	entrainment @	466	357	2	Hexane
PT	1.0	entrainment @	600	504	2	MIBK
	1.0	entrainment @	580	530	2	Oil
	1.0	entrainment @	603	599	3	Hexane

impeller type	C/D ratio	Njs	Power	Njd	Power	Dispersed Liquid
DT	1.0	482	6	412	4	MIBK
	1.0	464	5.5	445	5	Oil
	1.0	485	6	451	4.5	Hexane
	1.0	379	0.5	672	5	MIBK
	1.0	370	0.5	684	5	Oil
	1.0	386	0.5	812	9	Hexane

Dispersed Liquid	$\sigma^{1/12} \Delta\rho^{5/12}$
MIBK	11.144
Oil	11.705
Hexane	14.765

Table 5

Effect of Solid Concentration on Njs

Solid: Glass beads (150 microns); concentration = (by weight)

Dispersed Liquid: White mineral oil; concentration = 5% (volume)

Continuous Liquid: Distilled Water

T = 11.5"; D(disk turbine) = 4"; D(A310) = 3.8"

impeller type	C/D ratio	Njs	Power	Njd	Power	Solid Conc.
DT	0.744	337	10	400	16	0.5
	0.744	365	12	398	16	1
	0.744	400	16	403	17	2
A310	0.744	401	0.5	847	8.5	0.5
	0.744	528	1.5	830	8	2
	0.744	561	2	844	9	3
	0.744	604	3	839	8	3.5
	0.744	668	4	842	9	4

Table 6

Effect of Liquid Concentration on Njd

Solid: Glass beads (150 microns); concentration = 4.0% (weight)

Dispersed Liquid: White mineral oil; concentration = (by volume)

Continuous Liquid: Distilled Water

T = 11.5"; D(disk turbine) = 4"; D(A310) = 3.8"

impeller type	C'/D ratio	Njs	Power	Njd	Power	Liquid Conc.
DT	1.0	entrainment	(@ 370)	273	5	5
	1.0	entrainment	(@ 360)	291	6	10
	1.0	entrainment	(@ 365)	317	8	15
	1.0	entrainment	(@ 363)	334	9	20
A310	1.0	864	8	802	7	5
	1.0	885	9	922	12	10
	1.0	845	8	977	13	15
	1.0	856	8	995	14	20

Table 7

The Effect of Scale-up on Njs

Solid: Glass beads (150 microns); concentration = 0.5% (weight)

Dispersed Liquid: White mineral oil; concentration = 5% (volume)

Continuous Liquid: Distilled Water

T = 7.5" - 23.25"

impeller type	C/D ratio	Njs	Power	Njd	Power	Vessel Diameter
DT	0.5	349	1	709	6	7.625
	0.5	311	1.5	592	11	9.5
	0.5	248	3	456	20	11.5
	0.5	142	23	255	135	23.25
	1.0	500	3	516	3	7.625
	1.0	464	5.5	445	5	9.5
	1.0	368	13	380	14	11.5
	1.0	207	84	214	93	23.25
PT	0.5	411	0.5	738	3.5	7.625
	0.5	315	0.5	610	4	9.5
	0.5	262	1	511	10	11.5
	0.5	145	8	310	77	23.25
	1.0	491	0.5	874	3.5	7.625
	1.0	370	0.5	684	5	9.5
	1.0	361	3	584	14	11.5
	1.0	220	23	330	75	23.25
FT	0.5	422	3	760	4	7.625
	0.5	374	1	739	12	9.5
	0.5	299	2	excessive torque		11.5
	0.5	176	20	358	170	23.25
	1.0	686	4	782	6	7.625
	1.0	587	7	667	10	9.5
	1.0	509	18	570	26	11.5
	1.0	305	97	333	140	23.25

Table 8

The Effect of Scale-up on Njd

Solid: Glass beads (150 microns); concentration = 0.5% (weight)

Dispersed Liquid: White mineral oil; concentration = 5% (volume)

Continuous Liquid: Distilled Water

T = 7.5" - 23.25"

impeller type	C'/D ratio	Njs	Power	Njd	Power	Impeller Diameter
DT	1.0	entrainment @ 527		386	1	7.625
	1.0	entrainment @ 485		325	2	9.5
	1.0	entrainment @ 390		273	5	11.5
	1.0	entrainment @ 225		170	42	23.25
	1.875	500	3	516	3	7.625
	1.875	464	5.5	445	5	9.5
	1.875	368	13	380	14	11.5
	1.875	207	84	214	93	23.25
PT	1.0	entrainment @ 782		657	1	7.625
	1.0	entrainment @ 580		530	2	9.5
	1.0	entrainment @ 515		474	7	11.5
	1.0	entrainment @ 312		268	37	23.25
	1.875	491	0.5	874	3.5	7.625
	1.875	370	0.5	684	5	9.5
	1.875	361	3	584	14	11.5
	1.875	220	23	330	75	23.25
FT	1.0	entrainment @ 717		524	1	7.625
	1.0	entrainment @ 445		420	1.5	9.5
	1.0	entrainment @ 516		390	6	11.5
	1.0	entrainment @ 280		212	49	23.25
	1.875	686	4	782	6	7.625
	1.875	587	7	667	10	9.5
	1.875	509	17	570	26	11.5
	1.875	305	97	333	140	23.25

Table 9

Effect of Impeller Diameter on Nje

Solid: Glass beads (150 microns); concentration = 0.5% (weig

Dispersed Liquid: White mineral oil; concentration = 5% (vol

Continuous Liquid: Distilled Water

T = 11.5"; D(disk turbine) = 2.5-4"; D(A310) = 3.8-4.5"

impeller type	C'/D ratio	Nje	Njd	Power	Impeller Diameter
DT	1.0	900	623	5	2.5
	1.0	658	409	4	3
	1.0	390	273	5	4
PT	1.0	1190	1120	7	2.5
	1.0	807	760	7	3
	1.0	515	474	7	4

Table 10

The Effect of Vessel Diameter on Nje

Solid: Glass beads (150 microns); concentration = 0.5% (weig

Dispersed Liquid: White mineral oil; concentration = 5% (vol

Continuous Liquid: Distilled Water

T = 7.5" - 23.25"

impeller type	C'/D ratio	Nje	Njd	Power	Impeller Diameter
DT	1.0	527	386	1	7.625
	1.0	485	325	2	9.5
	1.0	390	273	5	11.5
	1.0	225	170	42	23.25
PT	1.0	782	657	1	7.625
	1.0	580	530	2	9.5
	1.0	515	474	7	11.5
	1.0	312	268	37	23.25
FT	1.0	717	524	1	7.625
	1.0	445	420	1.5	9.5
	1.0	516	390	6	11.5
	1.0	280	212	49	23.25

Table 11

Physical Properties of the Liquids

Fluid	Density (kg/m^3)	Interfacial Tension with Water (dynes/cm)
Mineral Oil	828	46.6
Hexane	673	29.6
Methylisobutyl Ketone	789	9.2
Distilled Water	998	-

Table 12

Physical Properties of the Solids

Particle	Shape	Size (microns)	Density (kg/m^3)
Glass Beads	spherical	60	2500
Glass Beads	spherical	75	2500
Glass Beads	spherical	150	2500
Glass Beads	spherical	200	2500

Table 13

Vessel Dimensions

Diameter, T (in)	7.625	9.5	11.5	23.5
Liquid Height, H (in)	7.625	9.5	11.5	23.5
Volume, V (in^3)	348	673	1194	10193
Baffle Width (%)	10	10	10	10
Material of Construction	Perspex	Glass	Perspex	Perspex
Geometry	Cylindrical with Flat Base			

Table 14

Impeller Information

Type	No. of Blades	Diameter
Disk Turbine	6	2.5
		3
		4
		8
Flat Turbine	6	2.5
		3
		4
		8
Pitched Turbine	6	2.5
		3
		4
		8
A310 Impeller	3	3.8
		4.5

Chapter 11
References

1. Baldi, G., Conti, R., and Alaria, E.; "Complete Suspension of Particles in Mechanically Agitated Vessels", Chemical Engineering Science, 33:21 (1978).

2. Bourne, J.R., and Sharma, R.N. ~"Homogeneous Particle Suspension in Propeller-agitated Flat Bottom Tanks", Chemical Engineering Journal, 8:243, (1974).

3. Carpenter, K. J.; Proceeding of the 5th European Conference on Mixing, Wurzburg, West Germany, June 10-12, 1985, BHRA Publication (1985).

4. Chapman, C. M., Nienow, A. W., Cooke, M., and Middleton, J. C., ~"Particle-gas-liquid Mixing in Stirred Vessels: Part I, Particle-Liquid Mixing", Trans. Inst. Chemical Engineering (Chem. Eng. Res. Des.), 61:74 (1983).

5. Clarke, S. I. and Sawistowski, H.; Trans. Inst. Chem. Eng., 56 : 50 (1978).

6. Delichatsios, M. A., and Probstein, R. F., "The Effect of Coalescence on the Average Drop Size in Liquid-Liquid Dispersions", Ind. Eng. Chem. Fund., 15, 134 (1976).

7. Esch, D. D., D'Angelo, P. J., and Pike, R. W.; "On Minimum Power Requirements for Emulsification of Two-Phase Liquid Systems", Can.J.Chem.Eng., 49, 872 (1971).

8. Godfrey, J. C., Reeve, R. N., Grilc, V., and Kardelj, E.; "Minimum Conditions for the Production of Liquid-Liquid Dispersions in Agitated Tanks", I. Chem. E. Symp. Series No. 89

(Fluid Mixing II), 8, 107, (1984).

9. Kuboi, J.R., Komasawa I. and Otake T., Chem. Eng. Japan, 5:349, (1972).

10. Mc Cabe, W. L., Smith, J. C., and Harriot, P., Unit Operations in Chemical Engineering,

11. Musil, L. and J. Vlk.; "Suspending Solid Particles in an Agitated Conical-bottom Tank", Chemical Engineering Science, 33:1125 (1978).

12. Narayanan, S., Bhatia, V. K., Guha, D. K., and Rao, M. N.; Chemical Engineering Science, 23:223 (1959).

13. Perry, R., Chemical Engineer's Handbook.

14. Skelland, AHP. and Seksaria, R.; "Minimum Impeller Speeds for Liquid-Liquid Dispersion in Baffled Vessels", Ind. Eng. Chem. Proc. Des. Dev., 17, 56 (1978).

15. Susanto, J., Multiphase Solid-Liquid and Solid-Liquid-Gas Mixing in Stirred Tanks, Masters Thesis, New Jersey Institute of Technology (1989).

16. Tsai, D. H., Liquid-Liquid Mixing in Stirred Vessels, Masters Thesis, New Jersey Institute of Technology, (1989).

17. van Heuven, J. W. and Beek, W. J.; "Power Input, Drop Size, and Minimum Stirrer Speed for Liquid-Liquid Dispersions in Stirred Vessels", Proc. ISEC71, 70 (1971).

18. Zwietering, T. N., "Suspending Solid Particles in Liquids by Agitators", Chemical Engineering Science, 8:244 (1958).

Effect of Impeller Clearance on Njs

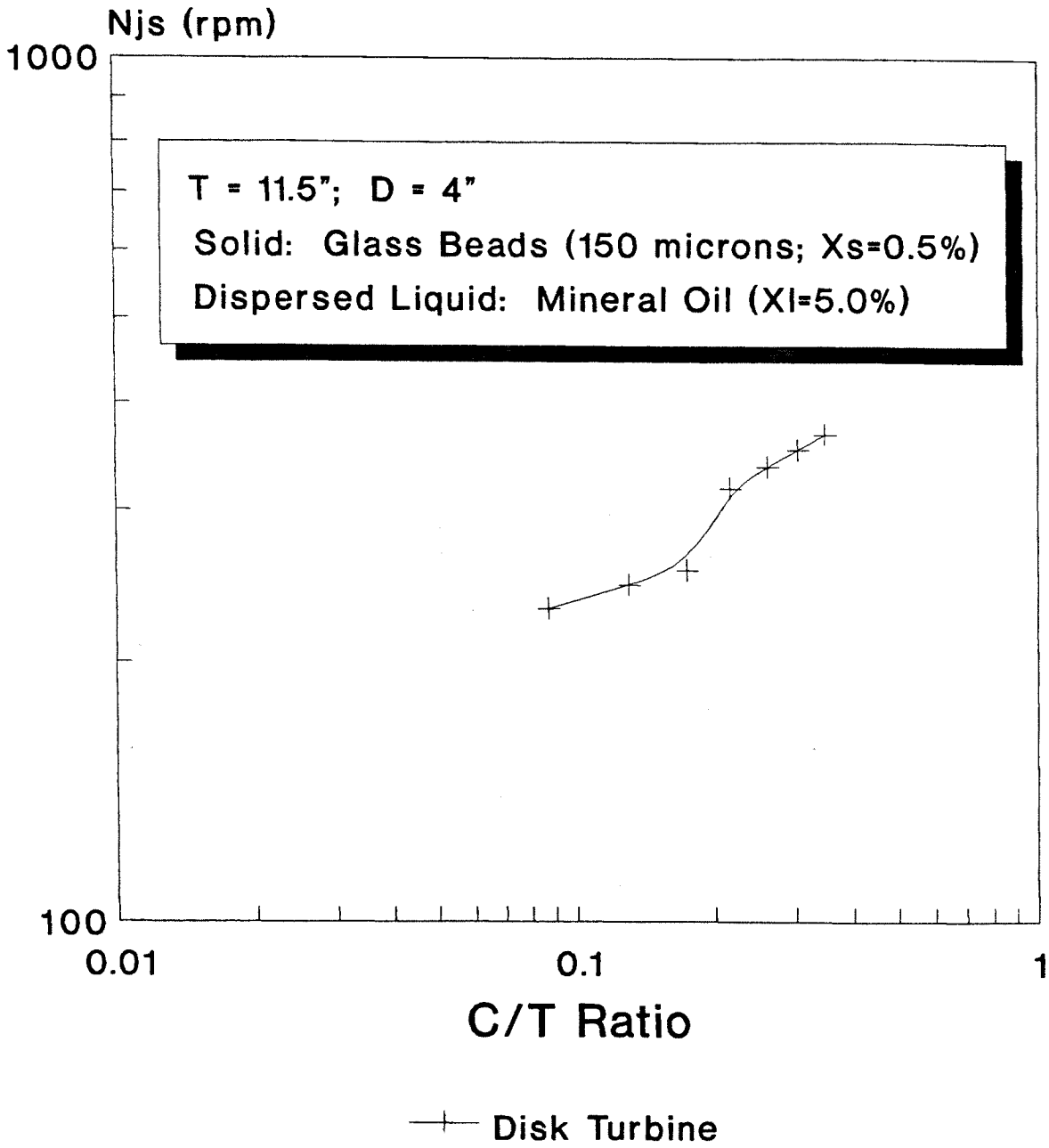

Figure 1

Effect of Impeller Clearance on Np

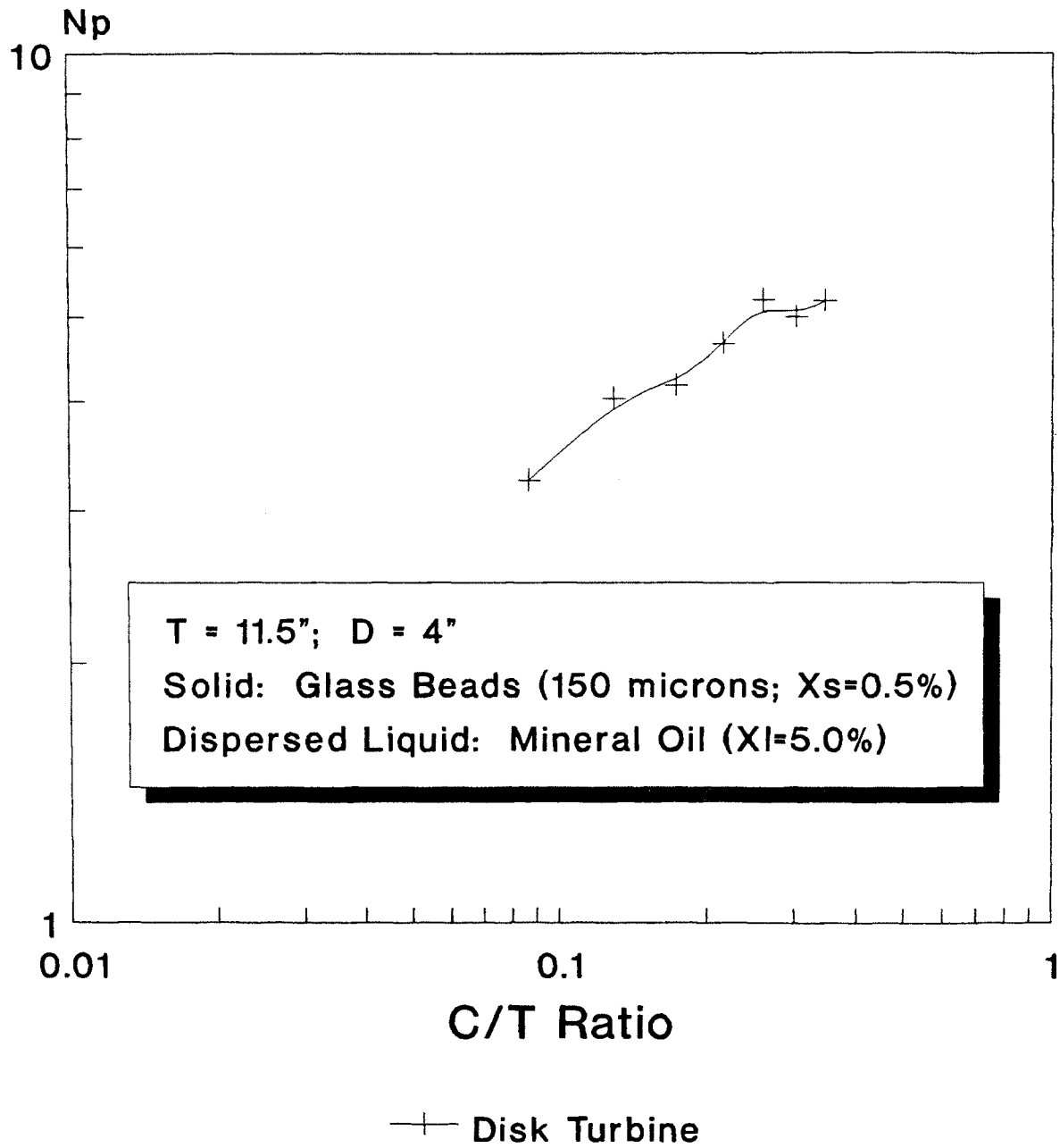

Figure 2

Effect of Impeller Clearance on Njs

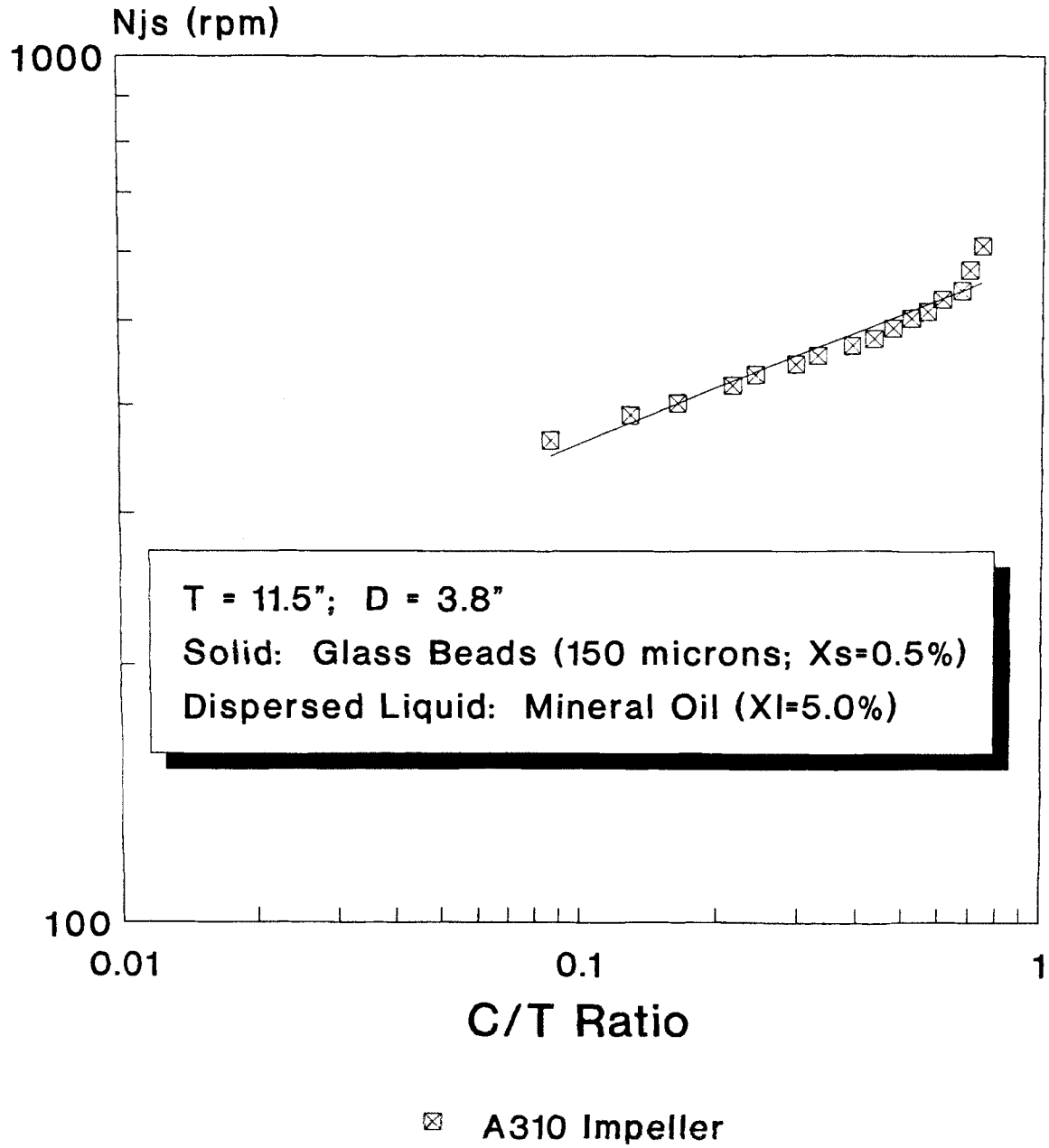

Figure 3

Effect of Impeller Clearance on Np

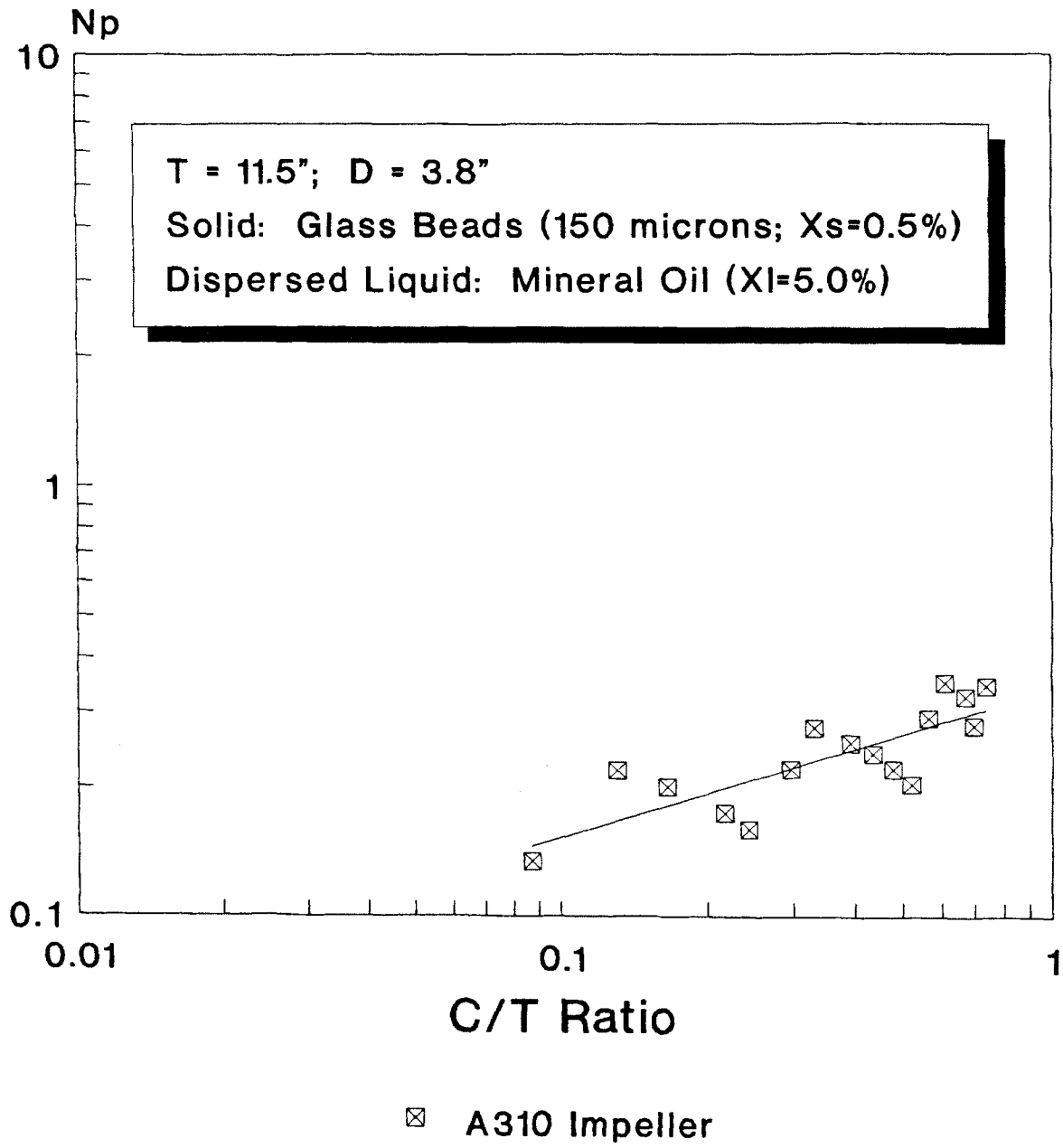

Figure 4

Effect of Impeller Clearance on Njd

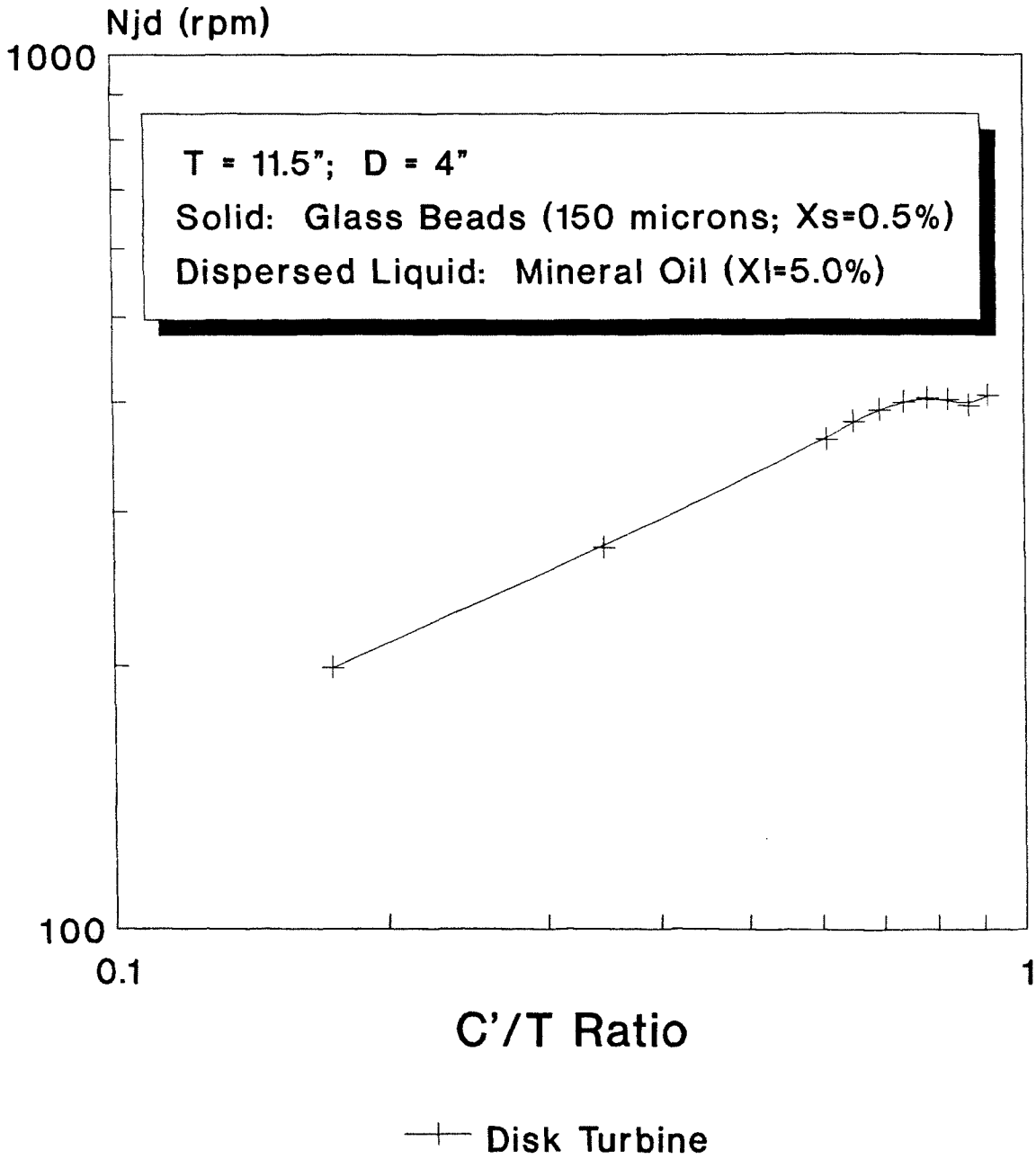

Figure 5

Effect of Impeller Clearance on Np

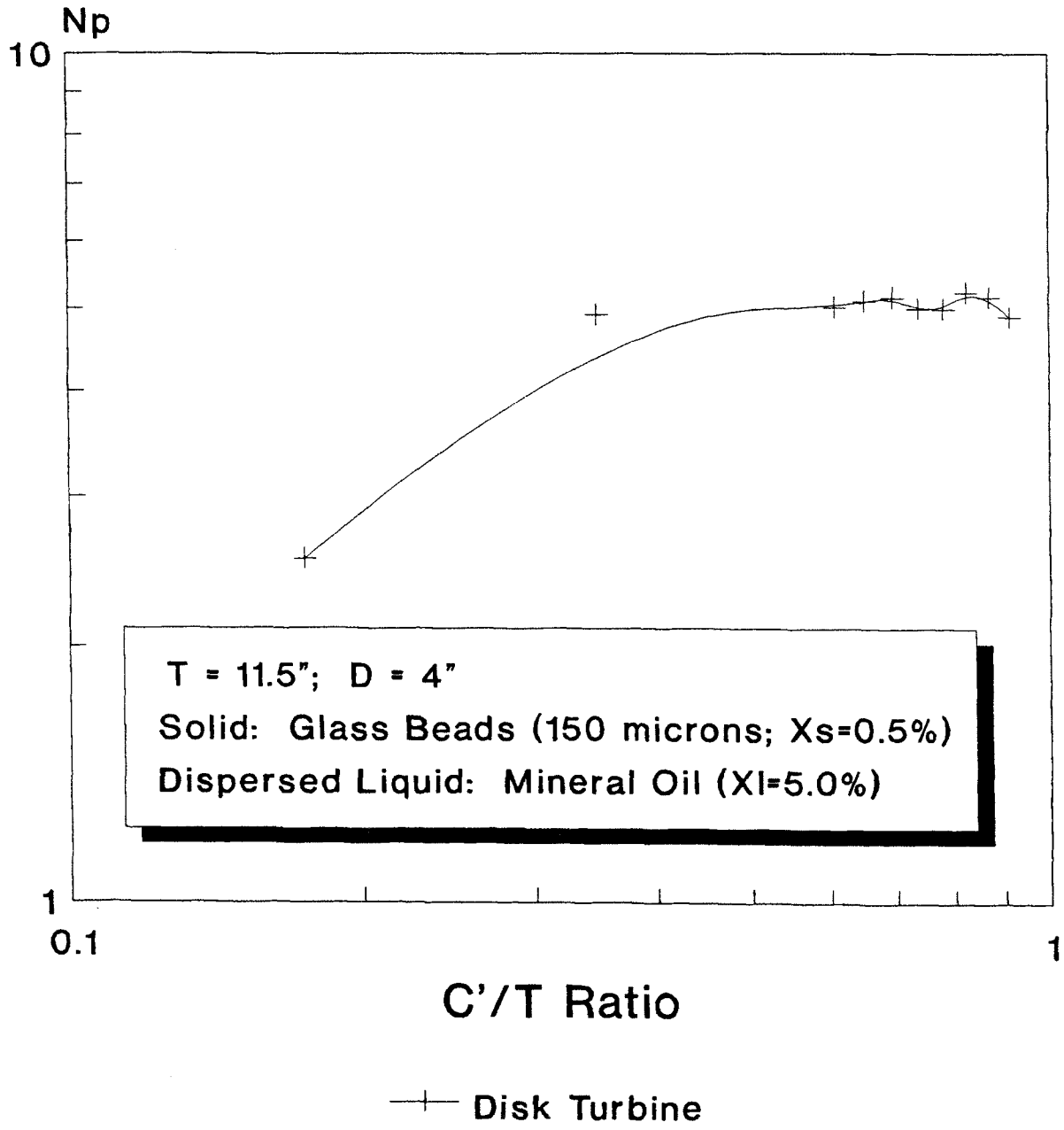

Figure 6

Effect of Impeller Clearance on Njd

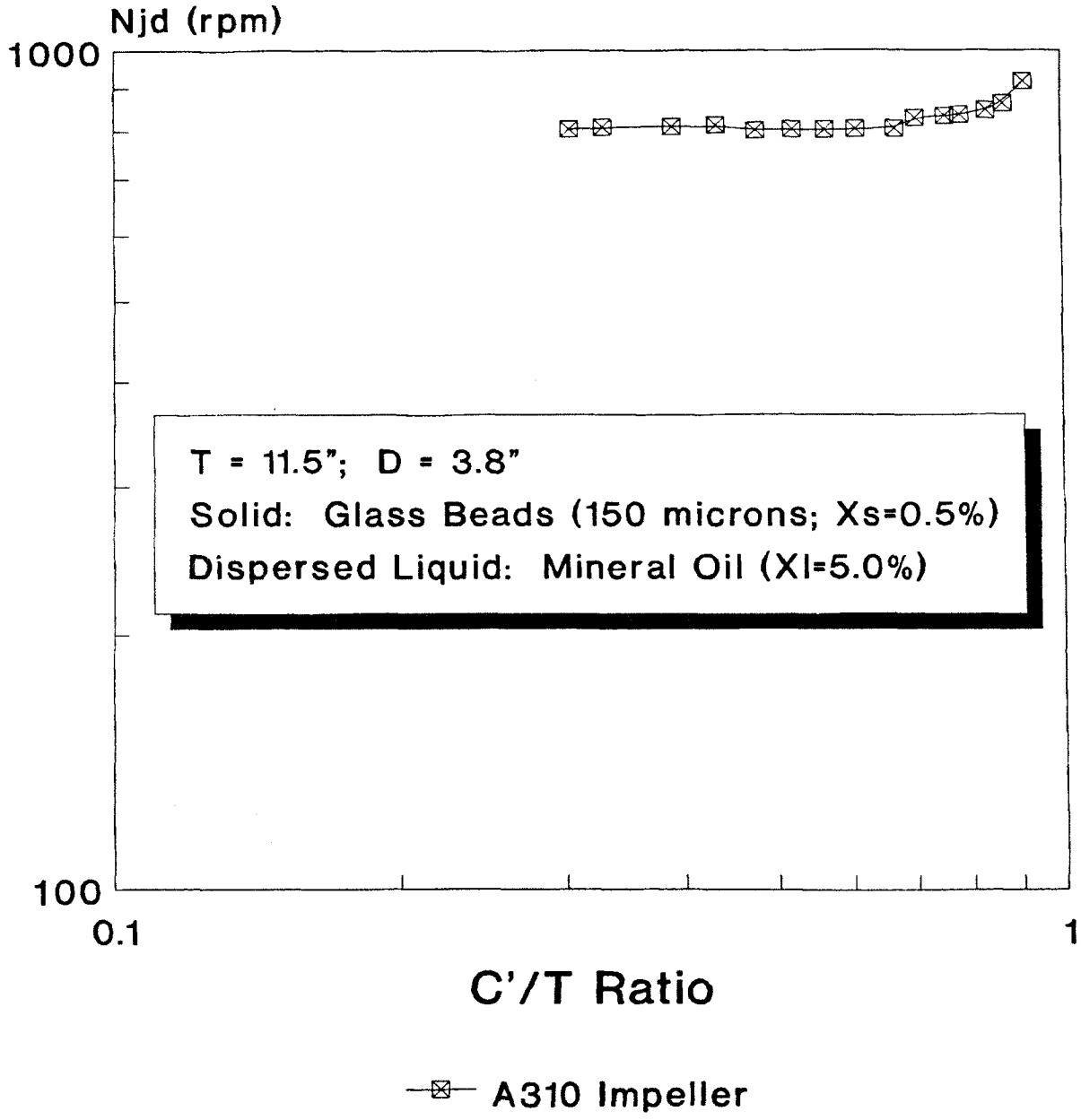

Figure 7

Effect of Impeller Clearance on Np

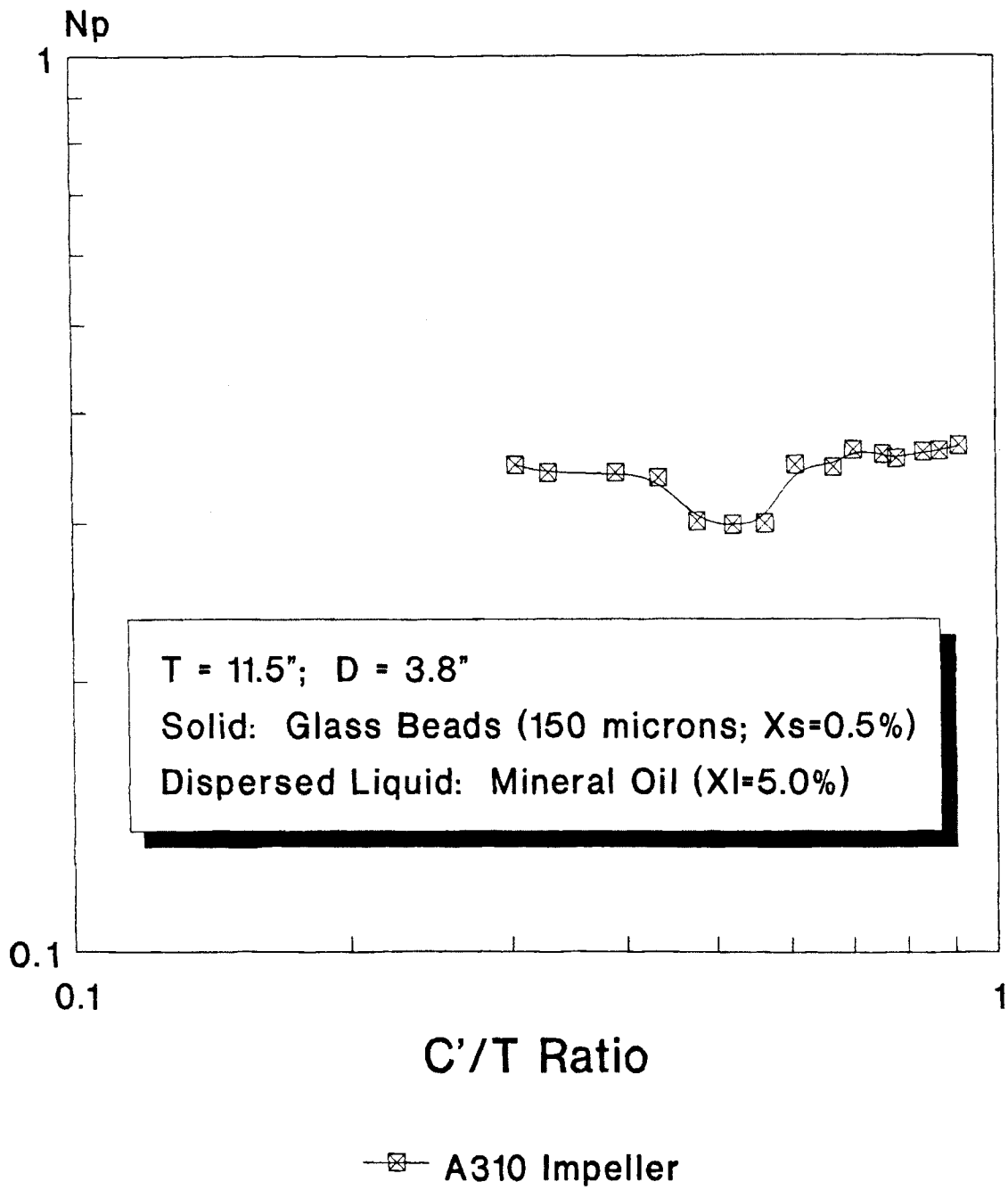

Figure 8

Effect of Impeller Diameter on Njs

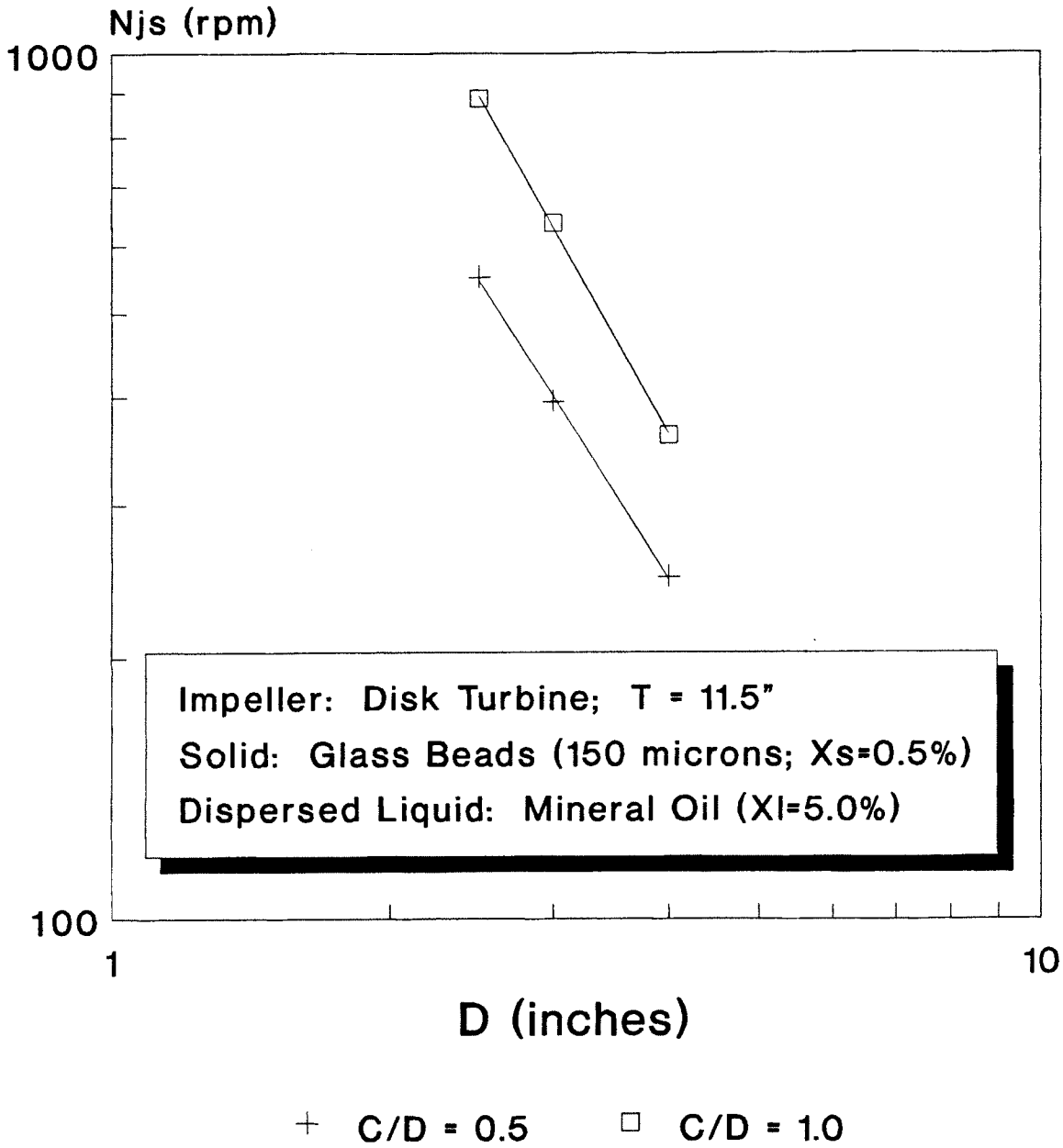

Figure 9

Effect of Impeller Diameter on Njs

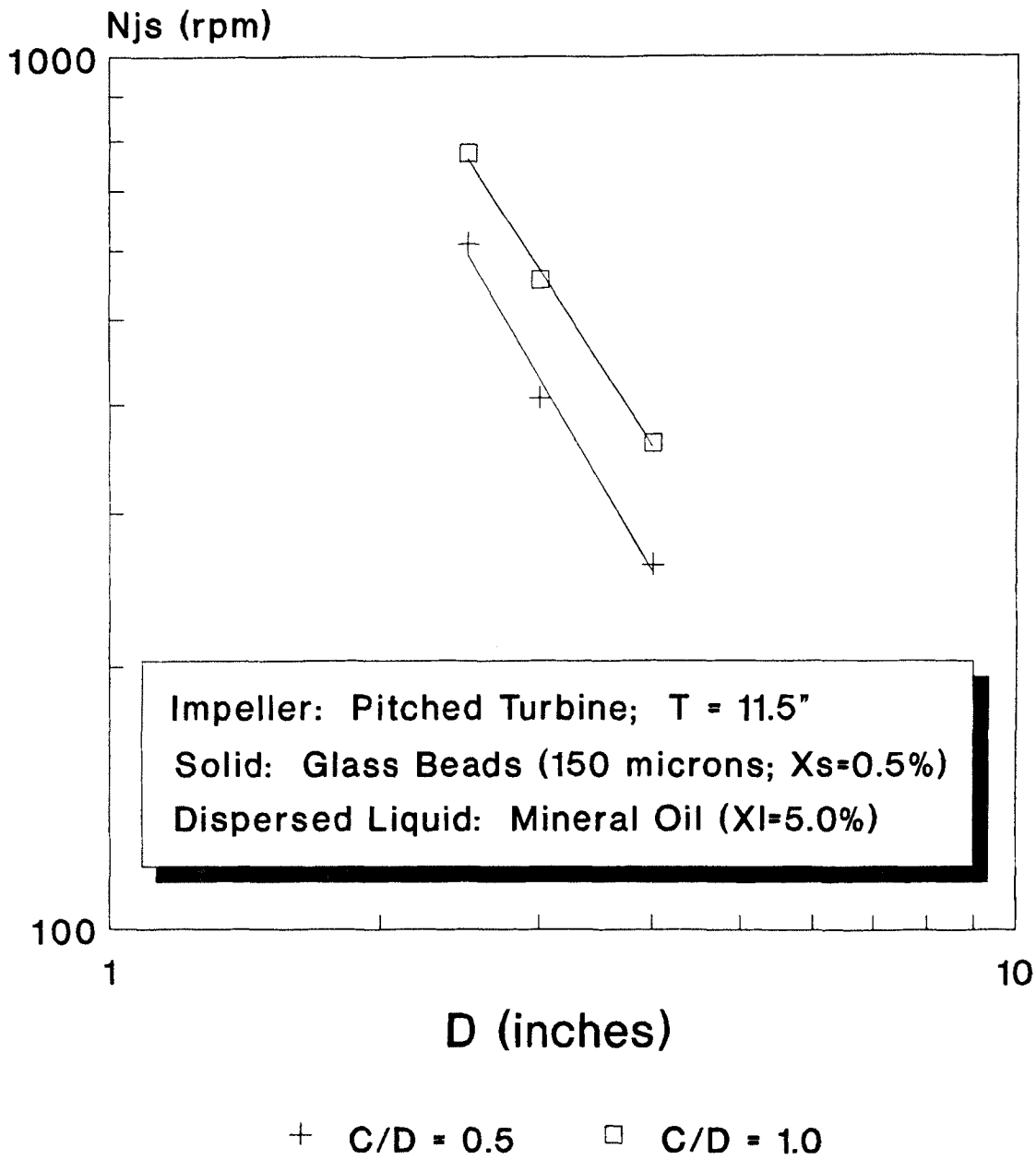

Figure 10

Effect of Impeller Diameter on Njd

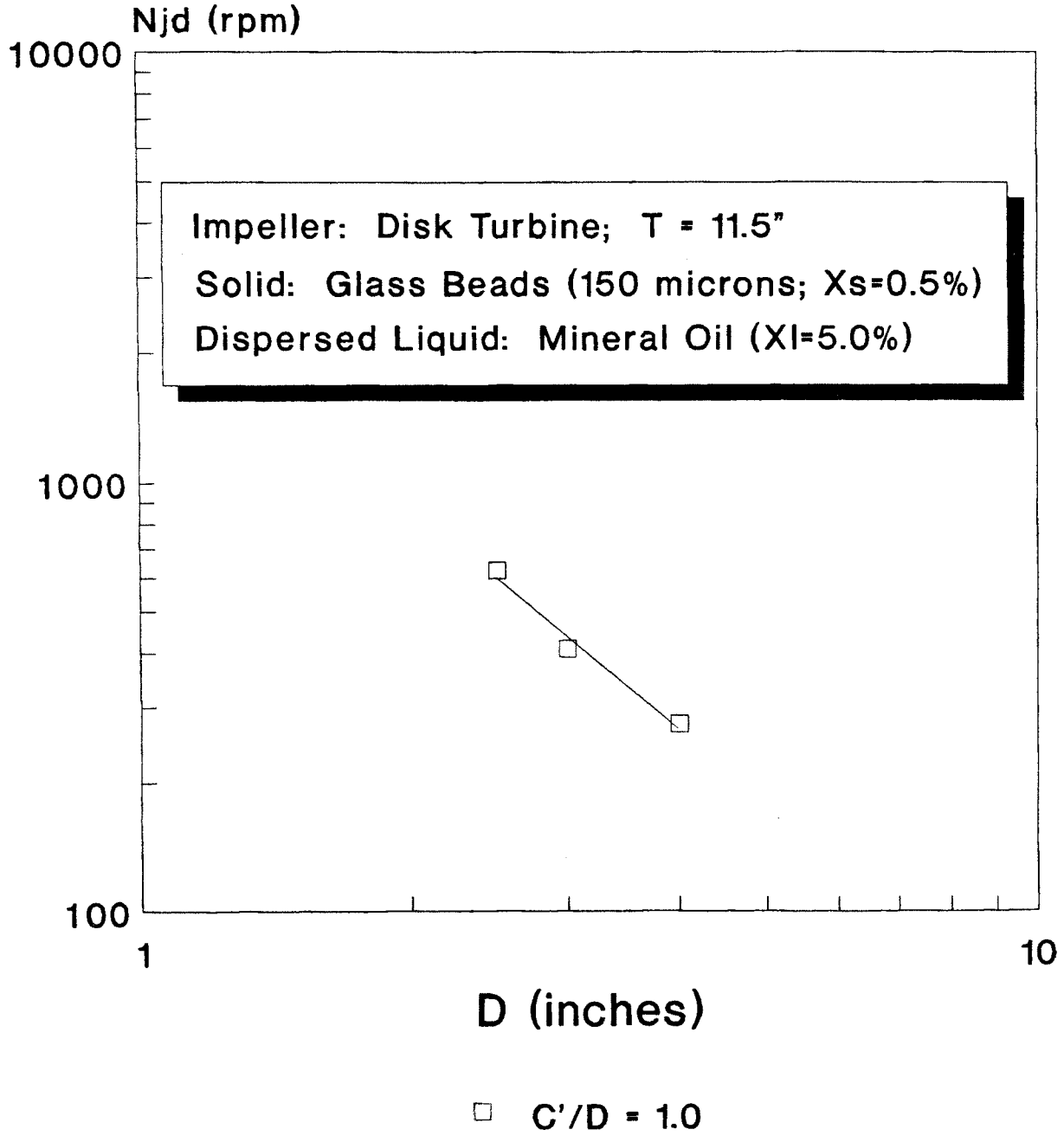

Figure 11

Effect of Impeller Diameter on Njd

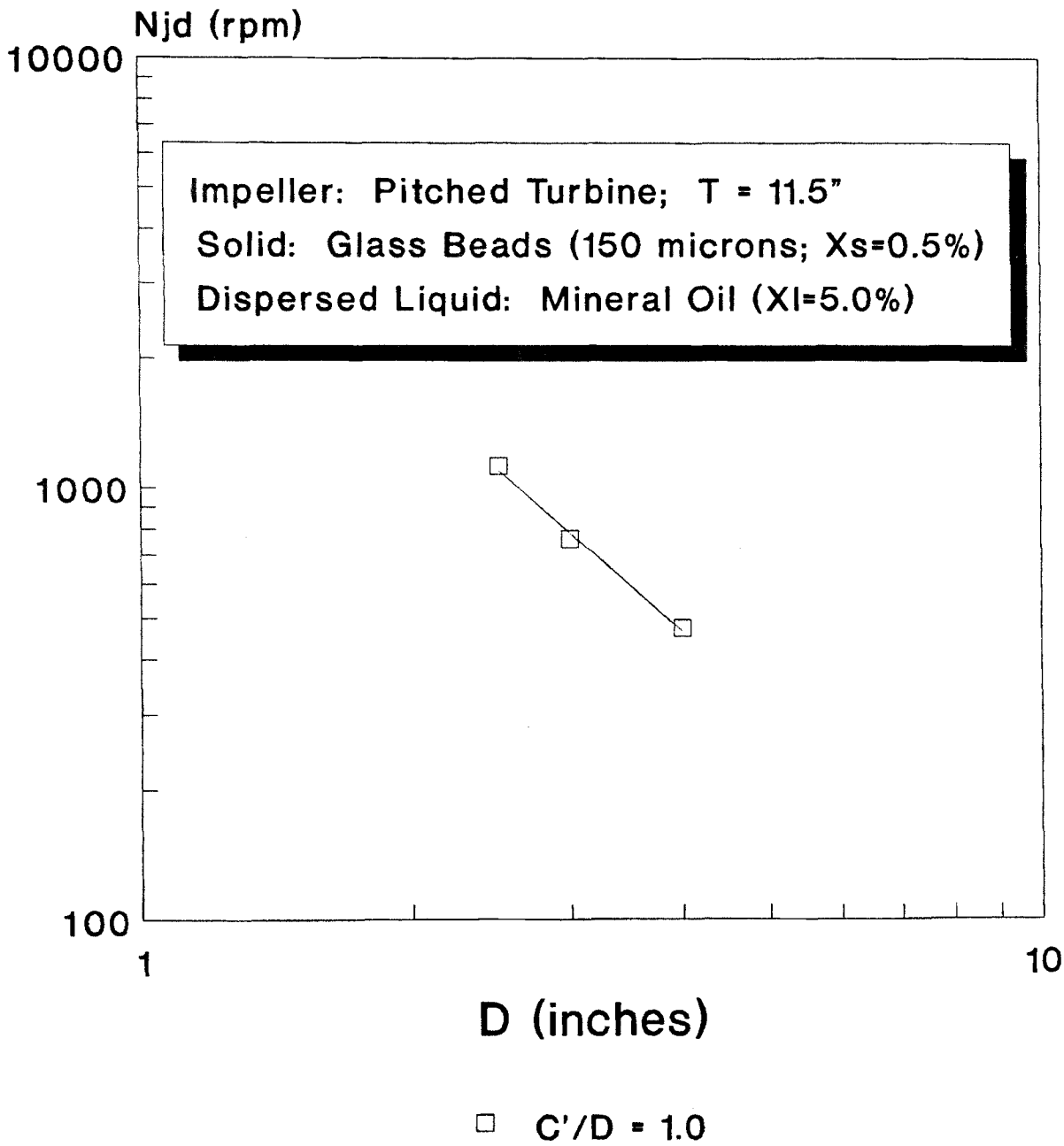

Figure 12

Effect of Particle Size on Njs

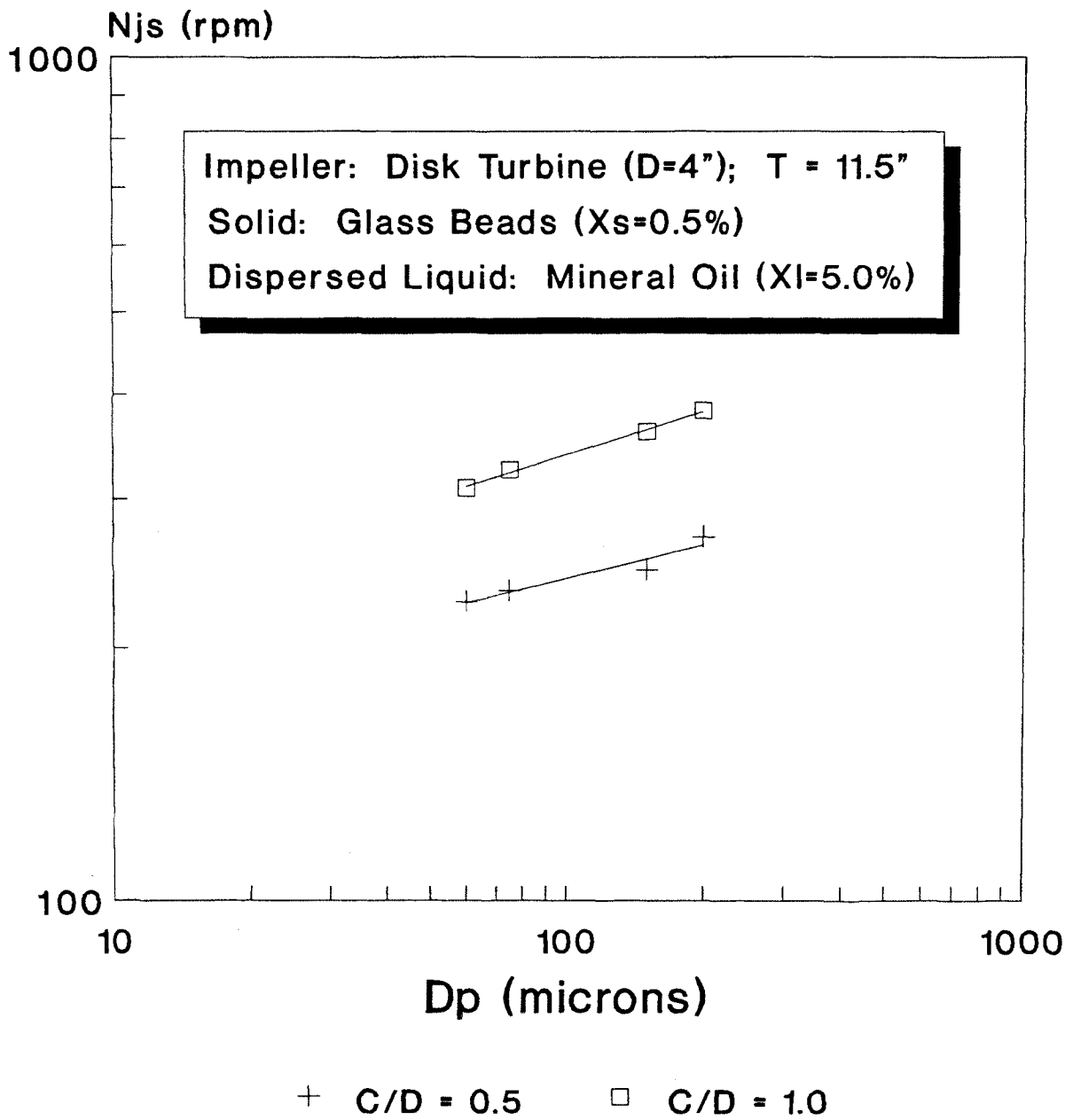

Figure 13

Effect of Particle Size on Njs, Njd

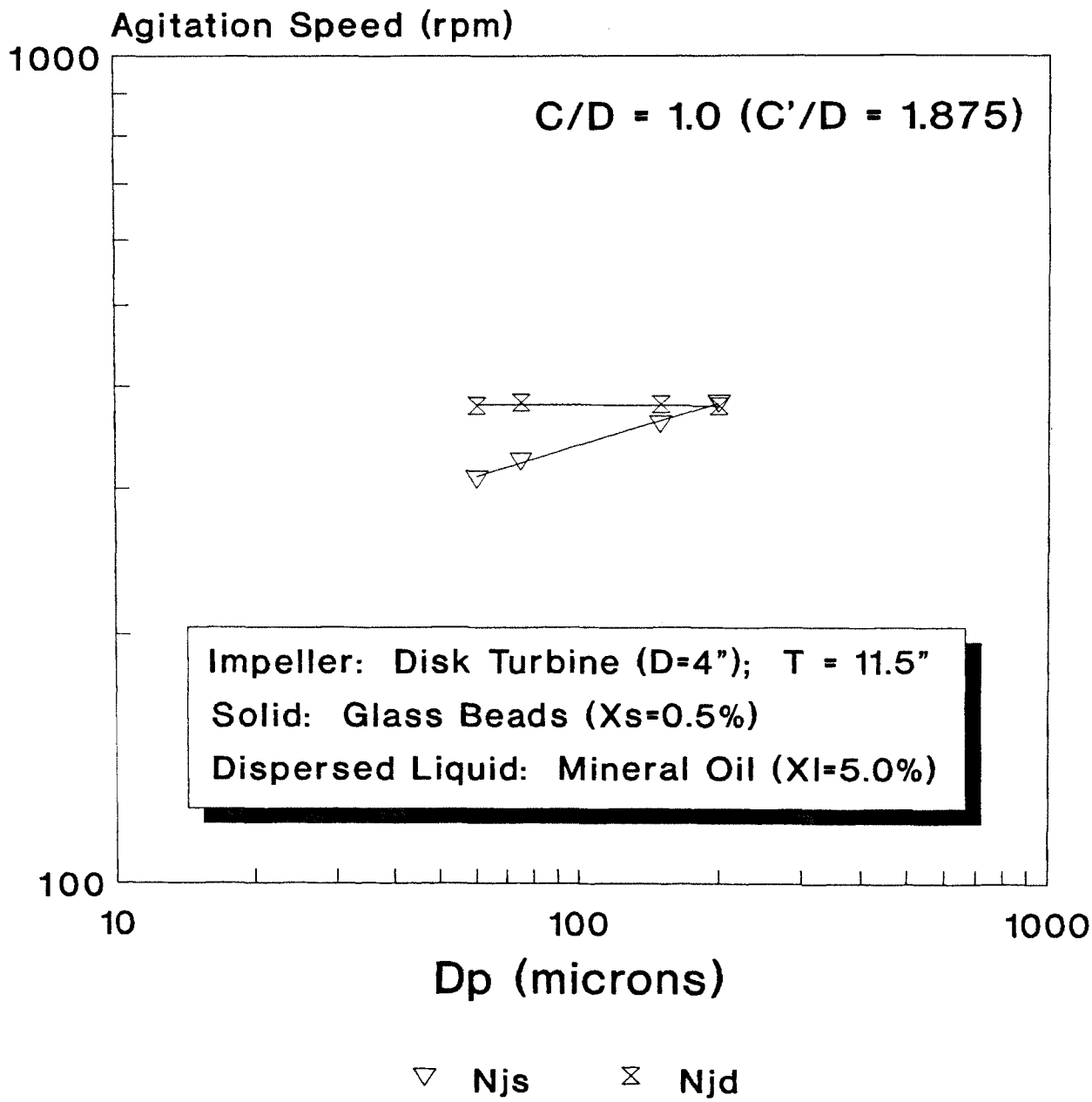

Figure 14

Effect of Particle Size on Njs, Njd

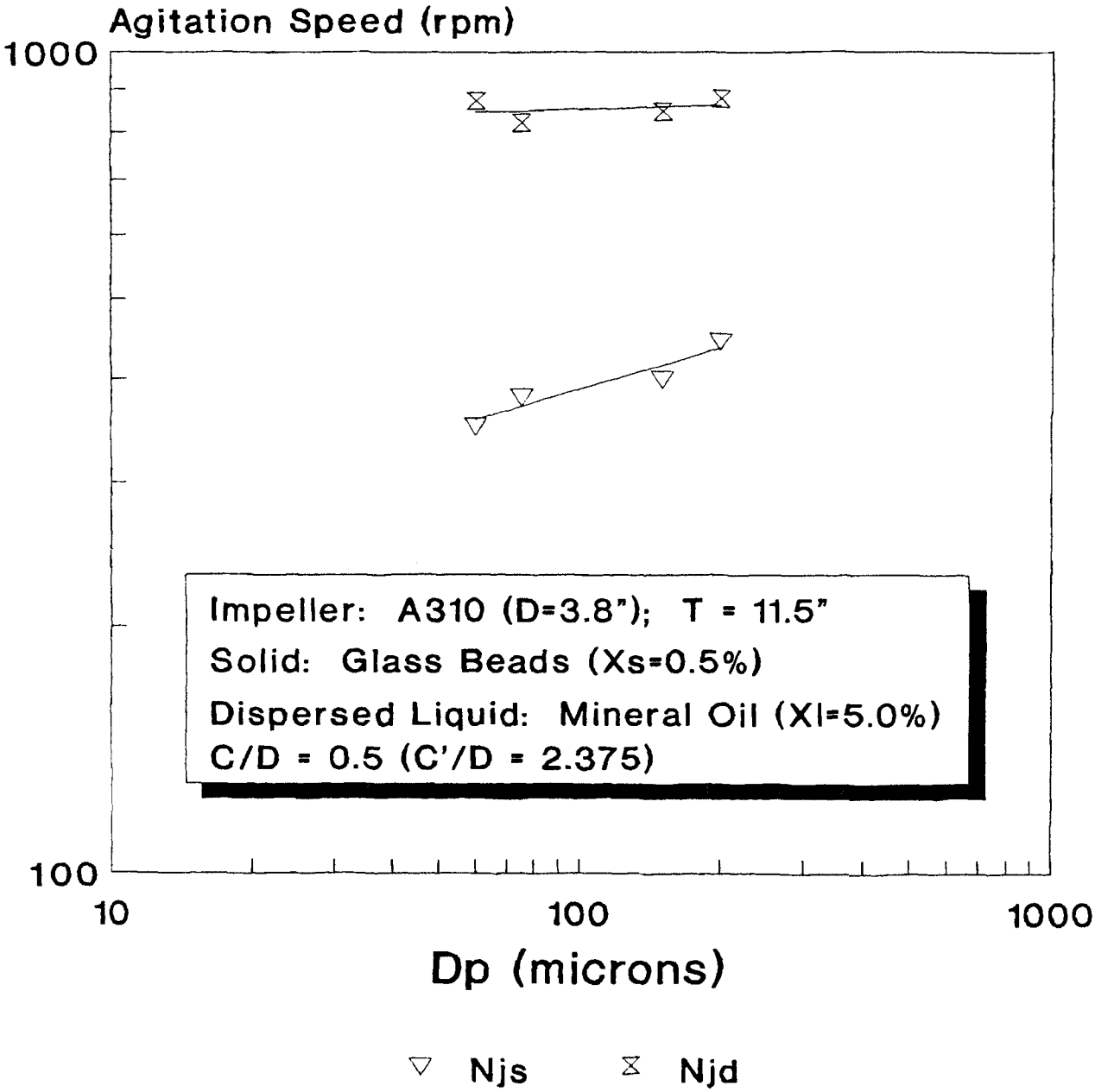

Figure 15

Effect of Particle Size on Njs, Njd

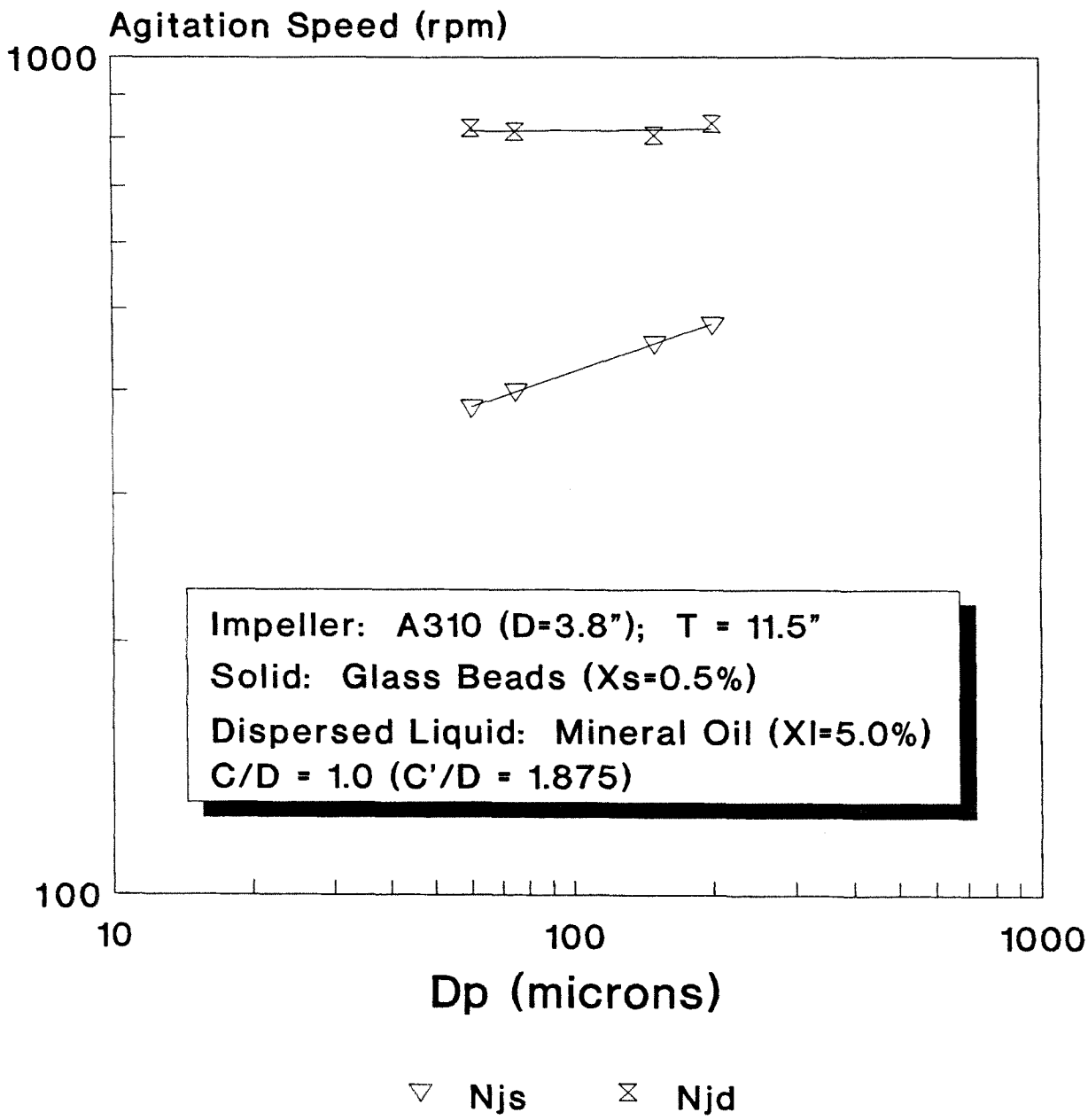

Figure 16

Effect of Liquid Properties on Njd

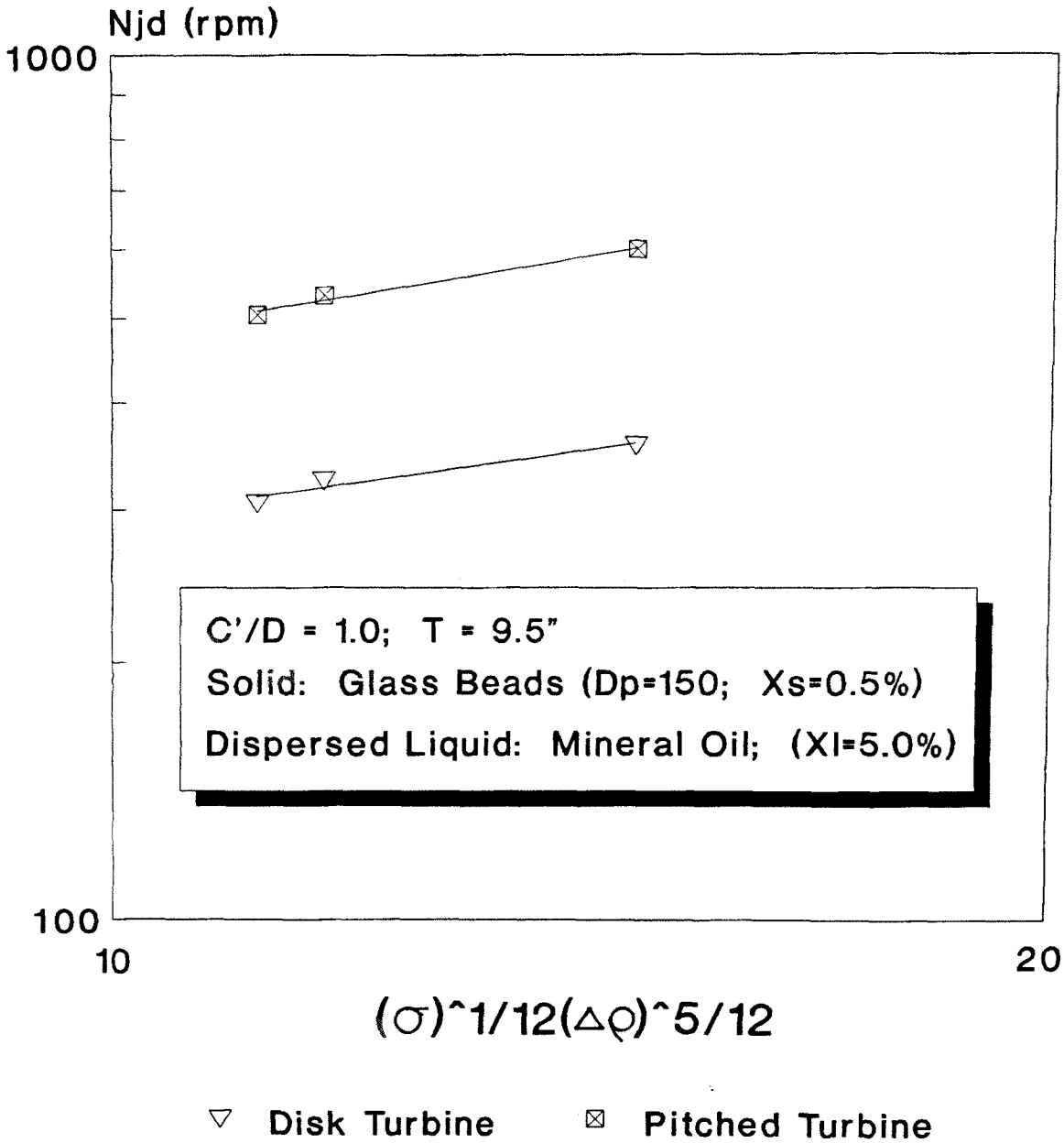

Figure 17

Effect of Liquid Properties on Njd

Using a Disk Turbine

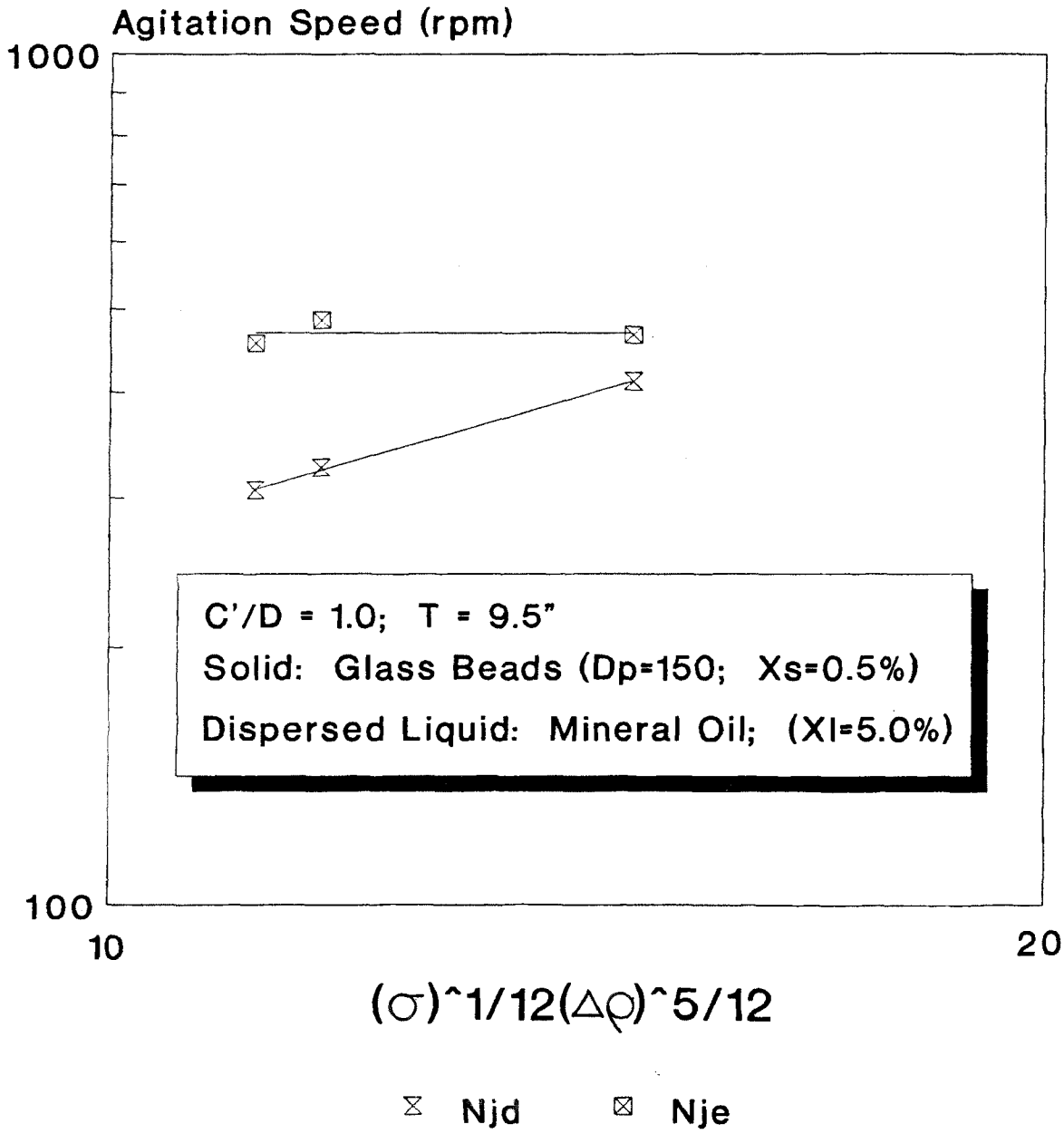

Figure 18

Effect of Liquid Properties on Njd

Using a Pitched Blade Turbine

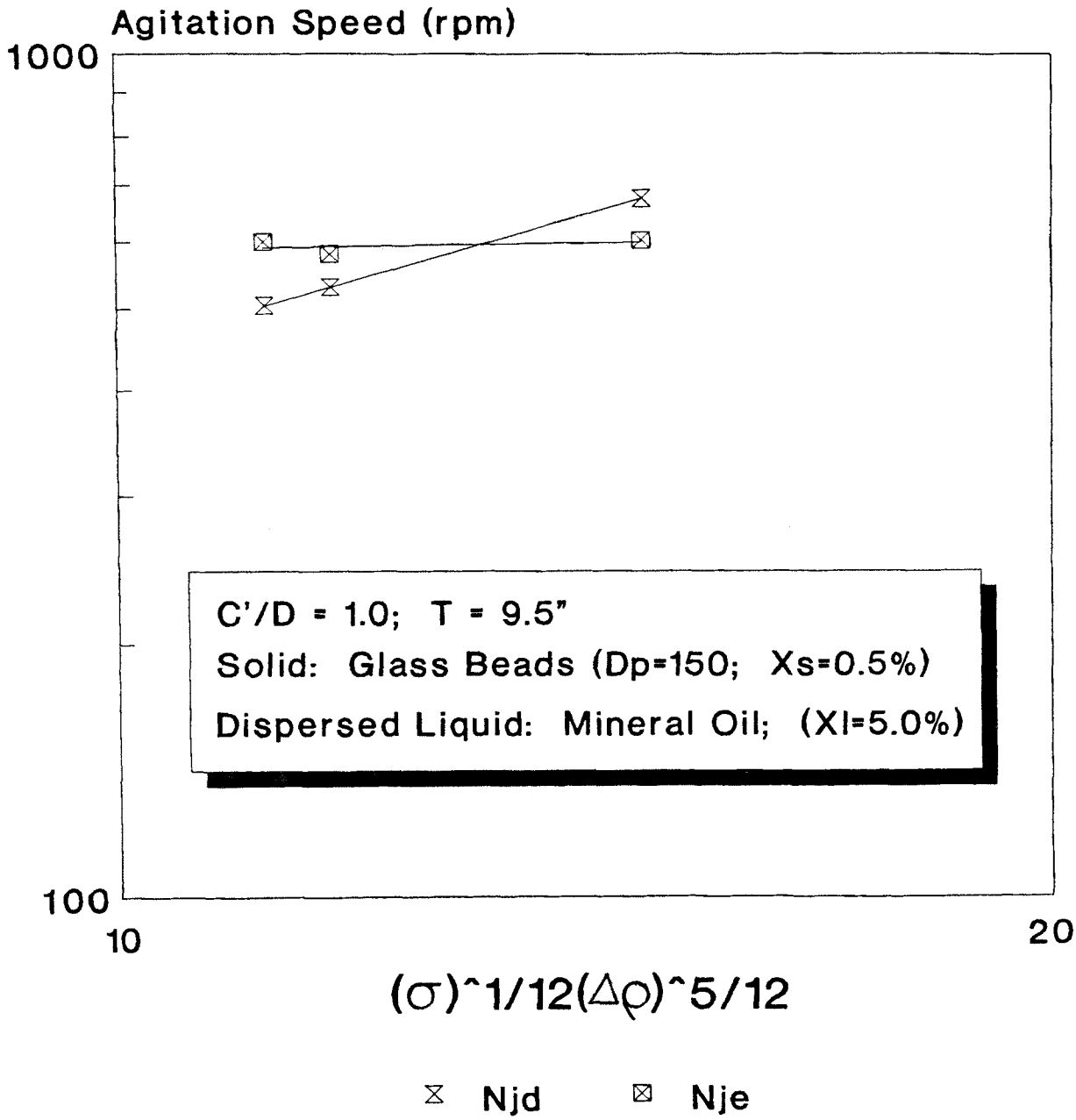

Figure 19

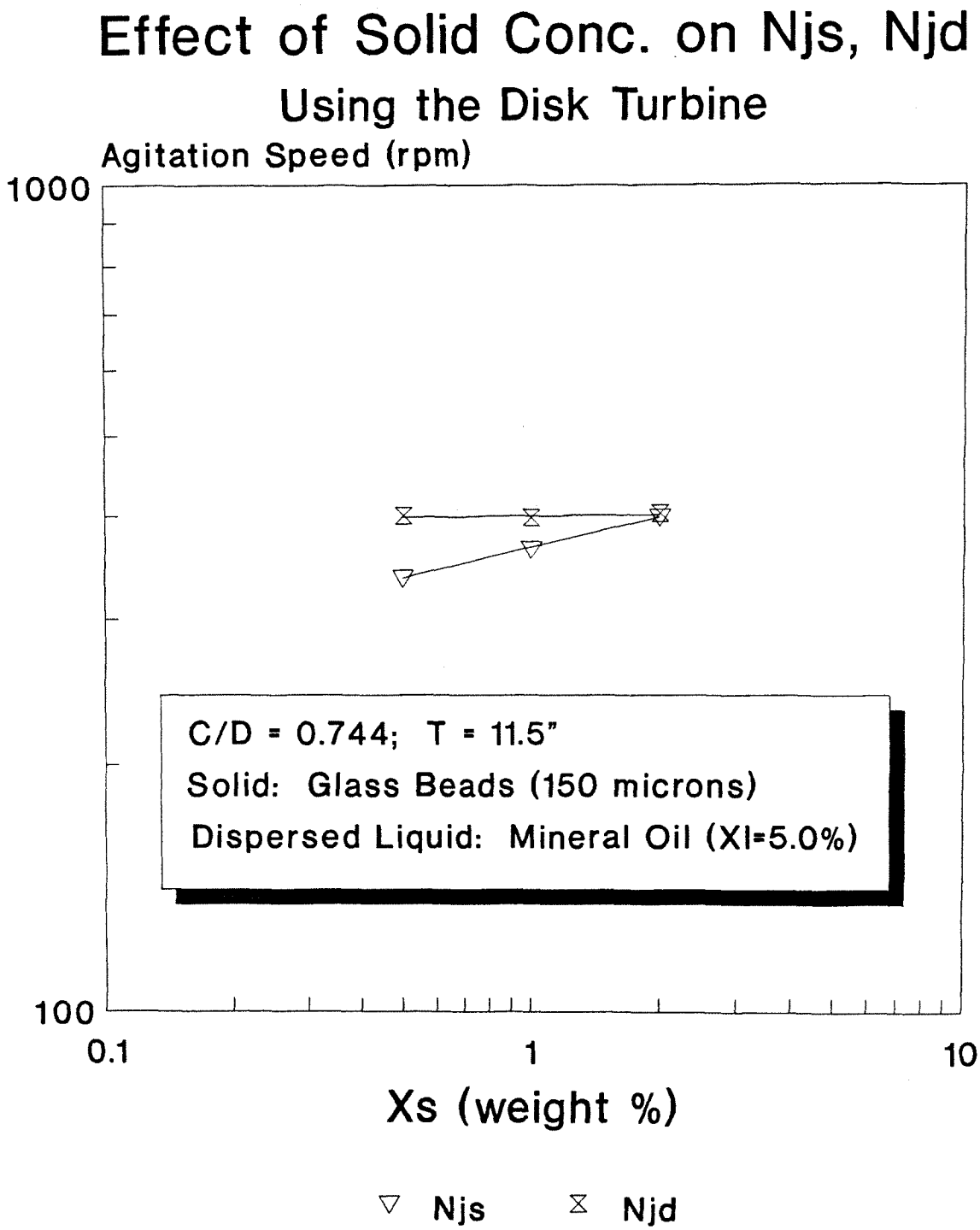
Effect of Solid Conc. on Njs, Njd
Using the Disk Turbine
Agitation Speed (rpm)
1000
100
0.1
1
10
Xs (weight %)
C/D = 0.744; T = 11.5"
Solid: Glass Beads (150 microns)
Dispersed Liquid: Mineral Oil (Xl=5.0%)
Njs
Njd

Figure 20

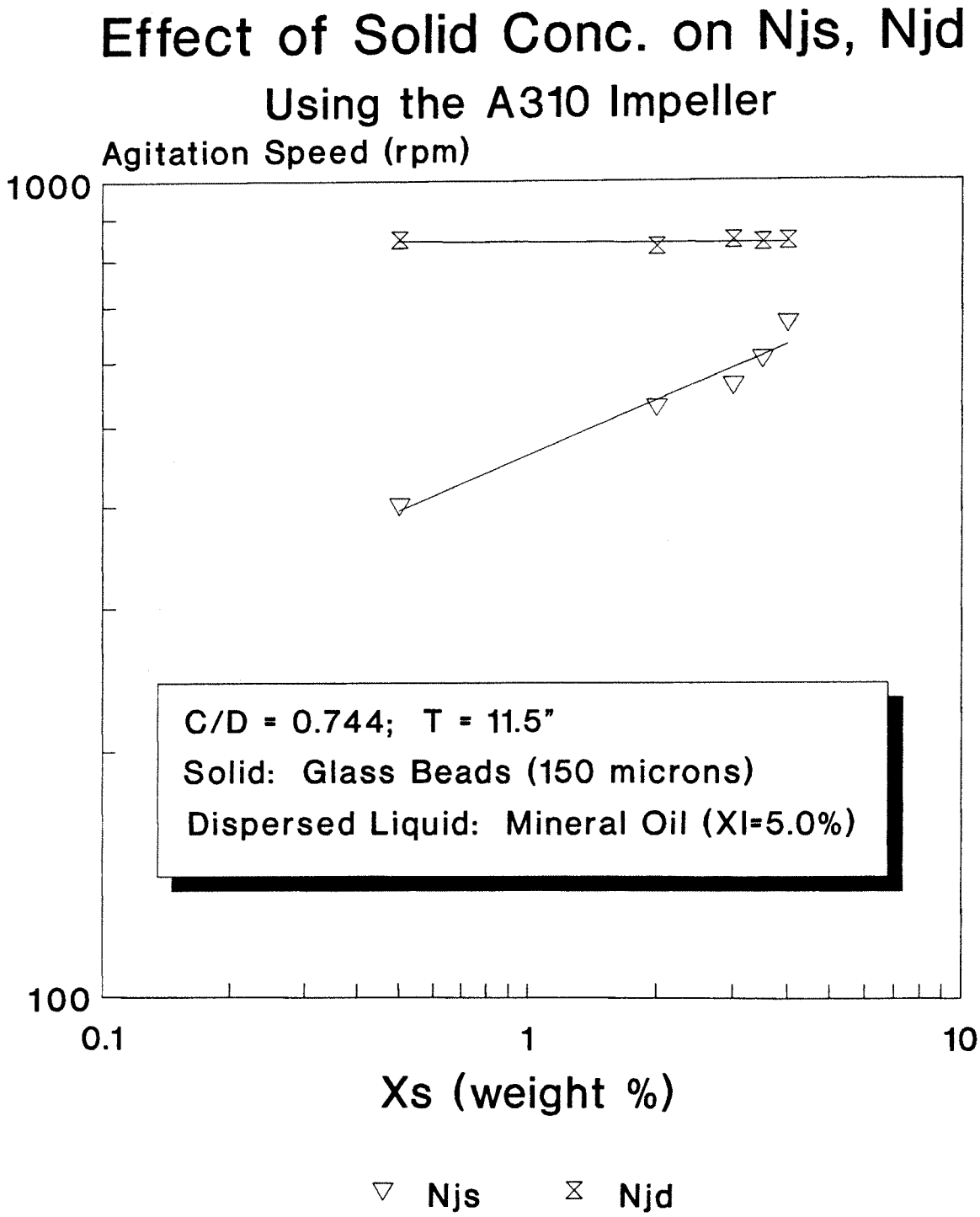
Effect of Solid Conc. on Njs, Njd
Using the A310 Impeller
Agitation Speed (rpm)
1000
100
0.1
1
10
Xs (weight %)
C/D = 0.744; T = 11.5"
Solid: Glass Beads (150 microns)
Dispersed Liquid: Mineral Oil (Xl=5.0%)
Njs
Njd

Figure 21

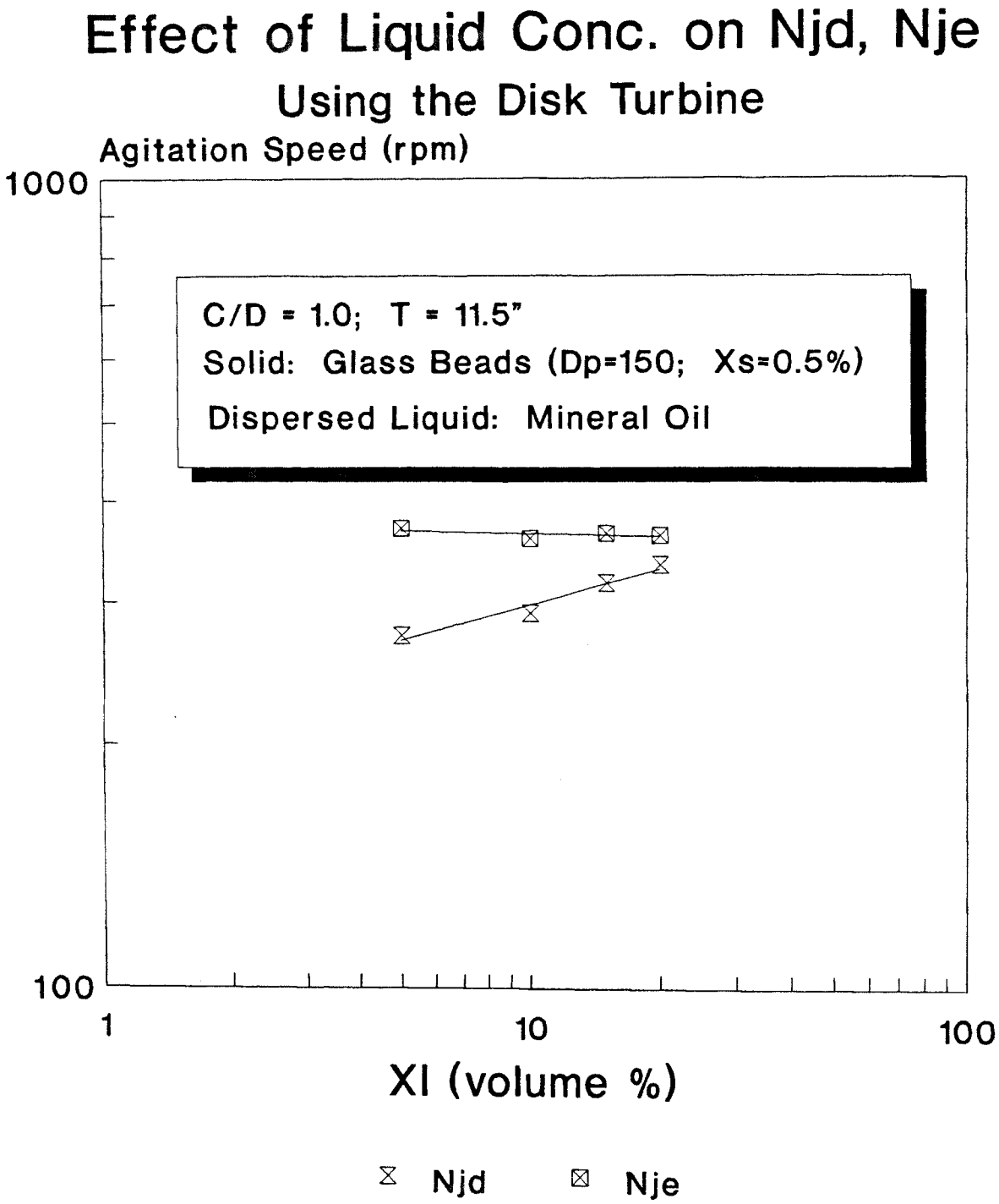
Effect of Liquid Conc. on Njd, Nje
Using the Disk Turbine
Agitation Speed (rpm)
1000
100
C/D = 1.0; T = 11.5"
Solid: Glass Beads (Dp=150; Xs=0.5%)
Dispersed Liquid: Mineral Oil
1
10
100
Xl (volume %)
Njd
Nje

Figure 22

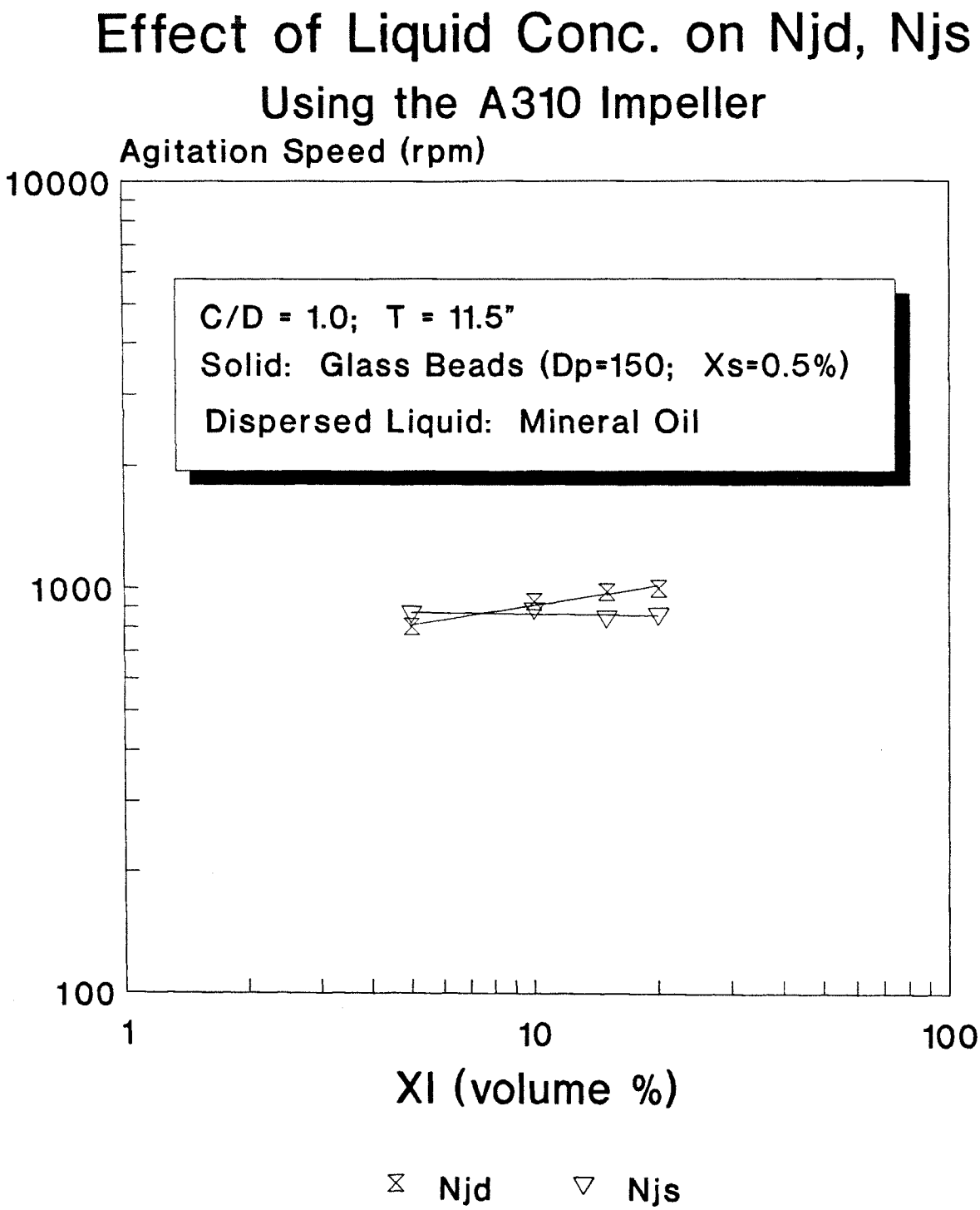
Effect of Liquid Conc. on Njd, Njs
Using the A310 Impeller
Agitation Speed (rpm)
10000
1000
100
C/D = 1.0; T = 11.5"
Solid: Glass Beads (Dp=150; Xs=0.5%)
Dispersed Liquid: Mineral Oil
1
10
100
Xl (volume %)
Njd
Njs

Figure 23

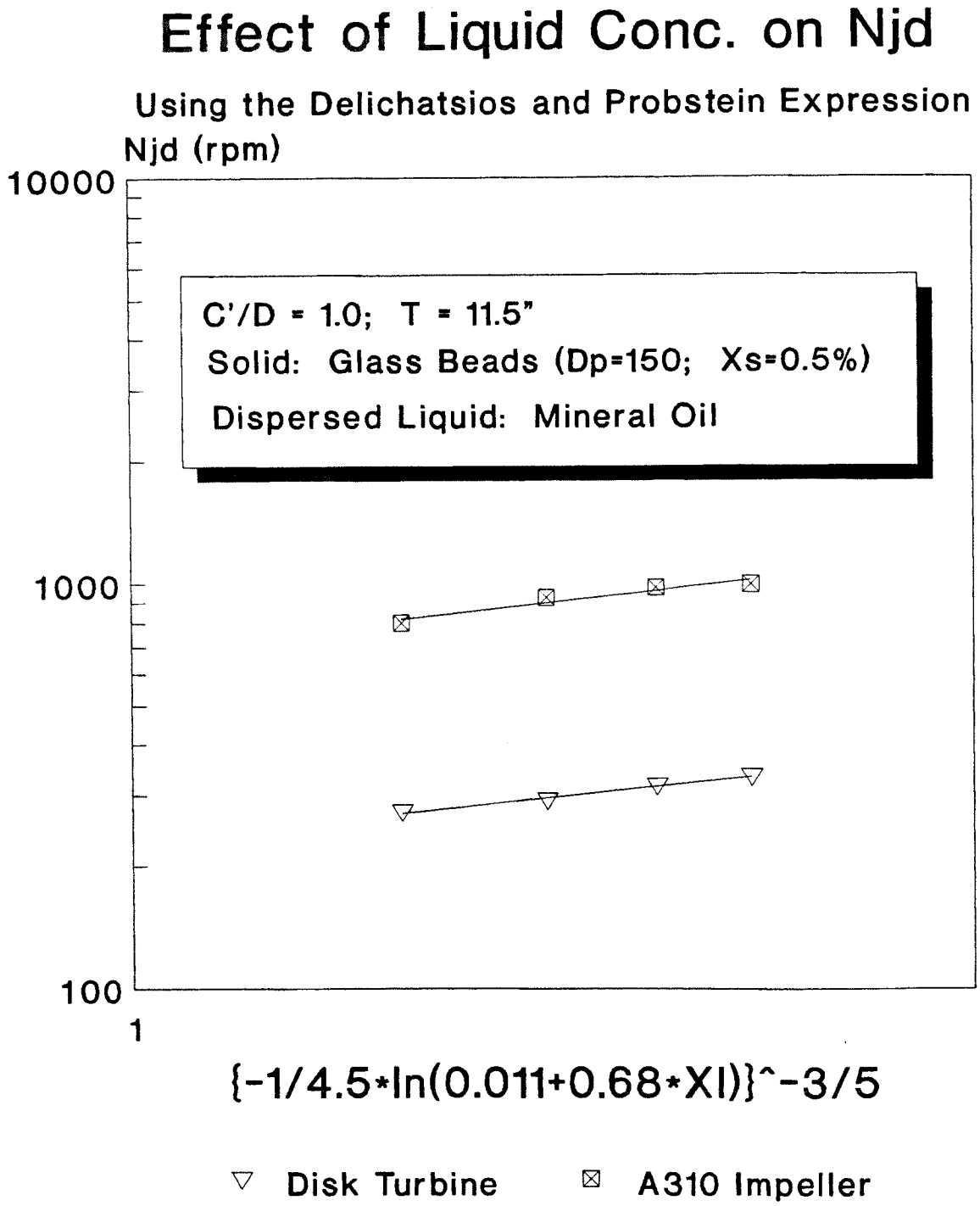
Effect of Liquid Conc. on Njd
Using the Delichatsios and Probstein Expression
Njd (rpm)
10000
1000
100
1
C'/D = 1.0; T = 11.5"
Solid: Glass Beads (Dp=150; Xs=0.5%)
Dispersed Liquid: Mineral Oil
{-1/4.5*ln(0.011+0.68*Xl)}^-3/5
Disk Turbine
A310 Impeller

Figure 24

Effect of Scale-up on Njs

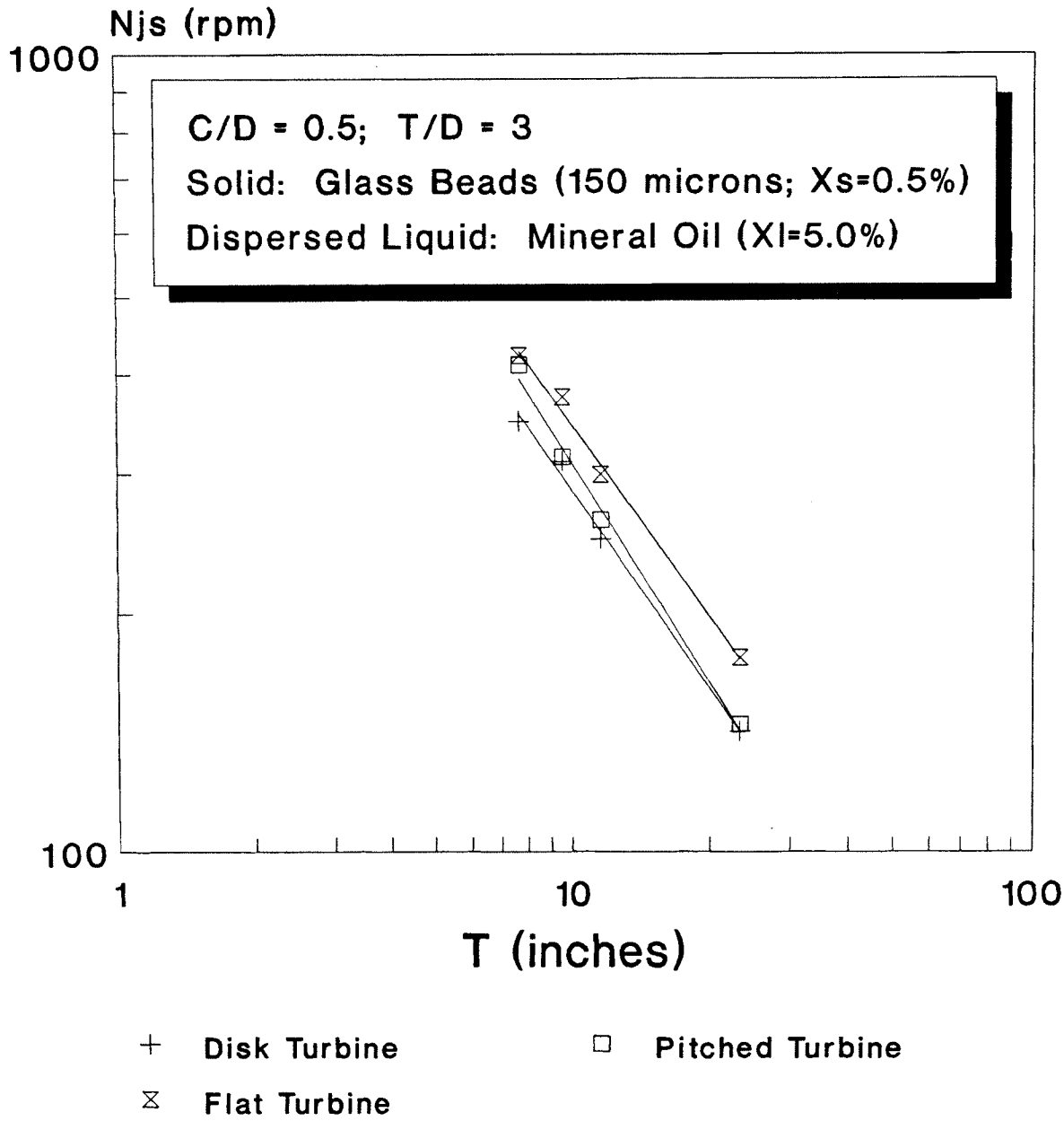

Figure 25

Effect of Scale-up on Njs

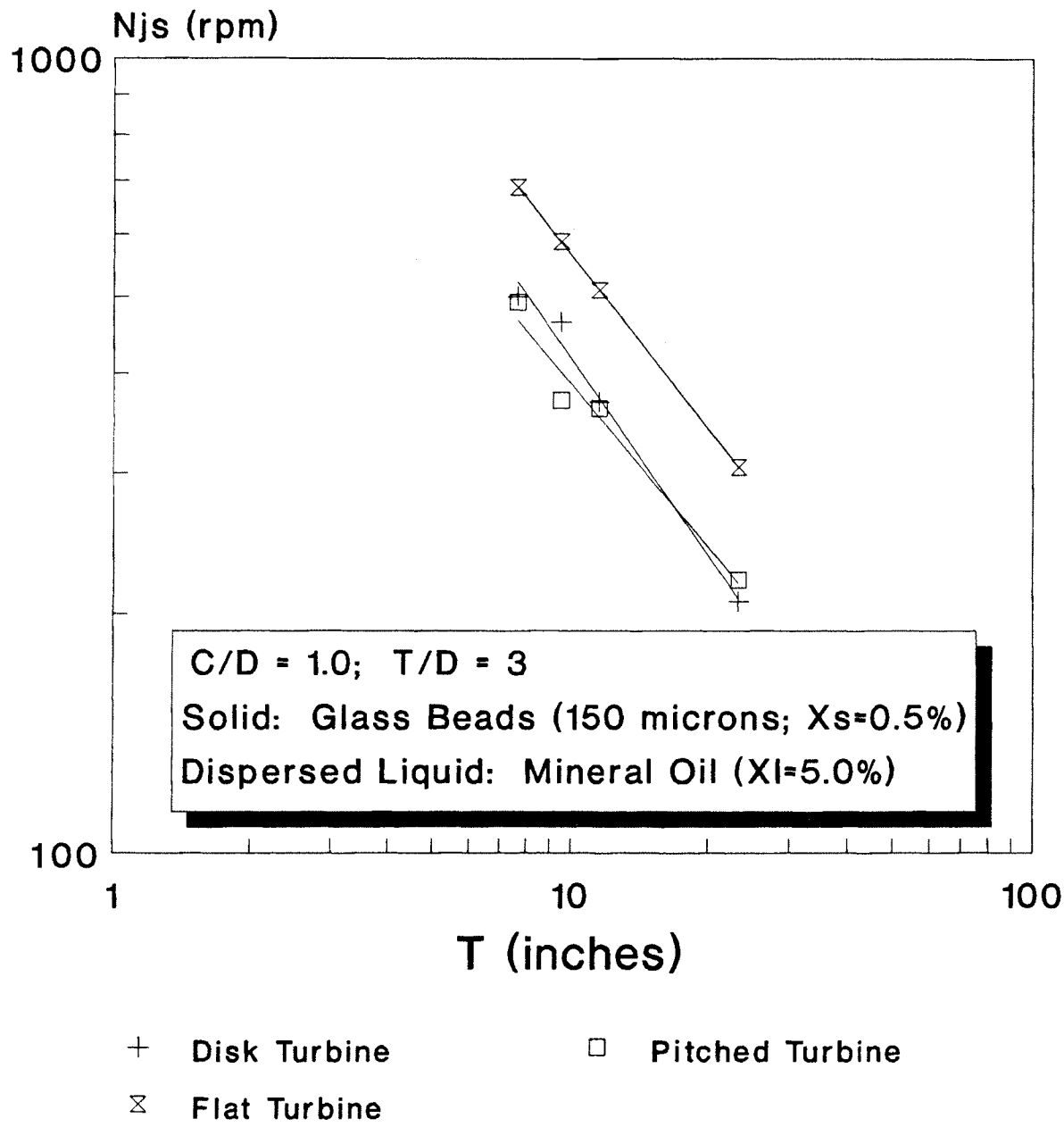

Figure 26

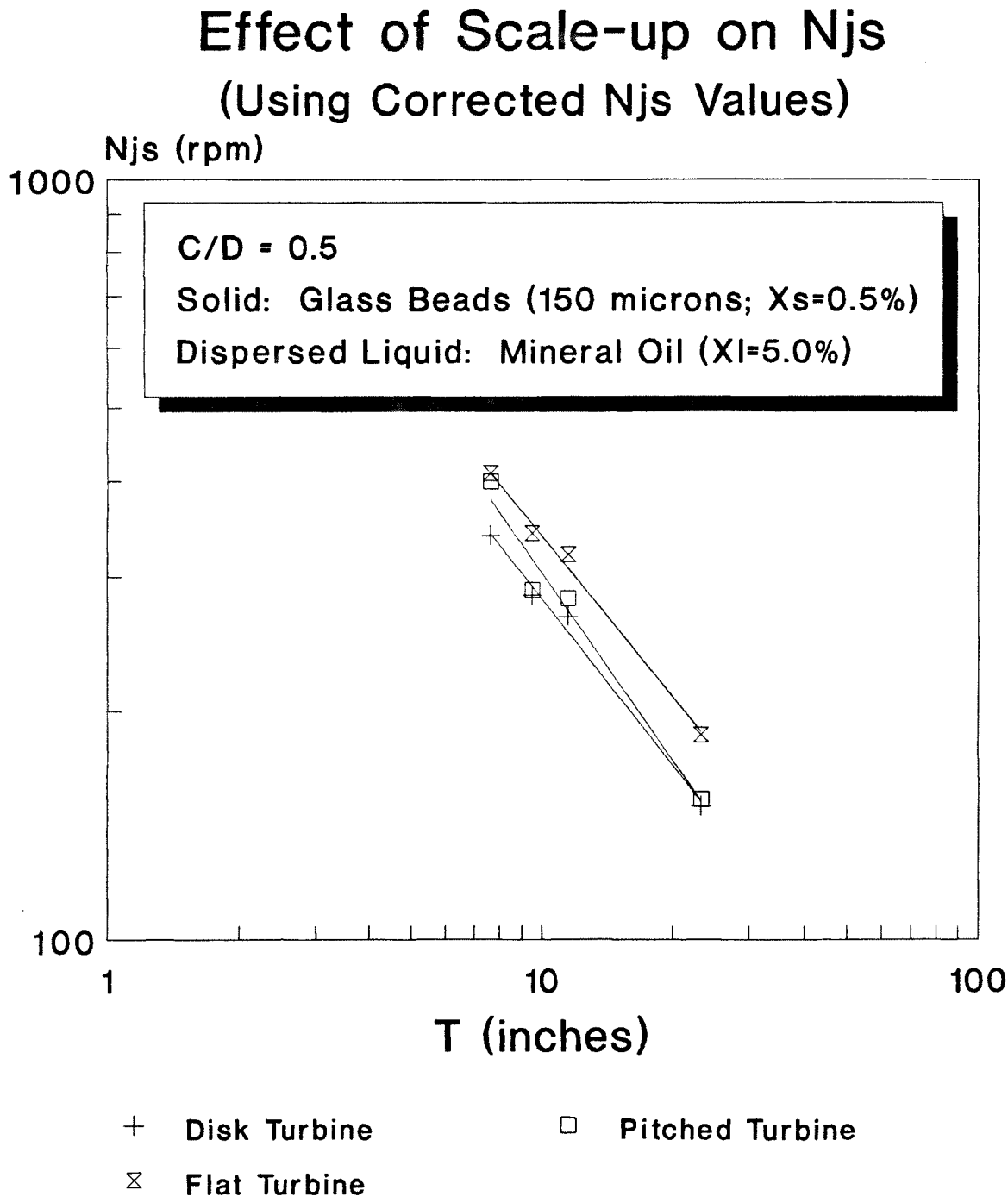
Effect of Scale-up on Njs
(Using Corrected Njs Values)
Njs (rpm)
1000
100
C/D = 0.5
Solid: Glass Beads (150 microns; Xs=0.5%)
Dispersed Liquid: Mineral Oil (Xl=5.0%)
1
10
100
T (inches)
Disk Turbine
Pitched Turbine
Flat Turbine

Figure 27

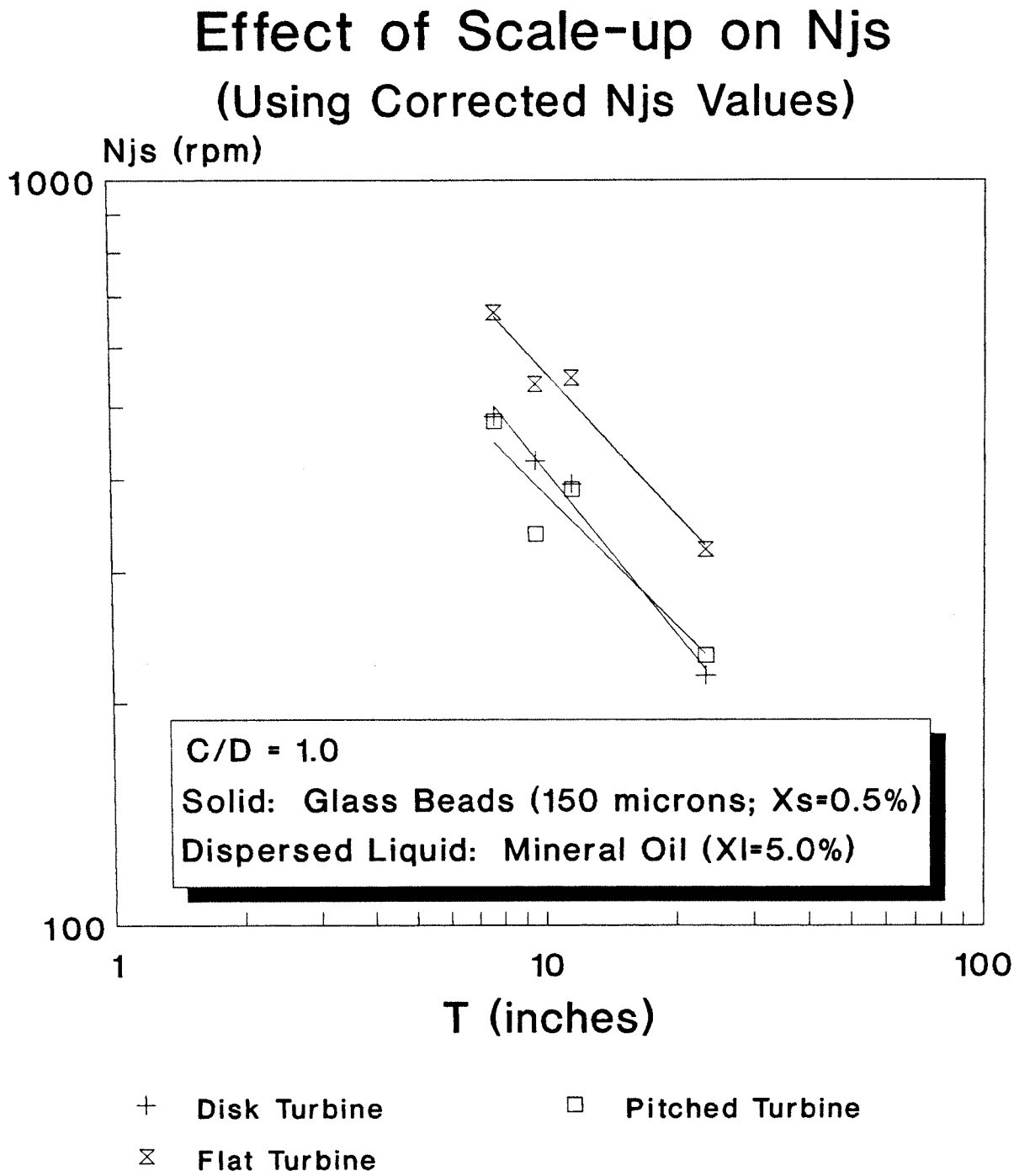
Effect of Scale-up on Njs
(Using Corrected Njs Values)
Njs (rpm)
1000
100
1
10
100
T (inches)
C/D = 1.0
Solid: Glass Beads (150 microns; Xs=0.5%)
Dispersed Liquid: Mineral Oil (Xl=5.0%)
Disk Turbine
Pitched Turbine
Flat Turbine

Figure 28

Effect of Scale-up on Njd

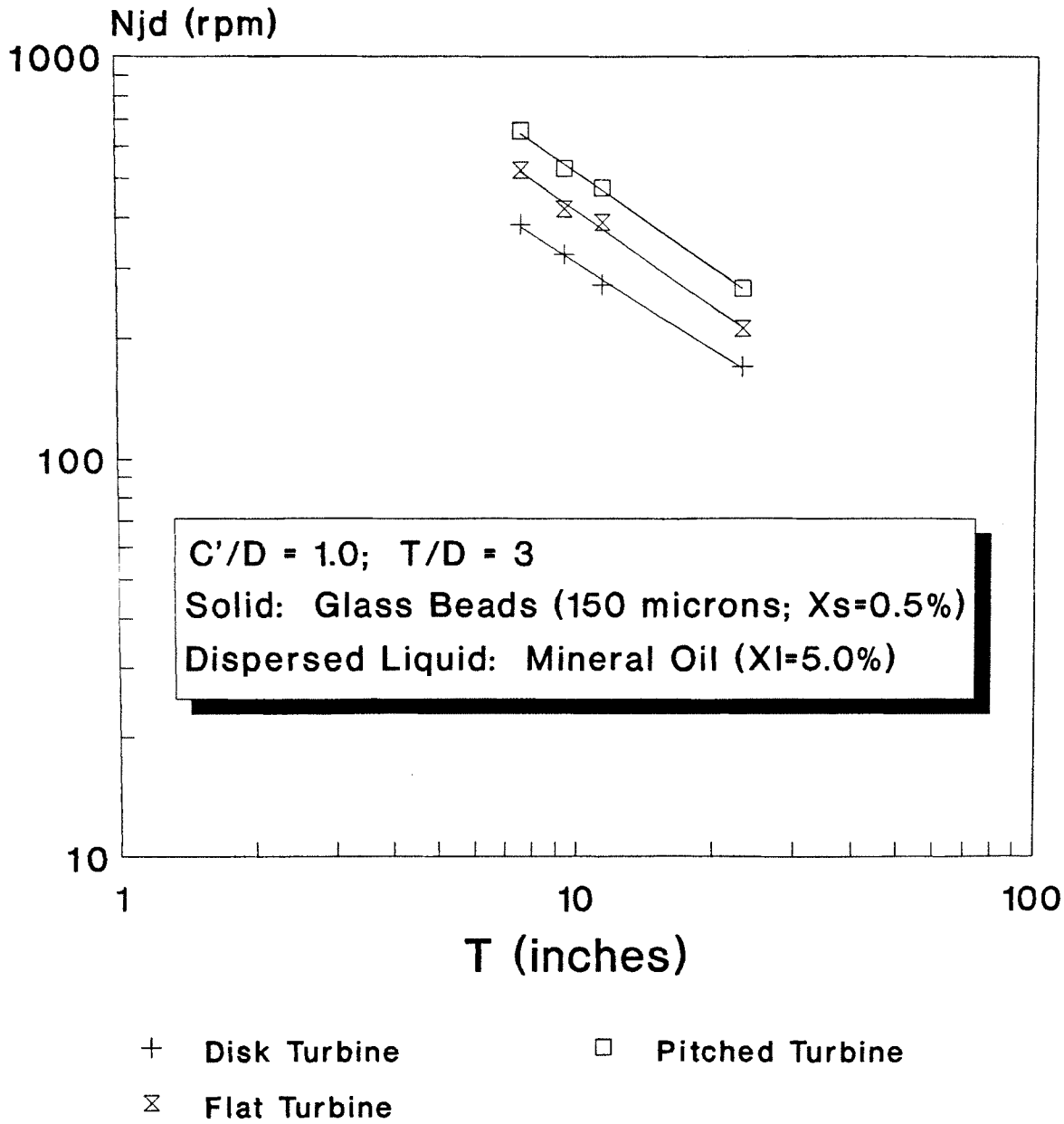

Figure 29

Effect of Scale-up on Njd

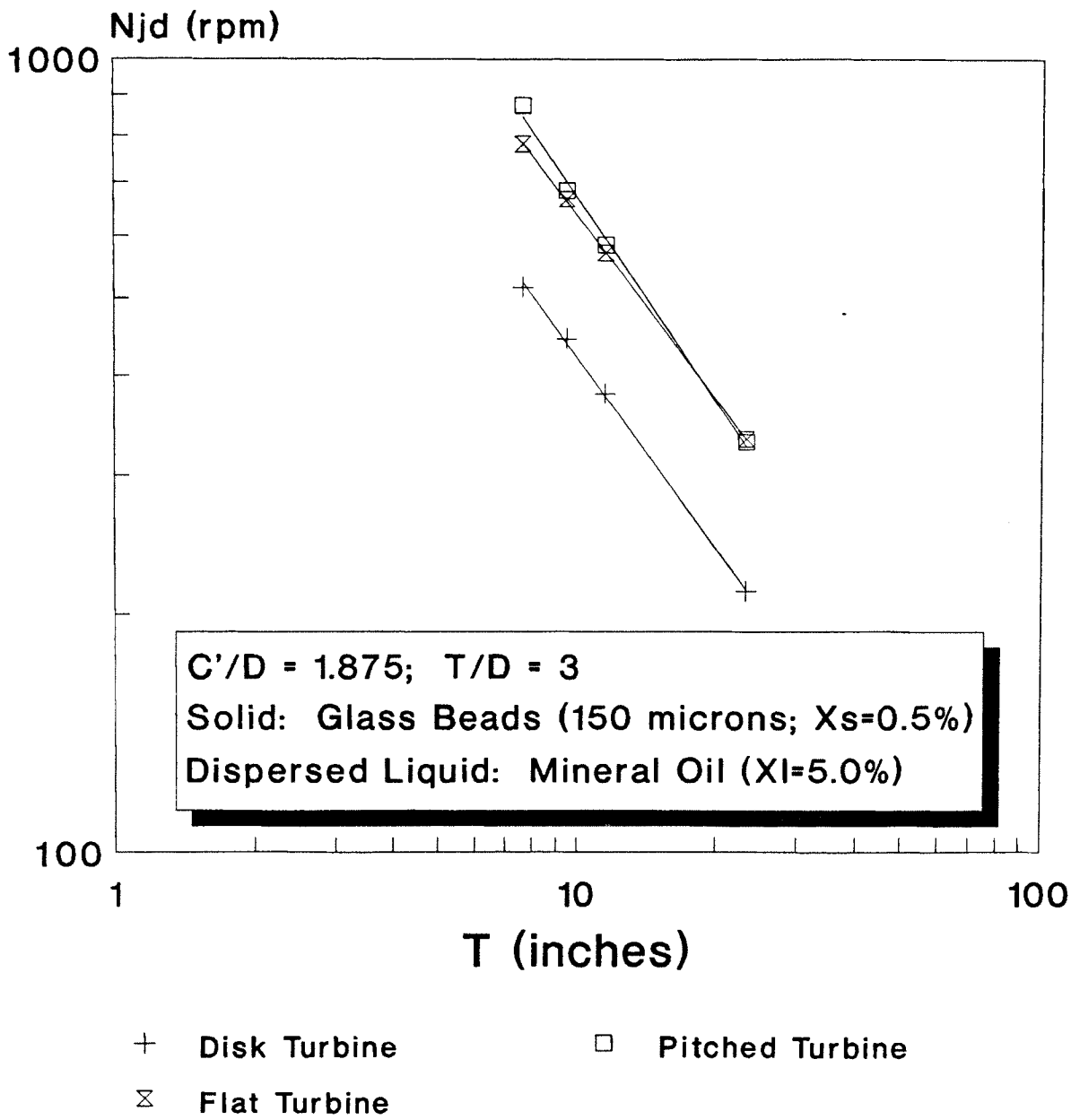

Figure 30

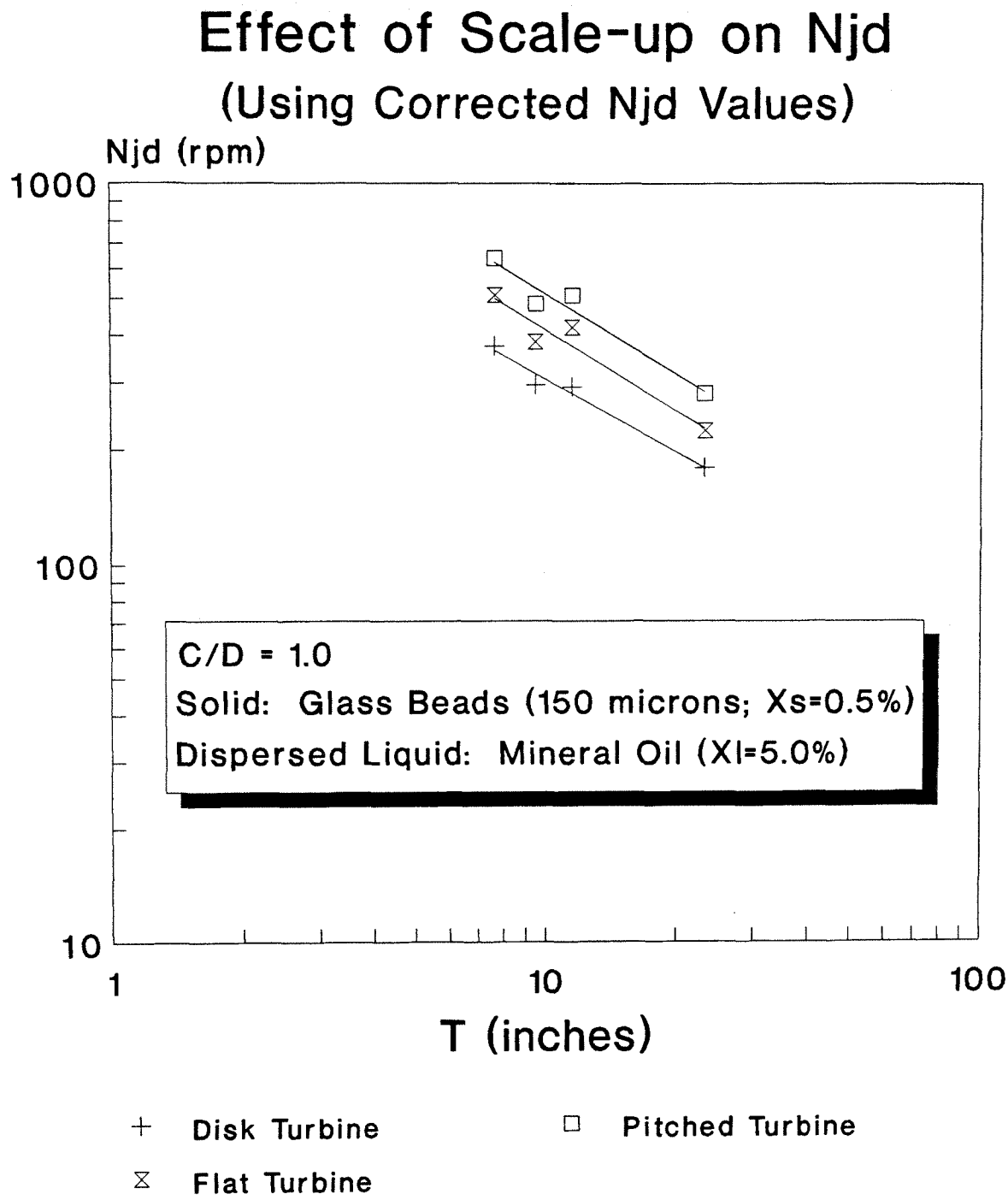
Effect of Scale-up on Njd
(Using Corrected Njd Values)
Njd (rpm)
1000
100
10
1
10
100
T (inches)
C/D = 1.0
Solid: Glass Beads (150 microns; Xs=0.5%)
Dispersed Liquid: Mineral Oil (Xl=5.0%)
Disk Turbine
Pitched Turbine
Flat Turbine

Figure 31

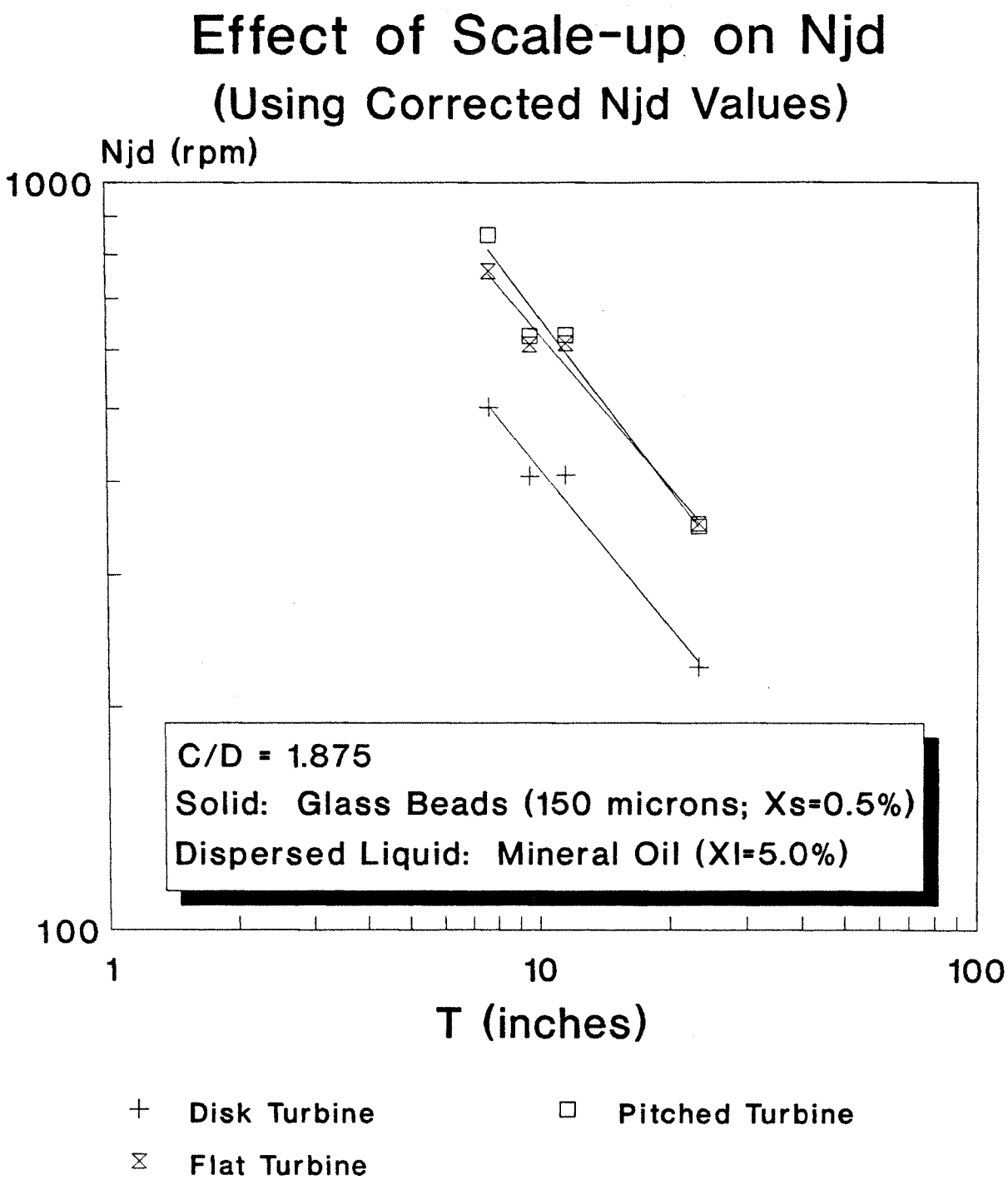
Effect of Scale-up on Njd
(Using Corrected Njd Values)
Njd (rpm)
1000
100
1
10
100
T (inches)
C/D = 1.875
Solid: Glass Beads (150 microns; Xs=0.5%)
Dispersed Liquid: Mineral Oil (Xl=5.0%)
Disk Turbine
Pitched Turbine
Flat Turbine

Figure 32

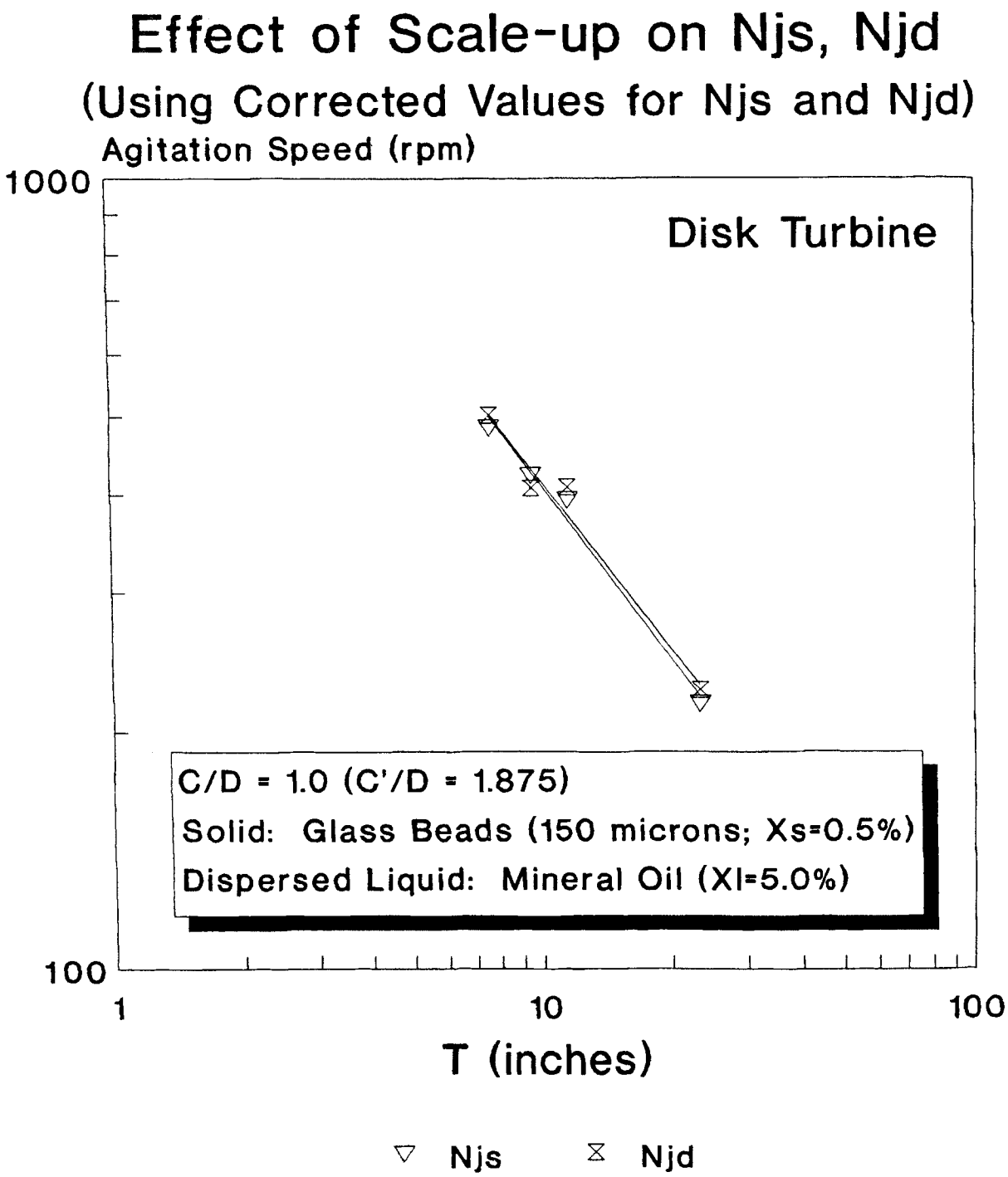
Effect of Scale-up on Njs, Njd
(Using Corrected Values for Njs and Njd)
Agitation Speed (rpm)
1000
100
Disk Turbine
C/D = 1.0 (C'/D = 1.875)
Solid: Glass Beads (150 microns; Xs=0.5%)
Dispersed Liquid: Mineral Oil (Xl=5.0%)
1
10
100
T (inches)
Njs
Njd

Figure 33

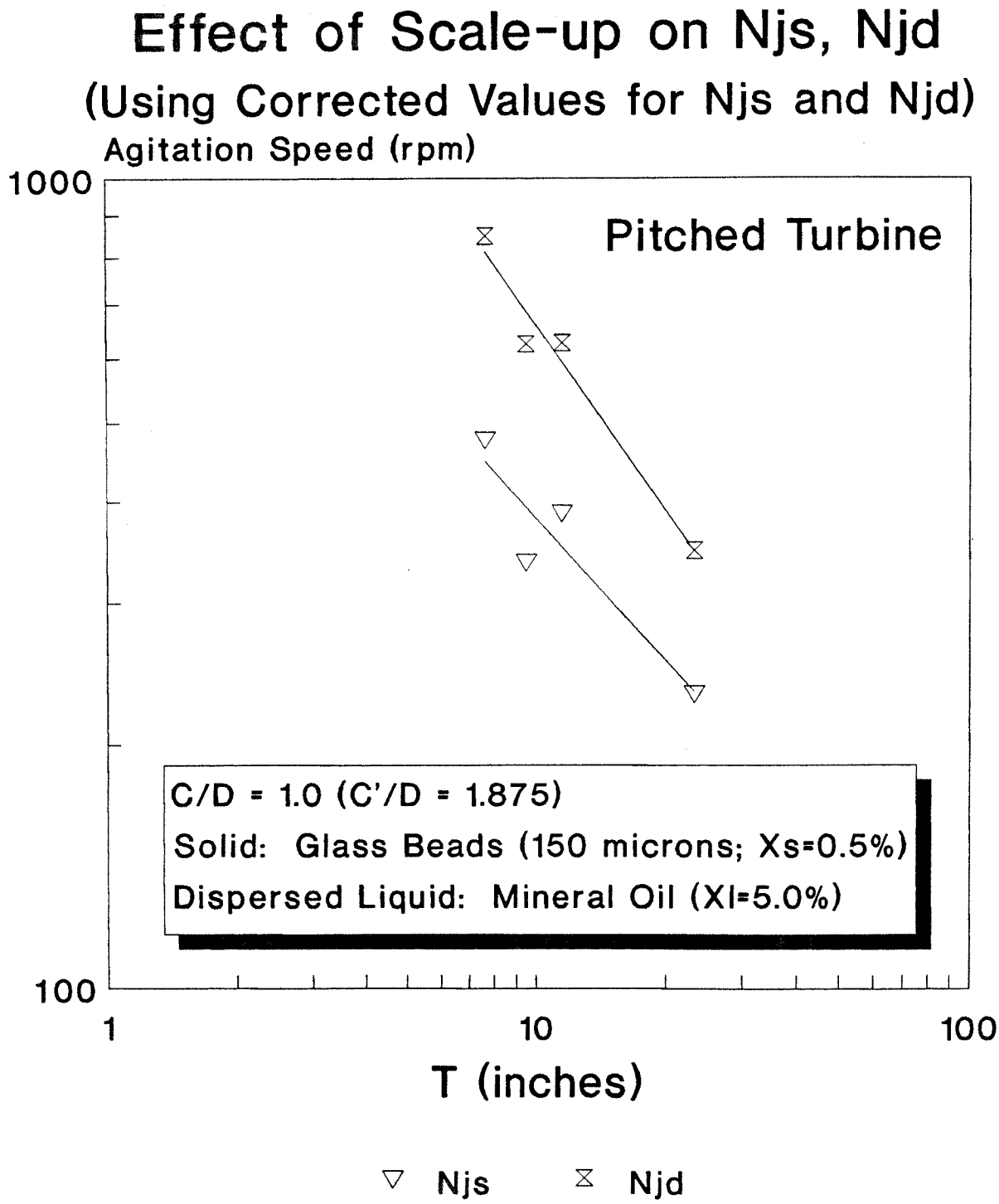
Effect of Scale-up on Njs, Njd
(Using Corrected Values for Njs and Njd)
Agitation Speed (rpm)
1000
100
Pitched Turbine
C/D = 1.0 (C'/D = 1.875)
Solid: Glass Beads (150 microns; Xs=0.5%)
Dispersed Liquid: Mineral Oil (Xl=5.0%)
1
10
100
T (inches)
Njs
Njd

Figure 34

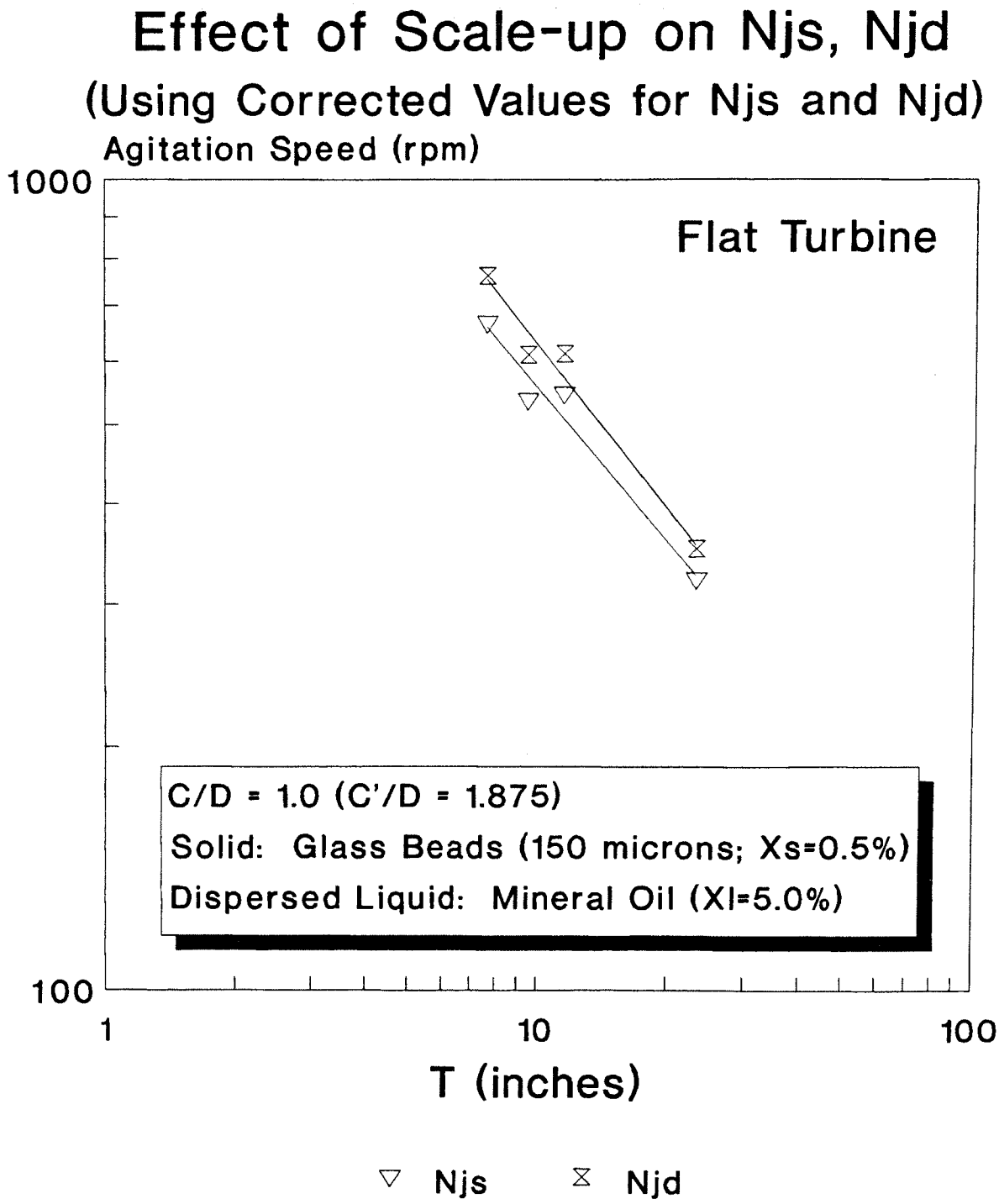
Effect of Scale-up on Njs, Njd
(Using Corrected Values for Njs and Njd)
Agitation Speed (rpm)
1000
100
Flat Turbine
C/D = 1.0 (C'/D = 1.875)
Solid: Glass Beads (150 microns; Xs=0.5%)
Dispersed Liquid: Mineral Oil (Xl=5.0%)
1
10
100
T (inches)
Njs
Njd

Figure 35

Effect of Impeller Diameter on Nje

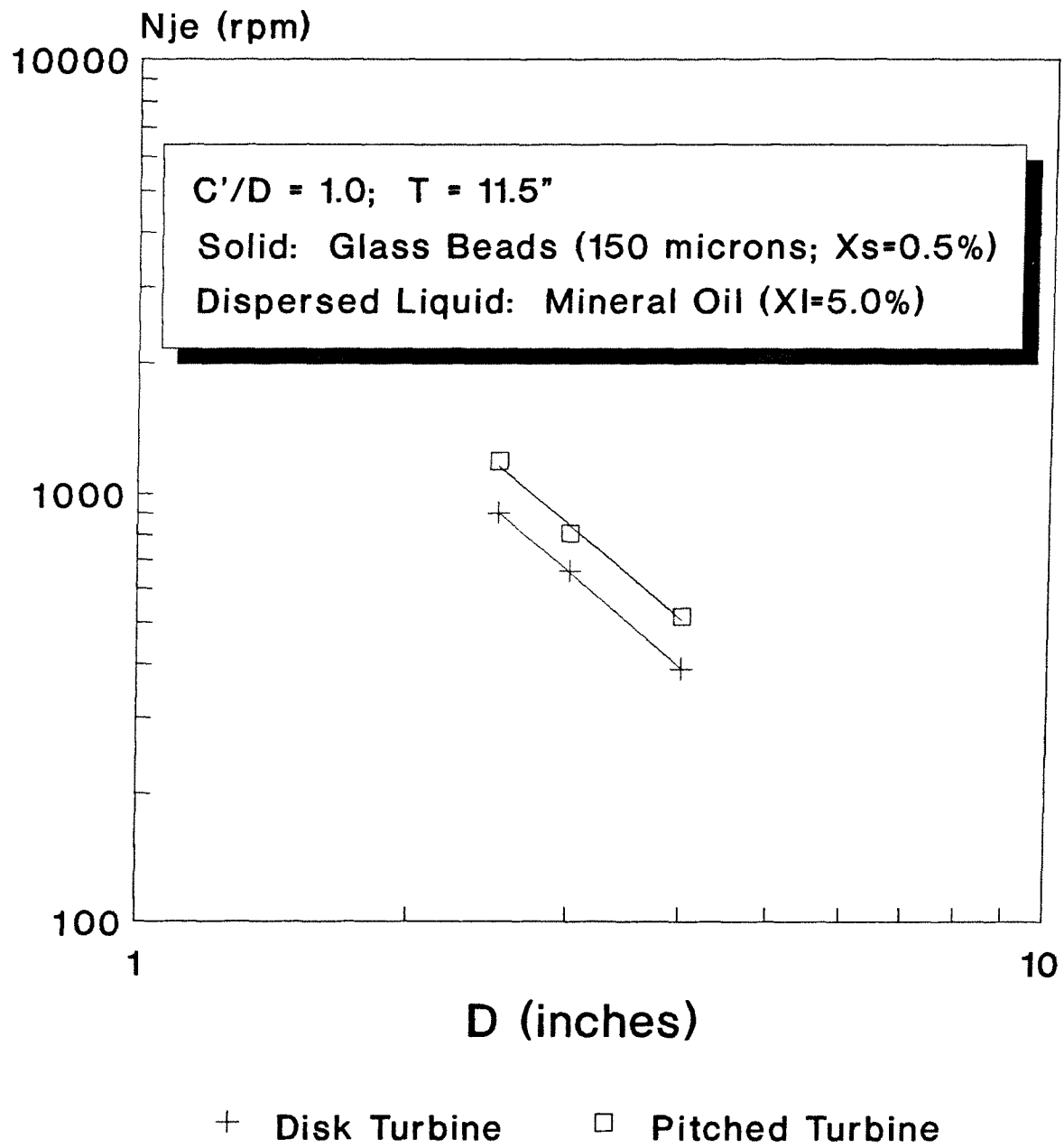

Figure 36

Effect of Scale-up on Nje

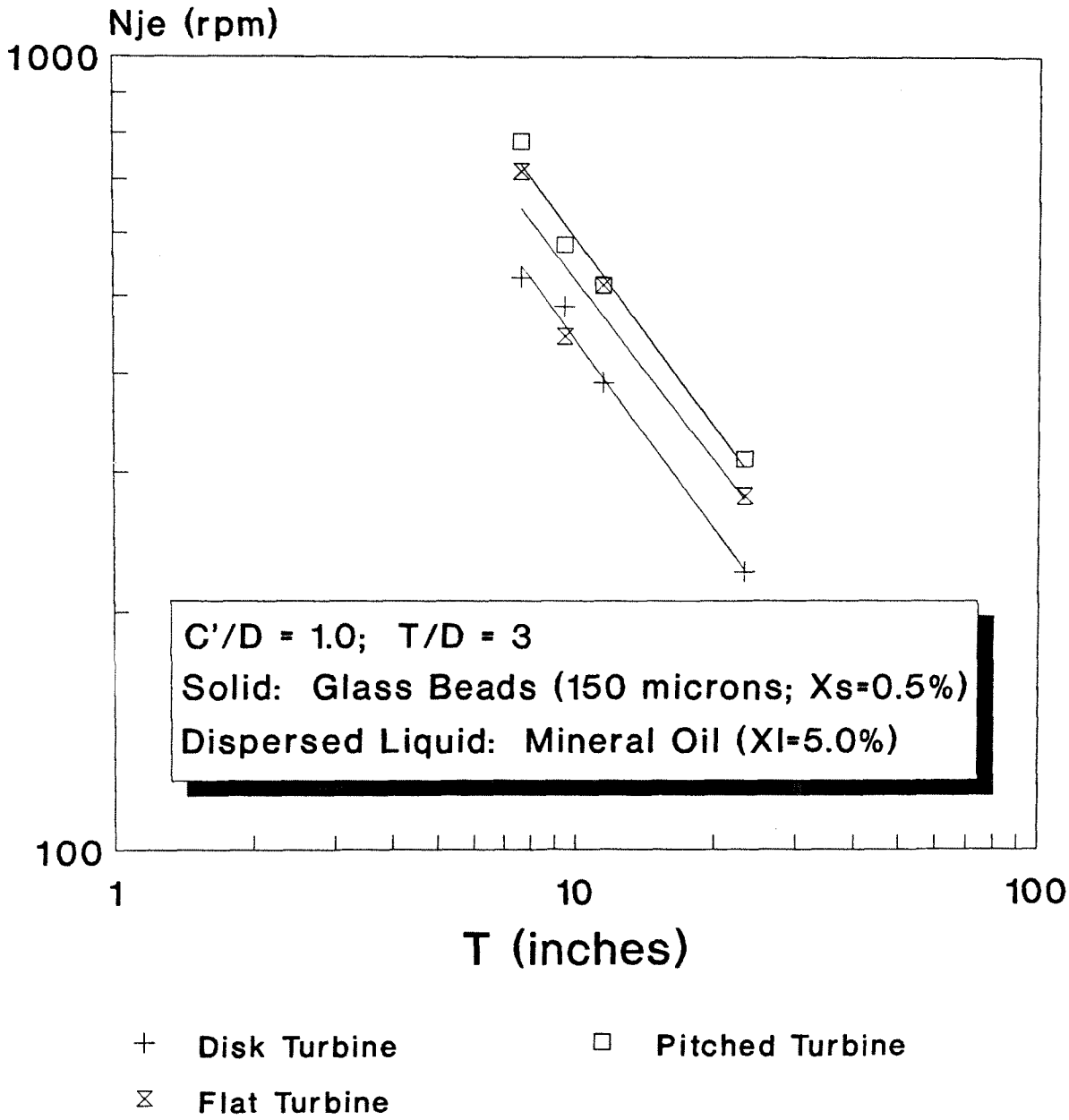

Figure 37

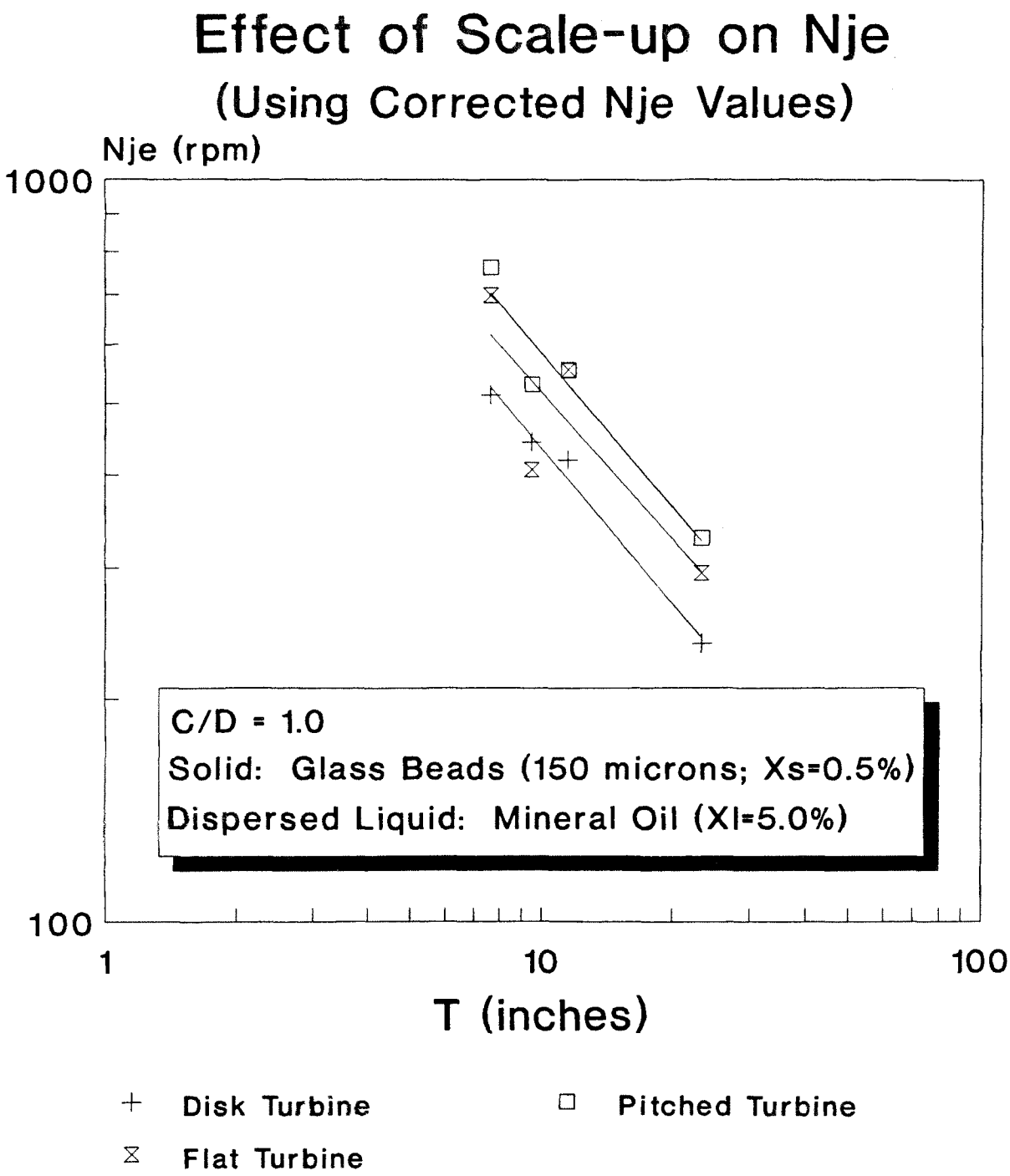
Effect of Scale-up on Nje
(Using Corrected Nje Values)
Nje (rpm)
1000
100
1
10
100
T (inches)
C/D = 1.0
Solid: Glass Beads (150 microns; Xs=0.5%)
Dispersed Liquid: Mineral Oil (Xl=5.0%)
Disk Turbine
Pitched Turbine
Flat Turbine

Figure 38

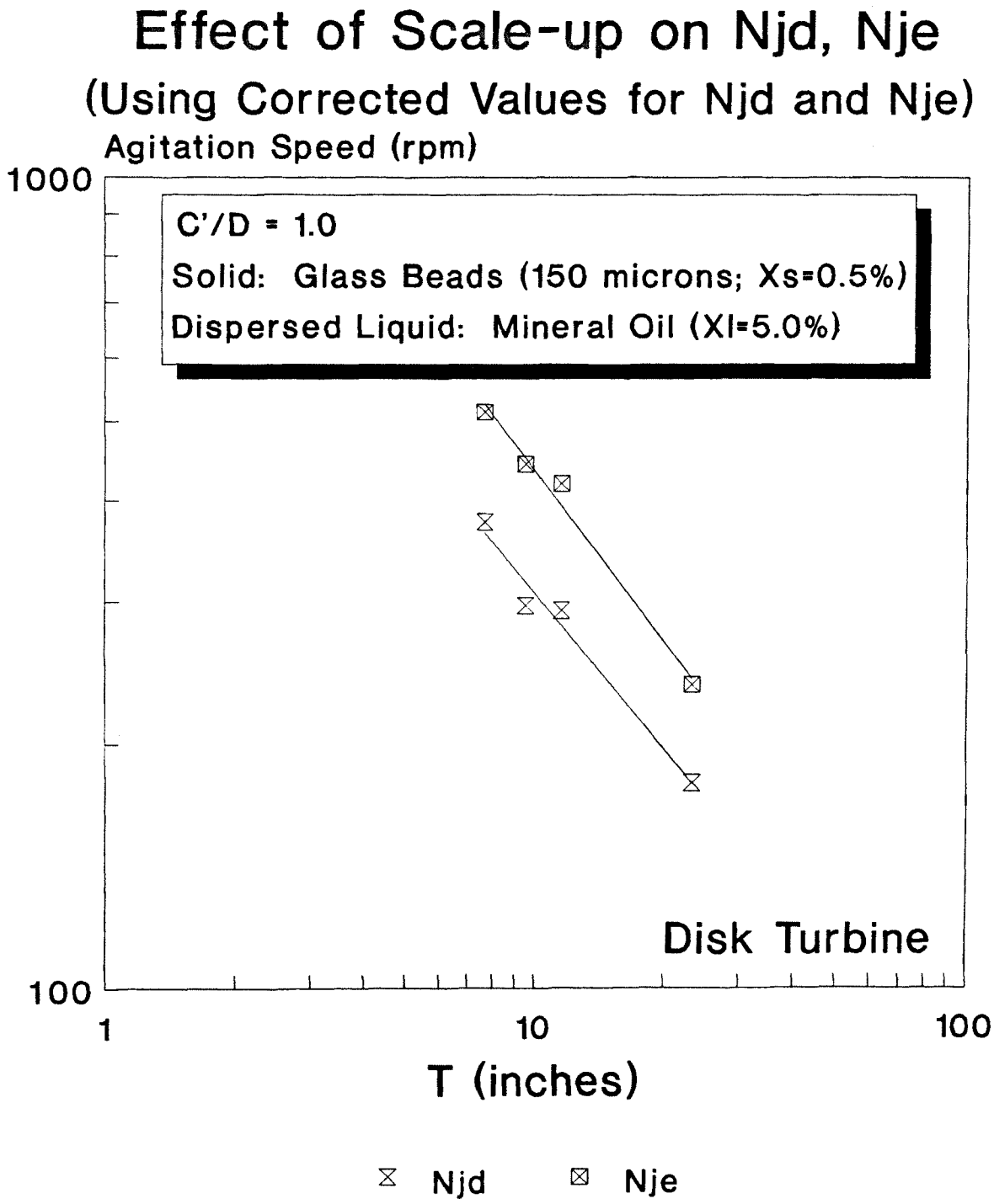
Effect of Scale-up on Njd, Nje
(Using Corrected Values for Njd and Nje)
Agitation Speed (rpm)
1000
100
C'/D = 1.0
Solid: Glass Beads (150 microns; Xs=0.5%)
Dispersed Liquid: Mineral Oil (Xl=5.0%)
Disk Turbine
1
10
100
T (inches)
Njd
Nje

Figure 39

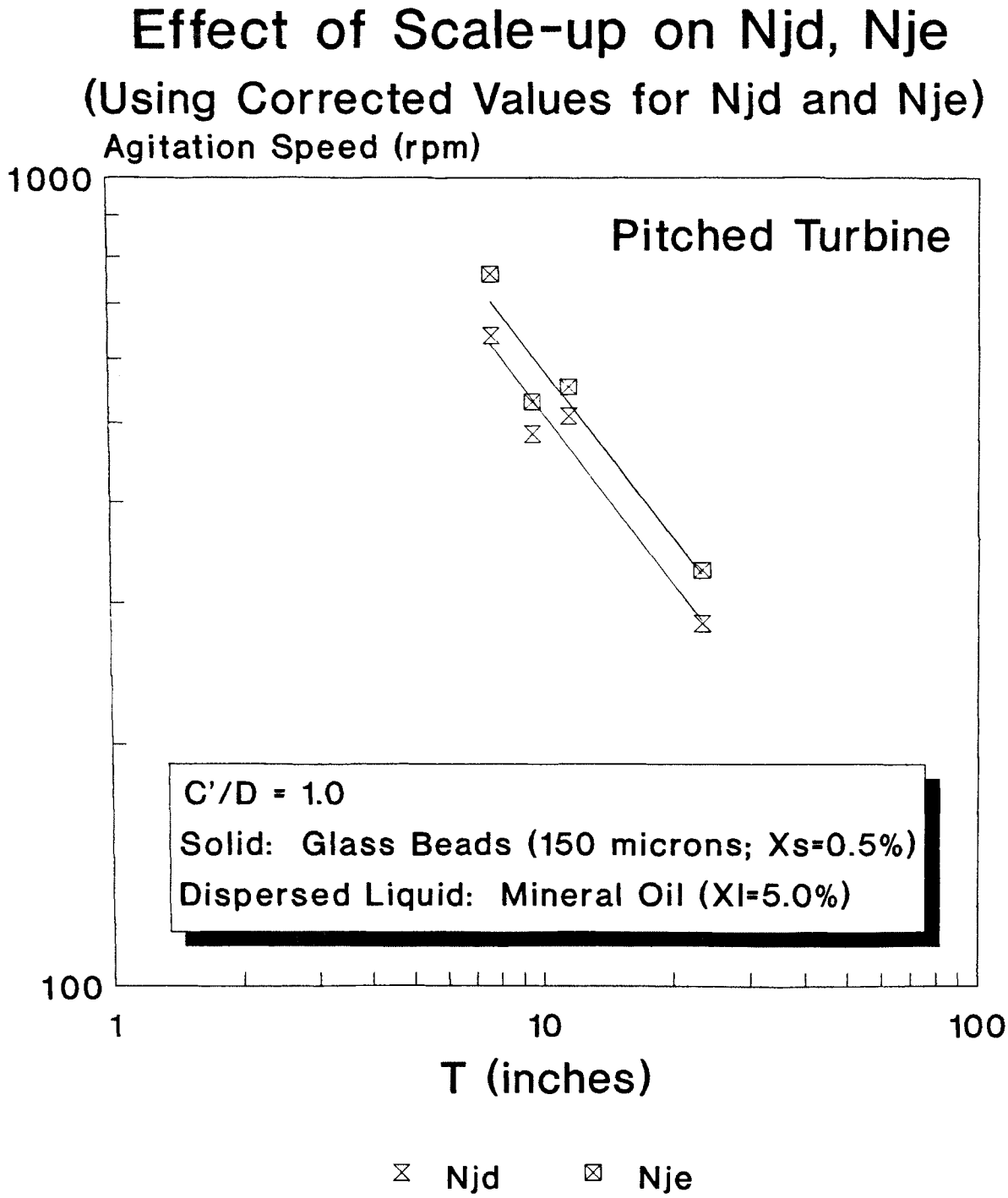
Effect of Scale-up on Njd, Nje
(Using Corrected Values for Njd and Nje)
Agitation Speed (rpm)
1000
100
Pitched Turbine
C'/D = 1.0
Solid: Glass Beads (150 microns; Xs=0.5%)
Dispersed Liquid: Mineral Oil (Xl=5.0%)
1
10
100
T (inches)
Njd
Nje

Figure 40

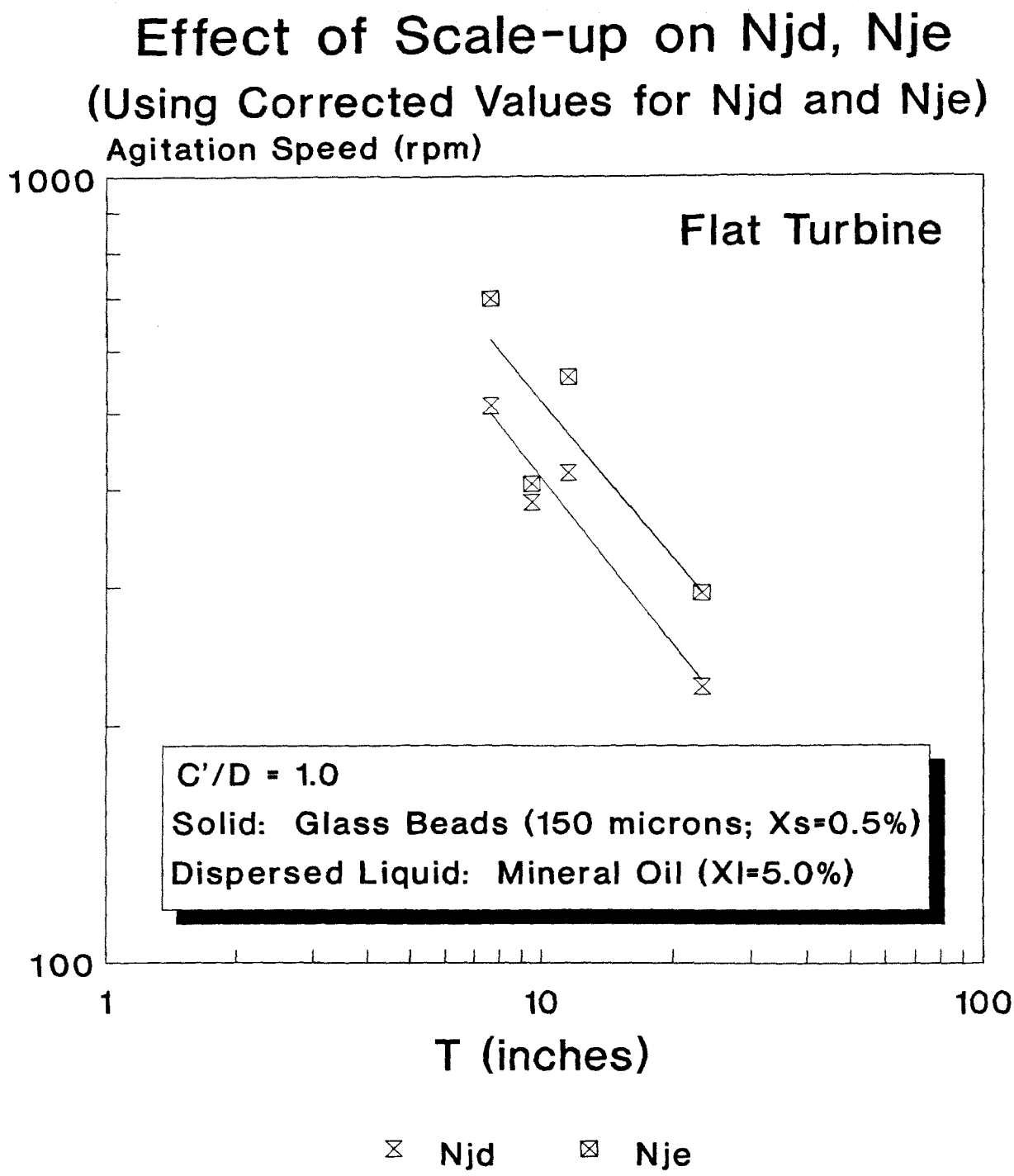
Effect of Scale-up on Njd, Nje
(Using Corrected Values for Njd and Nje)
Agitation Speed (rpm)
1000
100
Flat Turbine
C'/D = 1.0
Solid: Glass Beads (150 microns; Xs=0.5%)
Dispersed Liquid: Mineral Oil (Xl=5.0%)
1
10
100
T (inches)
Njd
Nje

Figure 41

Final Expression for Njs
Using the Disk Turbine

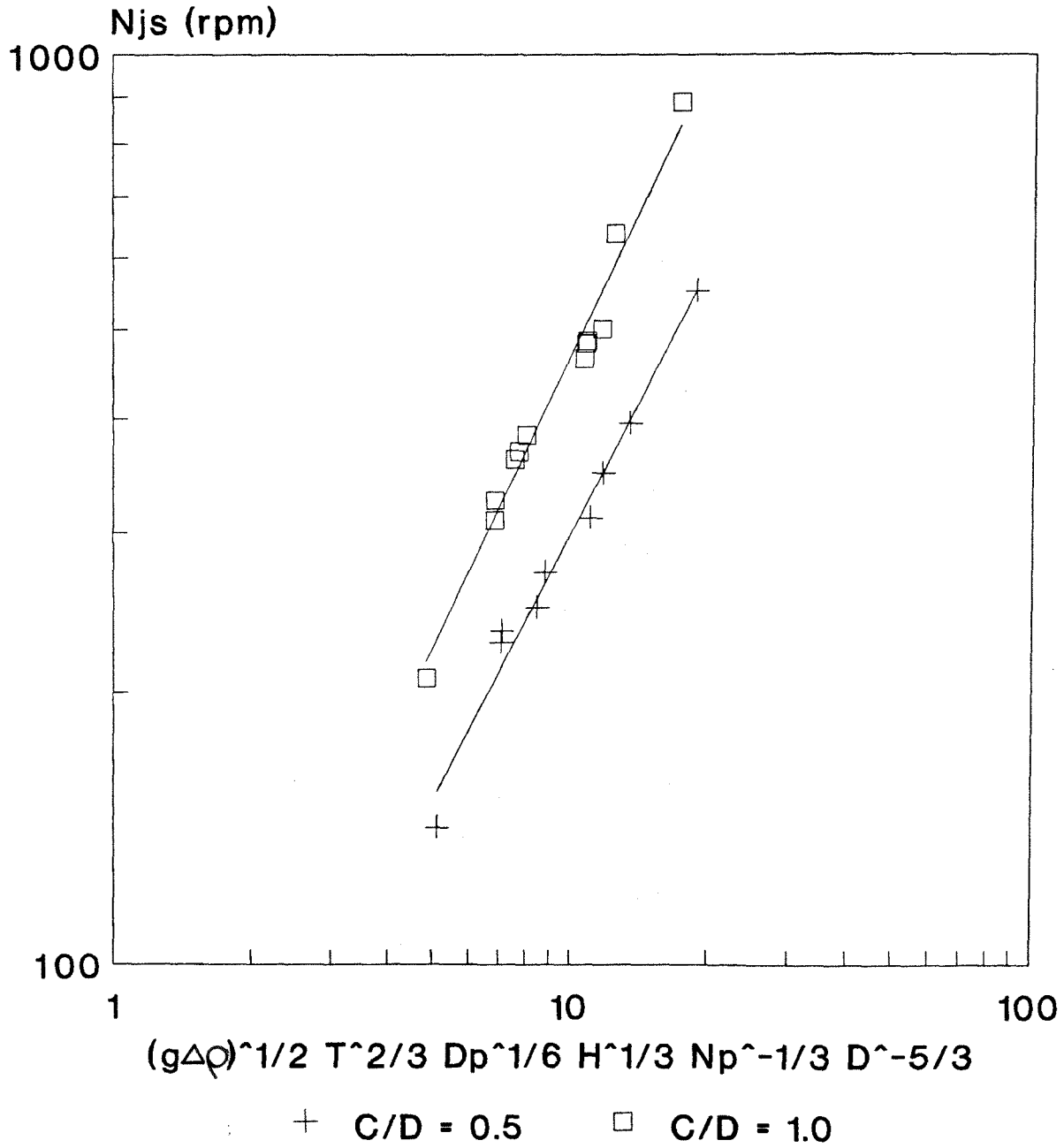

Figure 42

Final Expression for Njs
Using the A310 Impeller

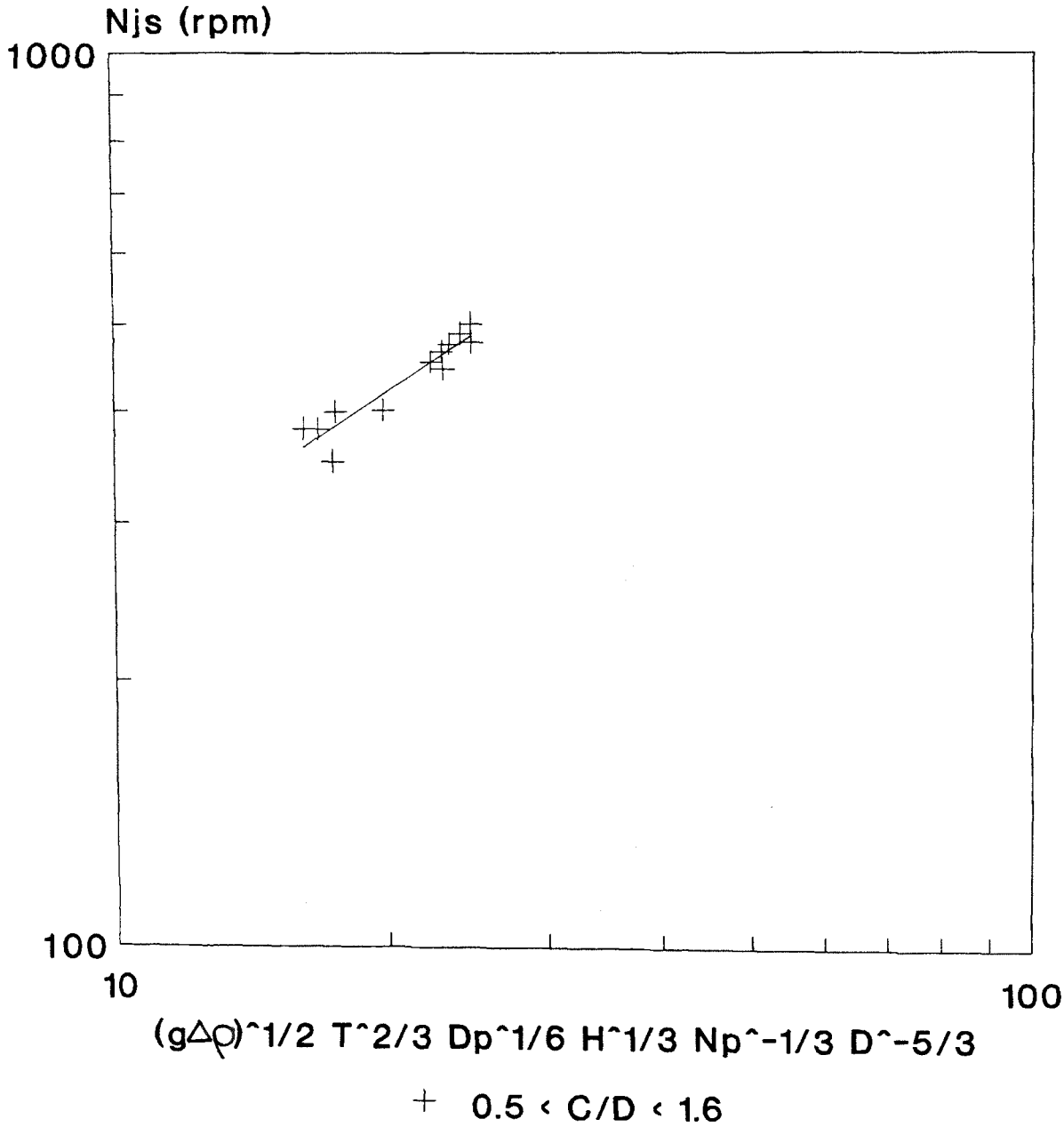

Figure 43

Final Expression for Njs
Using the Pitched Turbine

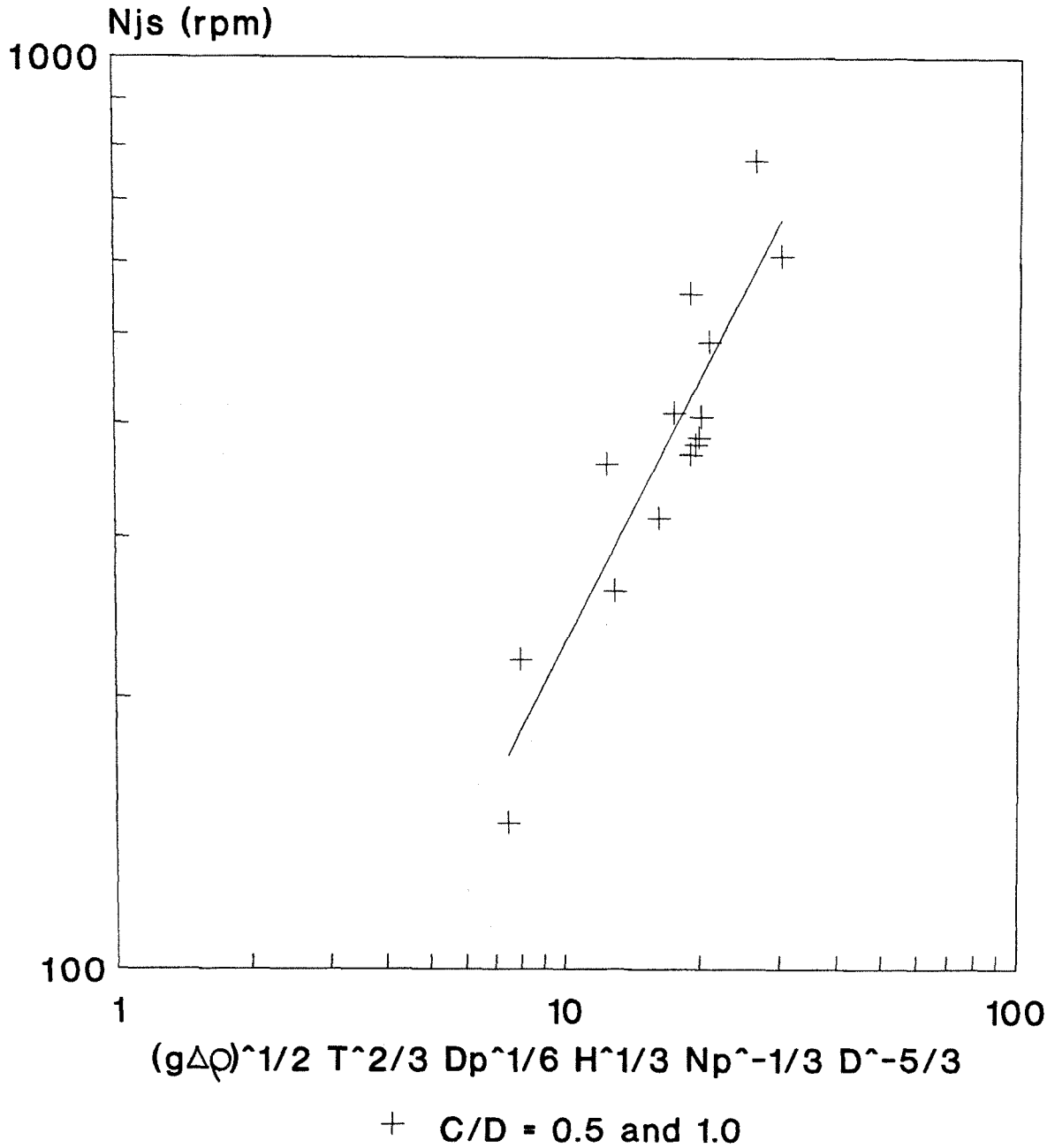

Figure 44

Final Expression for Njd
Using the Disk Turbine

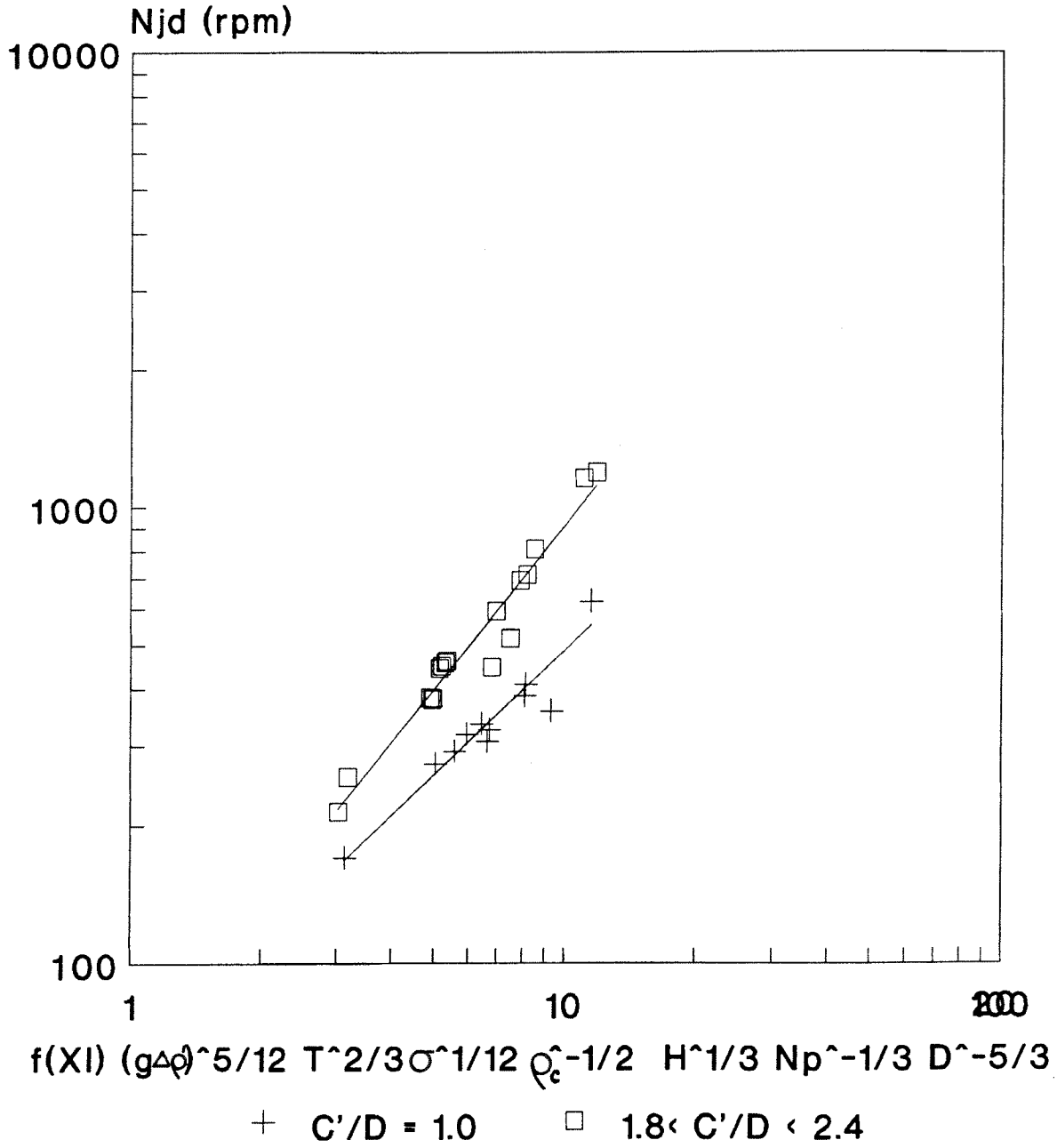

Figure 45

Final Expression for Njd
Using the A310 Impeller

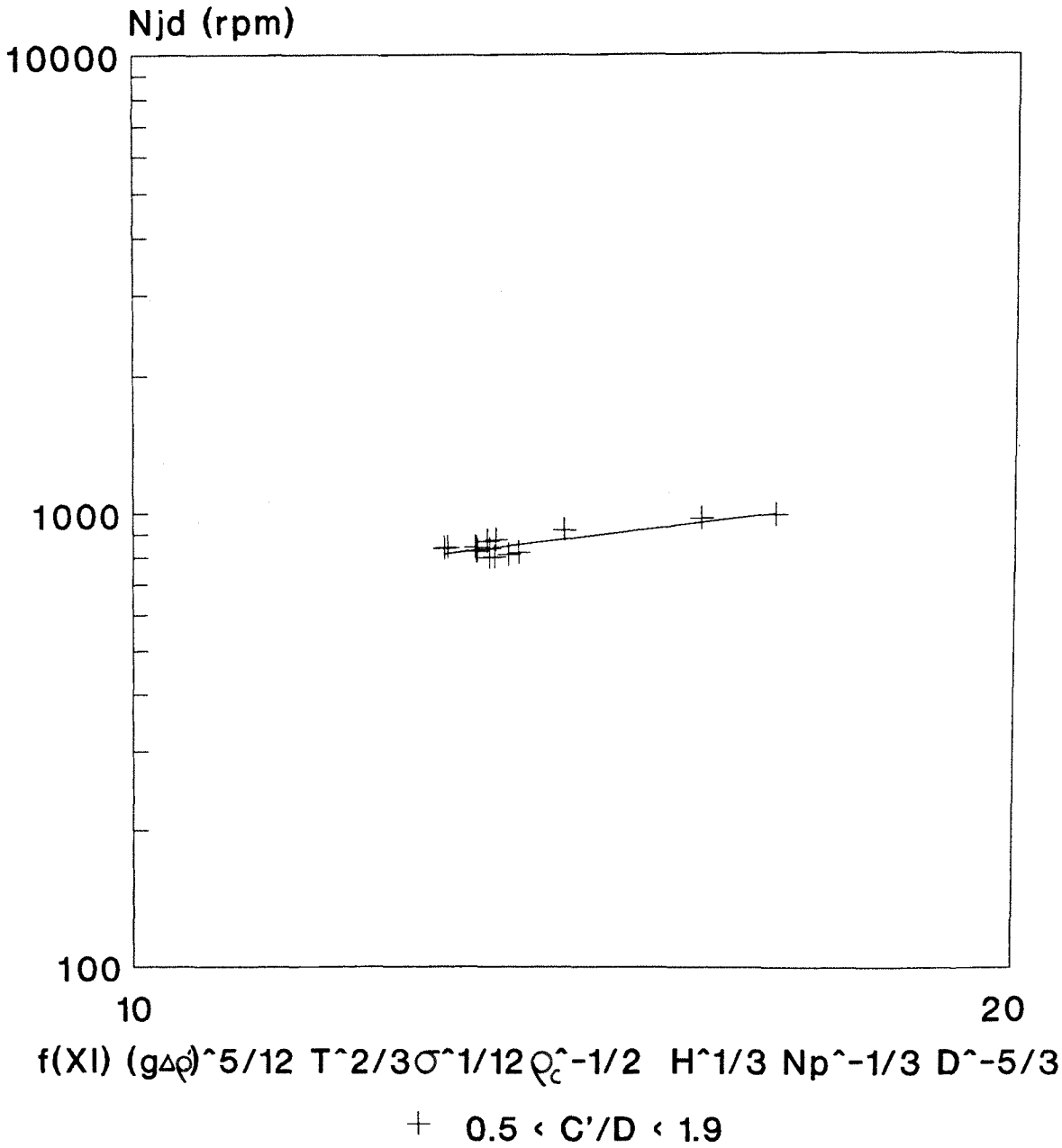

Figure 46

Final Expression for Njd
Using the Pitched Turbine

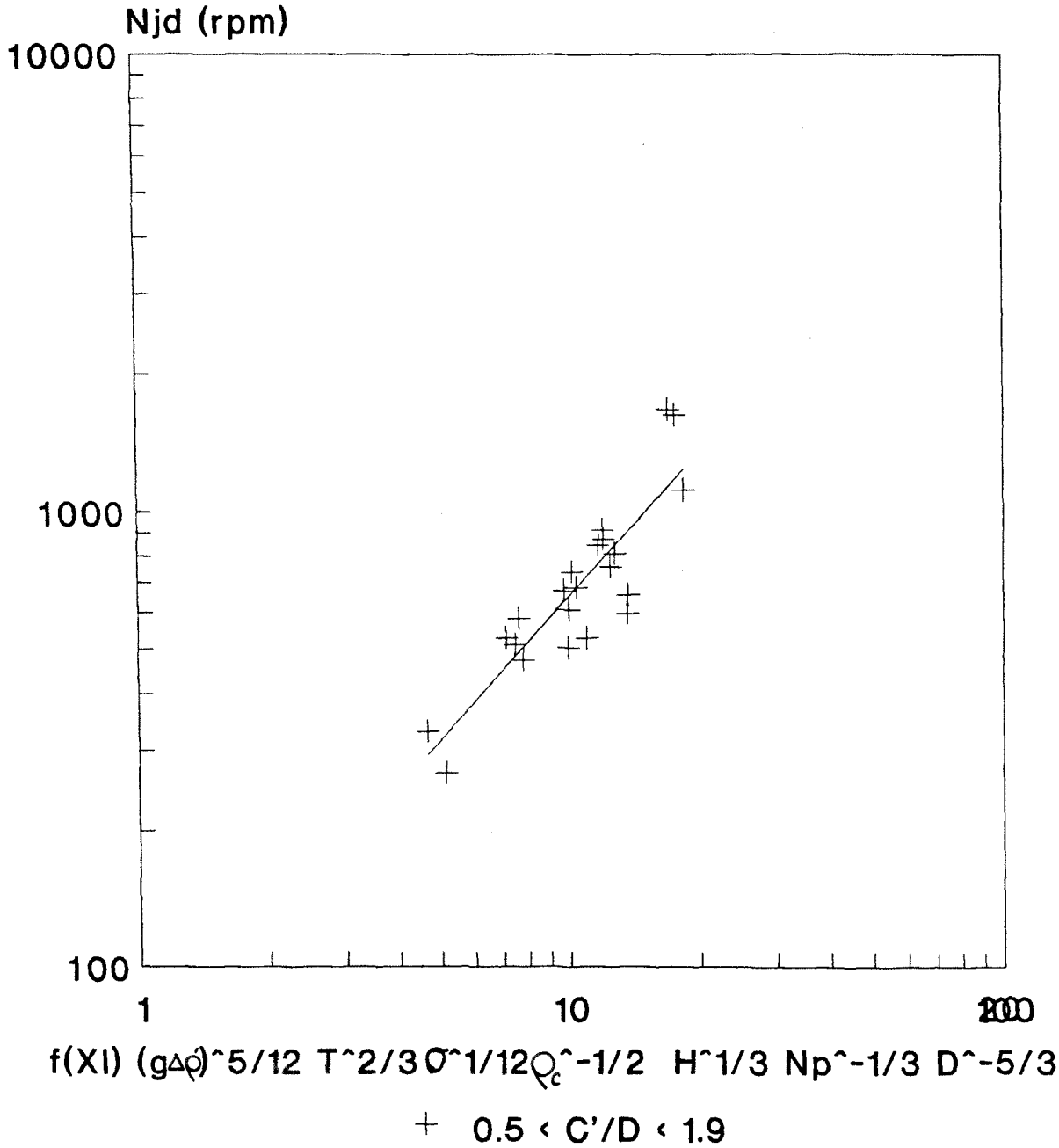

Figure 47